Development of a Novel Piezoelectric Implant to Improve the Success Rate of Spinal Fusions

BY

Nicholas Tobaben

Submitted to the graduate degree program in Mechanical Engineering

and the Graduate Faculty of the University of Kansas in partial fulfillment of the

requirements for the degree of Master of Science.

_____

Dr. Elizabeth Friis, Chairperson

_____

Dr. Carl Luchies, Committee Member

_____

Dr. Christopher Depcik, Committee Member

_____

Dr. Michael Detamore, Committee Member

Date Defended: 7/19/2012

The Thesis Committee for Nicholas Tobaben certifies

That this is the approved version of the following thesis:

Development of a Novel Piezoelectric Implant to Improve the Success Rate of Spinal Fusions

_____

Dr. Elizabeth Friis, Chairperson

_____

Date Approved

Abstract

The purpose of this thesis is to design and show preliminary proof of concept for a piezoelectric fusion cage, which will help stimulate bone growth during spinal fusions. The fusion cage will utilize a novel piezoelectric composite.

Back pain is one of the most common neurological diseases, second to only headaches. The primary surgical procedure to relieve lower back pain is known as a lumbar interbody fusion. The goal of this surgery is to stabilize the problematic spine segment by removing the intervertebral disc, stabilizing the segment with instrumentation, and growing bone between the vertebrae. This surgery, however, is far from perfect. Failure of the vertebrae to fuse occurs in 10 to 46% of all patients, depending on patients' inherent factors. Electrical stimulation has been found to significantly increase fusion rates, but requires extra instrumentation and is expensive. To overcome these issues, development has begun on a piezoelectric fusion cage, which will generate electricity as it is compressed between the vertebrae during normal activities.

A design for the implant has been developed that is made primarily of a piezoelectric composite, but will include additional materials and circuitry. The implant will safely deliver a bone-growing, negative electric potential to the fusion, while protecting the fusion from the bone-resorbing, positive electric potential.

A theoretical power analysis and material generation research were conducted simultaneously. The power analysis for piezoelectric composites was developed using a lumped parameters model based off of previous piezoceramic models. It was used to find trends in the implant parameters to help generate the appropriate amount of current density to deliver to the fusion. The material generation research was conducted to validate the results of the theoretical model.

The current generated by the material followed the same trends as the theoretical model and values for theoretical maximum current were within 36% of the experimental results. Based on the results, the theoretical model should be acceptable to find trends in the current output. From these results, a composite generating the required current density should be feasible, meaning the implant could significantly increase the success rates of spinal fusions.

Acknowledgements

There are several people I would like to thank for the amazing graduate experience I have had at KU.

- Dr. Elizabeth Friis for her guidance and support over the past two years. I have always admired her focus on product development and innovation. Her drive has inspired me and will continue to have an impact as this project continues.
- John Domann and Dr. Paul Arnold, the other members of the piezoelectric implant team. John's experience and assistance in the lab has been invaluable my graduate education. Dr. Arnold has brought his unique insight as a neurosurgeon to this project and has provided the opportunity to get a first-hand understanding of spinal fusions.
- Dr. Carl Luchies, Dr. Christopher Depcik, and Dr. Michael Detamore for agreeing to be part of my thesis committee and for their time and insight on my thesis.
- The Department of Mechanical Engineering, which has been a constant in my life over the past seven years and has helped shape the person I've become today.
- Erin Mannen, Nikki Galvis, Adam Cyr, Sami Shalhoub, Lauren Ferris, Fallon Fitzwater, and my other fellow researchers. You all have made my graduate experience truly memorable. I always looked forward to our game lunches and our great conversations. It wouldn't have been the same without you.
- Jim and Anita Tobaben, my brothers Eric and Matt, and my girlfriend Lauren Schimming. You have always been there for me with your love and support and have made my life a blessing.

This work for supported in part through the Institute for Advancing Medical Innovation

Table of Contents

List of Figures

List of Tables

I. Problem Definition and Solution

The purpose of this thesis is to design and show preliminary proof of concept for a piezoelectric fusion cage, which will help stimulate bone growth during spinal fusions. The fusion cage will make use of a novel piezoelectric composite.

Back pain is one of the most common neurological diseases, second to only headaches (1). For some people, the pain goes away within days. For others, the pain becomes chronic and requires surgery. The primary surgical procedure to relieve lower back pain is known as a lumbar interbody fusion. The goal of this surgery is to stabilize the problematic spine segment by removing the intervertebral disc, stabilizing the segment with instrumentation, and growing bone between the vertebrae. This surgery, however, is far from perfect. Failure of the vertebrae to fuse occurs in 10 to 46% of all patients, depending on patients' inherent factors (2-6). The lowest success rates are found in the "difficult-to-fuse" population, which includes patients with risk factors such as smoking, obesity, or diabetes. These difficult-to-fuse patients comprise about half of the total spinal fusion patient population.

Adjunct therapies, such as electrical stimulation, and growth factors (GFs) like bone morphogenic proteins (BMPs), have been found to significantly increase fusion rates, however both of these methods have issues. Internal electrical stimulation requires extra implanted instrumentation and longer surgery times. External electrical stimulation relies heavily on patient compliance for months after surgery. Use of BMPs (most of which is off-label) has recently been shown to cause severe issues in some patients due to ectopic bone formation. These adjunct therapies both add around $5,000 per level of surgery to the already expensive spinal fusion surgery healthcare costs.

Due to these issues, a device that shows considerable improvement over the current standards could greatly improve results for patients, as well as fill a hole in the market. Recognizing this, research has begun on an implant that will not only improve the rate of fusion, but also minimize the problems that hold back current techniques. The device is a piezoelectric fusion cage, which will generate electricity as it is compressed between the vertebrae during normal activities. Just like a fusion cage normally used in a lumbar interbody fusion, the piezoelectric fusion cage will provide a measure of immediate stability to the spinal segment. As the implant is stressed, however, it will also generate an electrical potential that can be delivered to the vertebrae, stimulating bone growth to fuse the segment. The implant will be primarily made of a piezoelectric composite in order to overcome the brittle nature of most piezoelectric materials.

II. Background and Significance

Lumbar Spine Anatomy

In humans, the vertebral column, or spine, is located in the posterior section of the upper body, and is divided into four primary segments including the cervical, thoracic, lumbar, and sacrum sections (7) (Figure 1).

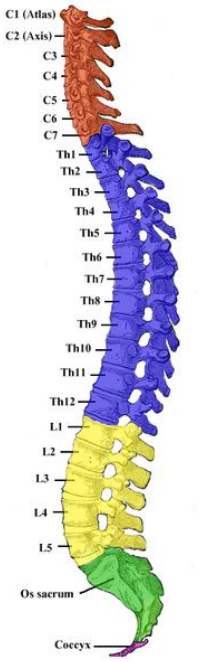

Figure 1. The different sections of the human vertebral column (Public Domain)

The cervical, thoracic, and lumbar sections are made of articulating vertebrae, each separated by a pad of fibrous cartilage, known as an intervertebral disc. The sacrum, however, is made of vertebrae that have been fused together. The cervical section is made of seven vertebrae and runs from the head to the base of the neck. The 12 thoracic vertebrae are immediately inferior to the cervical spine and are connected to the ribs. The lumbar spine has five vertebrae, is immediately below the thoracic spine, and supports much of the weight of the upper body (7). The primary functions of the spine are to provide support for the body and protect the spinal cord, which runs through the vertebral

foramen, or spinal canal. In this thesis, the primary focus will be on the lumbar spine, where the majority of back pain occurs (7, 8).

The majority of vertebrae share many characteristics. A vertebra can be divided into two sections: the vertebral body, and the vertebral arch, which is posterior to the vertebral body. The vertebral arch typically consists of two pedicles, two laminae, and seven processes (Figure 2). The intervertebral disc rests between the vertebral bodies of adjacent vertebrae. The majority of the upper body's weight is transferred through the vertebral body and intervertebral disc (7).

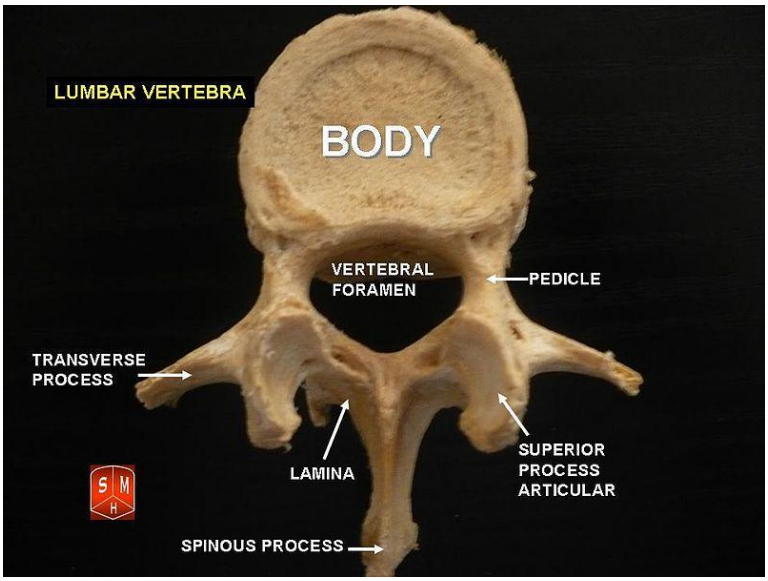

Figure 2. A typical lumbar vertebrae (Public Domain)

The lumbar vertebrae are larger than other vertebrae and carry more weight than any other section of the spine (7). Because of this, the lumbar segment is the most likely segment to have a compression injury to the vertebrae or intervertebral discs (7). The lumbar vertebrae do not connect to any ribs and allow a large degree of flexion and extension (forward and backward bending), moderate lateral bending, and a small amount of torsion.

Lower Back Pain

Back pain is the second most common neurological disease; only headaches occur more often (1). Most back pain is known as acute back pain and can last days to weeks. This type of back pain does not require surgery. If the back pain persists, however, it can become chronic and require surgery. The majority of back pain occurs in the lower back (8). In fact, low back pain is the most common cause of job-related disability in the United States (1). Over $50 billion is spent each year in the US alone for treatment (1).

There are many possible causes of lower back pain. The most common cause is a rupture or tear in an intervertebral disc, known as a herniated disc (7). Some other major causes of low back pain include degenerative disc disease, spinal stenosis, scoliosis, spondylolisthesis, trauma, and tumors (9).

Lumbar Fusions

The primary surgical procedure to relieve lower back pain is known as a lumbar interbody fusion. This procedure helps decrease lower back pain by stabilizing the symptomatic spine segment (10). The number of spinal fusions have increased dramatically over the last few decades (11), totaling over 432,500 in 2009 (12). Each spinal fusion costs the hospital an average of $26,000 in total health care costs (12).

Procedure

During a spinal fusion, the intervertebral disc between the vertebrae is removed and bone is grown between the vertebrae, literally fusing the vertebrae together. A cage is inserted into the intervertebral space to help stabilize the spine and maintain the correct distance between vertebrae while this occurs. Often posterior elements are added to help stabilize the spine, but much of the body weight is still transferred through the cage.

Most spinal fusions are also augmented with autograft (pieces of the patient's own tissue), which serves to improve fusion rates. Autografts are often taken from the patient's iliac crest or lamina and are packed into the intervertebral space in and around the fusion cage. Allograft tissue, which is taken from another person, can also be used, but autograft is preferable because there are no histocompatibility or immunogenic reactions (13) and it has been shown to have better fusion rates (14, 15).

There are several different surgical methods for completing lumbar interbody fusions; the primary ones including:

- Posterior Lumbar Interbody Fusions (PLIF)
- Transforaminal Lumbar Interbody Fusions (TLIF)
- Anterior Lumbar Interbody Fusions (ALIF)
- Extreme Lateral Interbody Fusions (XLIF)

For PLIF procedures, a 3-6 inch incision is made in the patient's back, the spinal muscles are retracted, and the lamina is removed. The surgeon is then able to remove the intervertebral disc and stabilize the spinal segment with fusion cages placed in the intervertebral space and posterior instrumentation.

TLIF procedures are similar to PLIF procedures. The main difference is that the incision in TLIF procedures occurs slightly more lateral to the spinal canal. This generally allows for a less traumatic experience for the spine (16).

ALIF procedures are done from the anterior of the patient rather than from the posterior, like the PLIF and TLIF techniques. For ALIF, an incision is made in the patient's lower abdomen and the disc is removed from the anterior side of the spine. The fusion cage is then placed in the intervertebral space.

This procedure avoids possible injury to nerve roots and provides the surgeon greater room to work on the disc space (10).

The XLIF procedure is a relatively new approach to spinal fusion. This is a minimally invasive technique that accesses the intervertebral space using a lateral incision, which avoids damage to the major back muscles.

Fusion Cages

Fusion cages are the one of the most vital instruments used in interbody fusions. A cage's primary role is to provide immediate stability to the spinal segment undergoing fusion (10, 17). In doing so, it provides support for the anterior column of the vertebrae, where the spine carries the greatest load (7). It also helps provide adequate intervertebral foramen distraction, preventing the vertebrae from pinching nerves and causing more pain (17). Lastly, it allows the annulus fibers of the intervertebral disc to maintain tension (17). The majority of cages are designed to allow bone graft to be packed inside. They usually have holes on the superior and inferior surfaces to allow bone graft to grow through the implant and connect with the vertebral bodies (10).

There are many different types of cages, which vary mainly depending on the method of surgical implantation (Figure 3). In general, ALIF cages are larger than the others since there is less obstruction in the way of the intervertebral space. They are usually fairly circular with a hole in the middle for placement of an autograft. PLIF cages are the smallest, usually shaped like small rectangles with a rectangular hole in the middle. Often, more than one cage is used in each intervertebral space during this type of surgery. TLIF cages are slightly larger than the PLIF variety. They look similar to the PLIF cages, except they are curved rather than straight like rectangles. Only one is used per level of the surgery. XLIF cages are larger than TLIF and PLIF cages and are rectangular with a large hole in the

middle. Only one cage is used per level. The top and bottom of the ALIF and TLIF cages are usually convex, while the PLIF and XLIF cages are normally flat.

Figure 3. From left to right: ALIF cage, PLIF cage, and TLIF cage

Other types of fusion cages exist, including threaded fusion cages and stand-alone cages that actually screw into the vertebral endplates. For the initial prototype, however, the focus shall be on the ALIF, PLIF, TLIF, and XLIF cages since they allow for the use of thicker composites and do not damage the endplates.

Complications associated with fusion cages are rare. Most cage failures occur due to difficulties during implantation or poor patient selection, rather than a mechanical problem with the cage itself (18). In the past, bone graft-only ALIFs and PLIFs have been attempted, but these showed a significant incidence of collapse and pseudoarthrosis, or failure to fuse (18). Overall, the benefits of fusion cages vastly outweigh any drawbacks.

Problems with Lumbar Fusions

Lumbar fusions are far from perfect surgeries. Failure to fuse is known as a nonunion or a pseudoarthrosis (19), and occurs in 10-15% of all patients (2-5). Assuming an 85% success rate, this means there are approximately 65,000 nonunions every year. Many risk factors can dramatically increase the rate of pseudoarthrosis. Patients such as those with a history of smoking, are obese, have diabetes, have osteoporosis, have a past history of failed fusion, have a multilevel fusion, or take certain medications have a significantly lower rate of success with the fusion (19). Patients with any of these qualifications are considered part of the difficult-to-fuse population. Failure rates in the difficult-to-fuse population can rise as high as 46% (6, 19).

Current Solutions to Low Fusion Rates

Efforts have been made to address the large number of unsuccessful fusions using electrical stimulation and growth factors (GFs). Both methods have shown promising results, but still leave room for improvement.

Growth Factors

Currently, GFs are used more often than electrical stimulation to increase the rate of spinal fusions. The type of GF used to stimulate bone growth comes from the group of GFs known as bone morphogenetic proteins (BMPs). Fourteen different BMPs have been discovered, but much of the research has been focused on BMP-2, -6, -7, -9, and -14 (20). Recombinant BMP-2 (rhBMP-2) is the primary GF used for spinal fusions and goes by the product name INFUSE® Bone Graft by Medtronic. When used instead of autograft, INFUSE® has shown equal or better fusion rates (21, 22), although the clinical application of BMP requires implantation of a high initial amount of the GF to retain desired levels through the therapeutic time period (19).

Problems with Growth Factors

There have been many problems associated with the application of a single GF to improve bone remodeling. Each BMP has its own functions and is not interchangeable, so the application of a single BMP requires recruitment of cells and other GFs to successfully remodel bone (19). Short residence time of the GF, prolific ectopic bone formation (bone forming in abnormal sites), and antibody formation against the GF have all been reported clinically (19, 23). In some cases, local soft tissue edema and bone resorption have also been found to occur (20, 23). Ectopic bone formation is particularly troublesome. Too much excess bone growth could easily cause pinched nerves, causing pain in the lower back, and defeating the purpose of the lumbar fusion.

INFUSE® in particular has some drawbacks. It is quite expensive, costing hospitals $5000 to $6000 per level of fusion (23). Also, INFUSE® is only approved for ALIFs, although it is predominantly used "off-label" for other spinal fusions (23). Insurance companies are increasingly not reimbursing for "off-label" use of INFUSE® (23). Moreover, within the last year, there has been a major controversy surrounding INSFUSE®. In July 2011, The Spine Journal dedicated its entire issue to a review of previous research on INFUSE®. They found that there was a systemic failure to report serious complications with INFUSE® and BMP-2. The new research found complication rates that were 10 to 50 times greater than those previously reported (13).

Electrical Stimulation

The current backlash against INFUSE® leaves the door open for the other main method of improving spinal fusion: electrical stimulation. Electrical stimulation was first shown to improve the fusion rate of both anterior and posterior fusions in 1974 (24). Even though bone formed by electrical stimulation has shown an increased growth rate, it still exhibits the same properties as normal bone (25).

The three types of electrical stimulation include direct current electrical stimulation (DC), capacitive coupling (CC), and inductive coupling (IC) (24). IC includes two variations: pulsed electromagnetic fields (PEMF) and combined magnetic fields (CMF). Although each method of electrical stimulation works through a slightly different mechanism, there are many similarities. Each delivers a negative electrical potential to the fusion, which promotes bone growth (19, 26). They also remove the positive electrical potential from the area since it has been found to resorb bone (19, 26).

Direct Current Electrical Stimulation

DC electrical stimulation, which is the most similar form of stimulation to the new piezoelectric implant, has been shown to be the most successful form of electrical stimulation (19). For DC stimulation, a power supply consisting of a battery and circuitry is encapsulated and placed in soft tissue during a spinal fusion. The power supply is then connected by insulated wires to two cathodes that deliver current to the vertebrae (24) (Figure 4). The cathodes deliver a negative potential to the fusion area, while the power supply acts as an anode, delivering a positive potential to the soft tissue (19). The power supply is placed 8 to 10 cm away from cathodes (24) in the soft tissue which serves to ground the implant and prevents the positive potential from causing bone resorption. The cathodes are placed in the lateral gutters touching the transverse processes to allow as much contact as possible with viable bone (24). Bone graft is placed around the fusion mass, completely covering the area of fusion (24). The bone graft acts as an insulator, preventing charge from transferring to any implanted fixation devices.

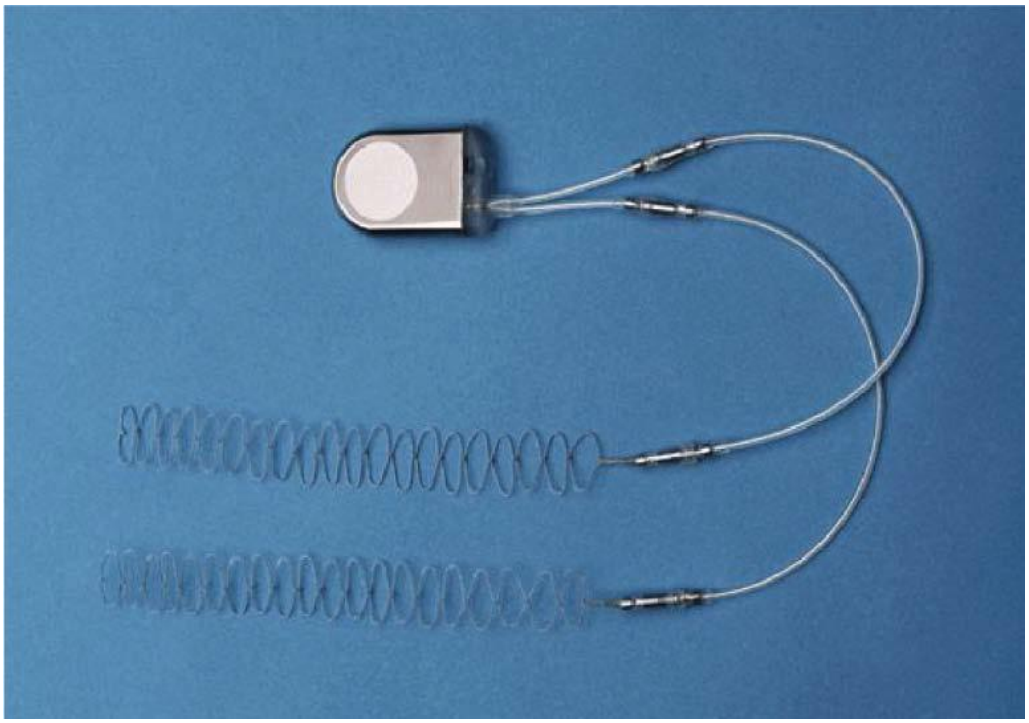

Figure 4. A direct current electrical stimulator device developed by Biomet (Image reprinted with permission of Springer ©)

Commercially available DC stimulators use titanium cathodes, which have generated successful results (26). In studies, DC power supplies deliver a constant current of 5-100 μA (24, 26-28), which generates an electric field extending 5-8 mm from the cathodes (19). One study showed that the fastest rate of growth and the strongest bone occurred at 100 μA, where 100 μA was the highest current delivered (28). Commercially, DC stimulators can deliver 60 μA or 40 μA to tissue resistances ranging from 0 to 40 kΩ (29). The DC stimulator remains functional for 6 to 9 months (24, 28). To stimulate the bone at 60 μA for 6 months, a large $LiMnO_2$ button cell battery 24.5 mm in diameter and 3 mm thick is used (29).

The value for current is vital to bone growth, but current density is what actually determines the rate of bone growth. The therapeutic window for current density is believed to range from 1 $\mu A/cm^2$ to approximately 150 $\mu A/cm^2$ (30). The current density delivered by commercially available DC devices is around 25 $\mu A/cm^2$ (29, 31). This is the primary target value for the piezoelectric implant.

DC electrical stimulation works primarily through two mechanisms: electric field effects and Faradic reactions (24). The electric fields generated through DC stimulation have been shown to up-regulate mRNA for bone growth stimulating GFs BMP-2, -6, and -7 (19, 26, 32), as well as TGF-ß (32). The amount that each GF is up-regulated fluctuates throughout the fusion process (32). This process is much more similar to natural bone growth (19, 32), unlike the brute-force method of overloading a single GF.

Faradic reactions also help to increase bone growth. Faradic reactions are chemical reactions that occur at the cathode-bone graft interface (24, 26, 32) and are represented by Equation 1.

$$O_2 + 2H_2O + 4e^- \rightarrow 4OH^- \quad (1)$$

Through this reaction, oxygen concentration is lowered, pH is increased, and hydrogen peroxide is produced (19, 26, 32), each of which stimulate bone growth. A decrease in oxygen content has been shown to increases osteoblastic activity, while an increase in pH increases osteoblastic activity and decreases osteoclastic activity (19, 32). At its most basic, osteoclasts remove bone and osteoblasts add bone, meaning both changes cause an increase in local bone growth. Hydrogen peroxide works through a different mechanism. It stimulates macrophages to release VEGF, an angiogenic GF (19). VEGF facilitates the growth of new blood vessels from existing ones, which is crucial to bone healing (19). Both mechanisms, electric field effects and Faradic reactions, also act together and separately to stimulate calcium intake (24).

DC stimulation has shown impressive results when applied to spinal fusions. Numerous studies show a dramatic increase in successful fusions, especially in the difficult-to-fuse population. Studies with patients undergoing posterolateral fusions with the addition of DC stimulation showed success rates ranging from 81%-95% compared to 54%-81% with autograft alone (6, 33-36). The difficult-to-fuse population, which has shown fusion success rates ranging from 54%-71% (6, 33, 34), has even shown over a 90% radiographic fusion success (19). DC also shows success in the long-term. In a ten-year follow

up study on patients who had DC stimulation, 100% showed successful fusion and no complications with the power supply or cathodes occurred (37).

Inductive Coupling

The other methods of electrical stimulation differ from DC in that they affect the fusion from outside the body, rather than as an implantable device. The devices used are not inserted during surgery, but rely heavily on patient compliance post-surgery.

There are two methods of inductive coupling: PEMF and CMF. In the operating room, the procedure is the same as a normal spinal fusion. After the surgery, however, one or two external coils are worn that generate an electromagnetic field and stimulate bone growth (24) (Figure 5). These coils must be worn for 3 to 8 hours a day for 3 to 6 months (24). The magnetic field generated by the coils is delivered in repetitive pulsed bursts or single pulsed signals (26).

Figure 5. EBI Bone Healing System- an IC device. The coil on the right is worn around the waist and delivers pulsed electromagnetic fields to the body. (Image reprinted with permission of Springer ©)

The mechanism for PEMF is less well understood than DC (24). The pulsed electrical field has been shown to up-regulate BMP-2 and TGF-ß1 (26), similar to DC. PEMF also causes calcium ions to be released from intracellular stores, which leads to increased cell proliferation (19).

CMF is similar to PEMF except that the time varying magnetic field is superimposed on a static magnetic field (24, 26). The device has to be worn for 30 minutes a day for up to nine months (24) Just like PEMF, CMF causes calcium ions to be released from intracellular stores, leading to increased cell proliferation (19). Unlike PEMF, though, CMF is found to increase IGF-II, which may help mediate the increase in bone cell proliferation (19). Overall, for similar treatment times the bone fusion rates remain similar for PEMF and CMF (24).

Capacitive Coupling

CC is another method of electrical stimulation that utilizes an external source for the electricity. Just like the IC methods, no change to the normal spinal fusion procedure is necessary. The electrical stimulation is implemented in the months following the surgery. Instead of using external coils like the IC methods, CC uses small electrodes that are attached to the surface of the skin over the fusion area (24, 28) (Figure 6). The electrodes are less obtrusive than the coils of the IC methods, but must be worn 24 hours a day for 6 to 9 months (28).

Figure 6. OrthoPak Capacitive Coupling Device (Image reprinted with permission of Springer ©)

CC has been shown to stimulate bone growth by up-regulating mRNA for BMP-2, -4, -6, and -7, TGF –ß, FGF-2, and VEGF (19). Like both methods of IC, CC causes an increase in intracellular calcium ions, leading to increased cell proliferation (19); however, CC utilizes a process that is much more effective than IC. CC opens voltage-gated channels, allowing calcium ions to enter the cells from the extracellular matrix (ECM). The amount of calcium ions in the ECM is infinite compared to the amount in intracellular stores, which some have hypothesized is the reason CC has shown improved results over IC (19).

Electrical Stimulation Summary

Although it is currently not as frequently used as INFUSE®, electrical stimulation has shown promise in spinal fusions. Electrical stimulation does not have the challenges presented by delivery of a single GF because they up-regulate the natural physiological expression of the GFs (19, 32).

There are several methods of electrical stimulation, but some have shown better results than others. Current clinical and science data establishes DC as superior to IC and CC, especially when used

during posterior spinal fusions (19, 21, 24). CC is not as successful as DC, but does show clinical superiority over IC (19, 24).

Electrical Stimulation Problems

Even though electrical stimulation, especially DC, has shown to be effective in improving spinal fusion rates, there are still some major problems holding it back.

For DC stimulation, battery placement takes 10-15 minutes, requires a second surgical site, and lengthens the time the patient is under anesthesia (28) It is not feasible to place a battery of the size needed between the vertebrae, so it requires extra instrumentation outside of the intervertebral space. The manufacturer also suggests the battery be removed in six months, requiring a second surgery (28). This surgery, however, is not as invasive and only requires local anesthesia. The extra equipment for DC stimulation is expensive, around $6,500 per surgery (38), roughly the same price as one level of INFUSE®.

IC and CC are not as successful as DC and for both of them, patient compliance is essential. Patient compliance has been a big issue for these methods. The coils used in IC are obtrusive and it is often difficult to ensure that the patient will continue wearing the device as much as prescribed (39). The electrodes used in CC are less obtrusive, but must be worn for 24 hours a day. The electrodes must also be replaced periodically (24).

III. The Piezoelectric Implant

From this information, it can be seen that there is room for improvement in the spinal fusion market. For such a common surgery, success rates are low; the current electrical stimulation and GF methods have been shown to significantly increase these success rates, but are each stymied by their own problems. An implant that improves upon these fusion rates, while at the same time minimizing many of the problems associated with current solutions, could be beneficial for the patient.

In order to improve upon existing treatments, it was necessary to create a device that would generate electricity without needing a large battery or outside stimulation to increase the rate of bone growth. From previous studies, it was clear that it would be best to deliver a current similar to DC, since it showed the best results of the electrical stimulation methods and did not have the ectopic bone formation issues of GFs. Another important factor in the implant design was to create an implant that would not require extra instrumentation. By doing this, surgery times would not increase and the increase in cost for the procedure would be minimized. The solution was to create a piezoelectric fusion cage, which would generate electricity as it was compressed between the vertebrae.

Piezoelectricity

At its most basic, a piezoelectric material is a material that generates charge when mechanically stressed. The opposite is also true. Piezoelectric materials can be used as actuators that strain when subjected to an electric field. When stressed, the electricity generated by the piezoelectric material spikes initially, but decreases quickly. Therefore, the piezoelectric material needs to be cyclically loaded to be utilized to its full potential.

Piezoelectric materials often have a crystalline structure, which can be represented by a periodic pattern created by identical, three-dimensional, microphysical structural units (40) (Figure 7).

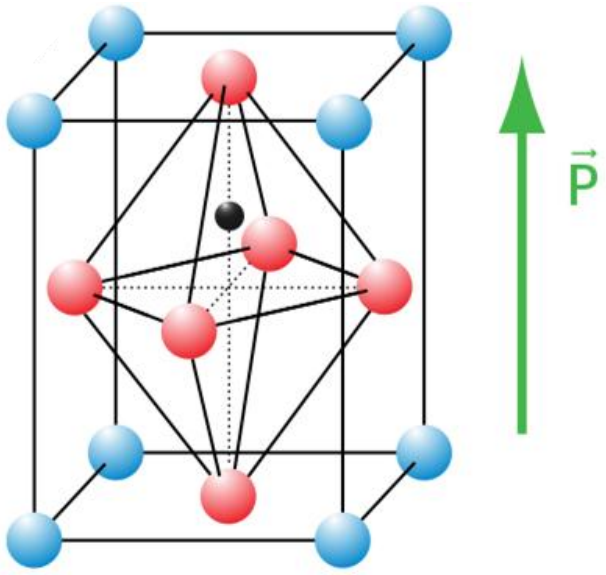

Figure 7. A typical piezoelectric structural unit. The non-symmetric location of the central atom causes the unit to have a piezoelectric dipole moment in the direction of the green arrow. (Public Domain)

The piezoelectric effect greatly depends on the symmetry of this crystal. If the crystal is sufficiently non-symmetric, it has a piezoelectric dipole moment and the application of stress will cause it to electrically polarize (40). For the bulk material to generate a net piezoelectric effect, the piezoelectric dipole moment of each crystal must be relatively aligned.

Piezoelectric materials have dielectric properties, meaning they readily polarize in an applied electric field. This polarization is distinct from the polarization that occurs when the material is stressed and plays an important role in several manufacturing methods.

A common measure of piezoelectricity of a material is the piezoelectric coefficient, d_{ij}. The piezoelectric coefficient is a measure of the amount of charge density per applied mechanical stress to the material, the units of which simplify to C/N. The most common piezoelectric coefficient used to describe a material is d_{33}, which is measured when the material is stressed in the direction it is poled (Figure 8). Most piezoelectric materials have a d_{33} coefficient in the 10^{-12} C/N range.

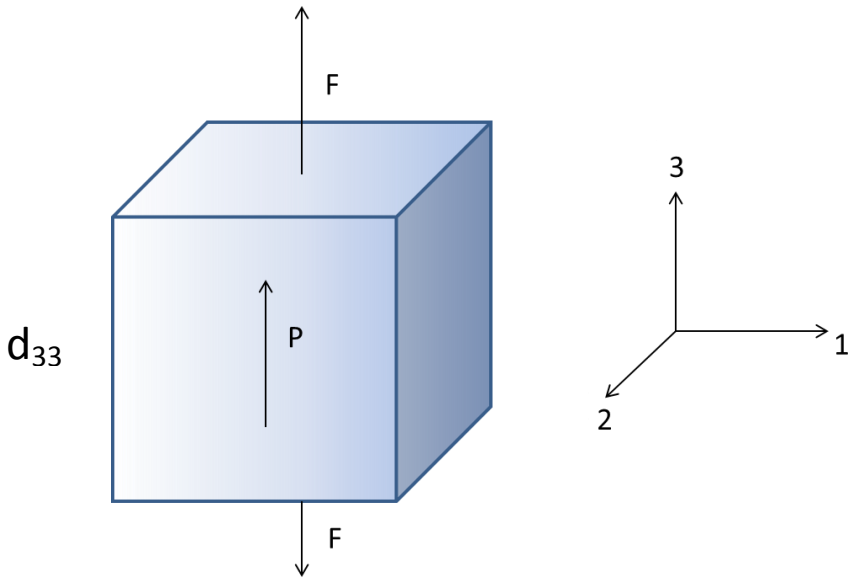

Figure 8. The piezoelectric charge coefficient d_{33} is expressed when a piezoelectric material is stressed in the direction it is poled. F is the force applied and P is the piezoelectric dipole moment.

Piezoelectric materials also have a property known as the Curie temperature, above which the material loses its piezoelectric properties. When the material drops back below the Curie temperature, the particles of the material regain their piezoelectric properties, although the dipole moment of each particle is facing a random direction. This is important because the manufacturing of the implant could eventually involve high temperature processes, depending on the materials used.

Piezoelectricity of Bone

Piezoelectric materials exist in nature, as well. In fact, dry bone itself is piezoelectric. When bone is put in compression, an electronegative potential is formed which triggers bone formation (26). In tension, however, an electropositive potential is formed which causes bone resorption (26). The piezoelectric effect is generated in bone's extracellular matrix, not the living cells (41). At rest, bone potentials can range from .1 to 10 mV (42). This number increases to 20 mV during ordinary physical activity and can reach negative potentials as high as 100 mV during compression (42).

Problems with Current Piezoelectric Materials

Although piezoelectric materials have been around for decades, to this point, they have found limited commercial use inside the body. Part of the reason for this stems from the issue that piezoelectric materials tend to have poor source properties for generating power, including high voltage, low current, and high impedance (43). The majority of piezoelectric materials are ceramics, many of which are lead based. Many of these materials have serious biocompatibility issues, although some, like $BaTiO_3$, are considered fairly safe and have found use in the body. The chief concern about ceramics, however, is their low toughness. Ceramics are brittle structures, so a spike in stress or manufacturing defect could cause a catastrophic failure, which is unacceptable in the body. Piezoelectric polymers also exist, but exhibit much lower piezoelectric properties than piezoceramics and practical applications are rather limited (44).

Piezoelectric Composites

To overcome these issues, a piezoelectric composite has been developed. Composites are made of a combination of two or more materials that can be used when the properties of a single material are insufficient to meet the needs of the application (45). For the composite used in the implant, a polymer matrix will be embedded with a dispersion of piezoelectric particles. The polymer matrix will provide a structural stability, while ceramic particles will provide piezoelectricity. When in bulk form, the particle material would be brittle, but with the support of the polymer matrix, there is much lower chance of material failure.

Piezoelectric composites consist of a combination of materials: a piezoelectric ceramic to provide electricity when stressed and a polymer to provide structural integrity. These composites exhibit high piezoelectric coefficients partially due to a low dielectric permittivity of the polymeric matrix (46). Depending on the way the ceramic is distributed within the polymer, the piezoelectric properties can be

greatly varied (46). The polymeric matrix also provides improved damping and resistance to mechanical shock, compared to brittle piezoelectric ceramics. Piezoelectric polymers offer some of the same mechanical benefits as the composites, but have low Curie temperatures, giving them a strong dependence on temperature (46).

All piezoelectric composites consisting of piezoelectric particles must be poled during manufacturing for the composite to actually exhibit piezoelectric properties. When the particles are originally mixed into the still-liquid polymer mixture, there is no specific piezoelectric dipole orientation. The dipoles will be randomly oriented causing them to cancel each other out. Current methods involve poling the material by passing an electric field over it after the material solidifies, causing the random orientation of dipoles to align in the direction of the field. The resulting composite is an anisotropic material, which displays piezoelectric properties in the direction the electric field was applied.

0-3 Composites

Several different forms of these composites exist. One of the easiest piezoelectric composites to mass produce is known as a 0-3 composite (46). This composite consists of a random distribution of unconnected piezoelectric particles dispersed throughout a continuous polymeric matrix (46) (Figure 9).

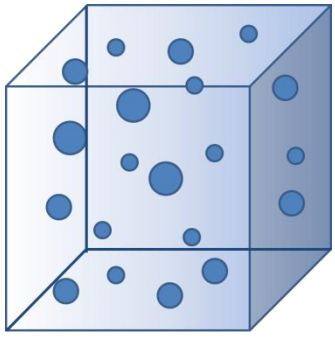

Figure 9. Example of a 0-3 Composite

0-3 composites are relatively easy to manufacture. The manufacturing process basically involves mixing an appropriate amount of particles into a liquid matrix and allowing the matrix to cure. After it

cures, the piezoelectric dipole moments of the particles are randomly oriented. In order for the composite to generate a net piezoelectric effect, it must then be poled to orient the dipole moments in the same direction. Even after poling, 0-3 composites have relatively low piezoelectric properties, especially at low volume fractions (Figure 11). As the volume fraction increases, however, the piezoelectric properties increase.

1-3 Composites

Another type of piezoelectric composite is known as a 1-3 composite. In 1-3 composites, the particles have connectivity in a single direction, forming chains through the continuous matrix material (Figure 10).

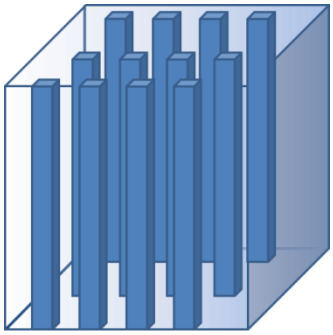

Figure 10. Idealized example of a 1-3 Composite

Composites of this structure exhibit orthotropic behavior and generally have much greater piezoelectric properties in the aligned direction than 0-3 composites (47). This is especially true at low volume fractions (Figure 11, 12). In 1-3 composites, the charge generated by the particles can travel particle to particle, whereas the charge in a 0-3 composite must travel through the resistive matrix to reach neighboring particles. For 0-3 composites with higher volume fractions, the particles are packed much closer together, making it easier for the charge to travel through the composite. This causes the structure of the composite to make less of a difference. As Figure 11 shows, the d_{33} coefficient for both 1-3 and 0-3 composites becomes similar, even at volume fractions as low as 60%. Dielectric constant

shows a fairly consistent increase for both 0-3 and 1-3 composites as volume fraction increases (Figure 12).

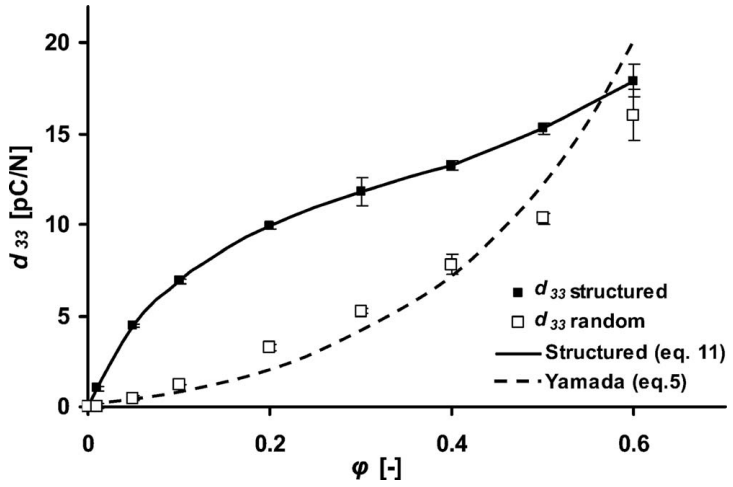

Figure 11. Piezoelectric charge coefficient (d_{33}) vs. Volume fraction (φ). PZT particles were used in an Epotek 302-3M matrix. Structured composite is 1-3; unstructured is 0-3. (Image reprinted with permission of American Institute of Physics ©)

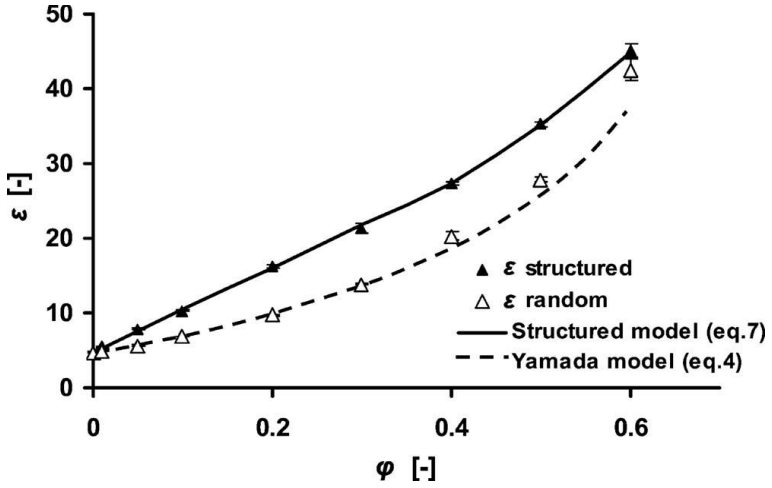

Figure 12. Dielectric constant (ε) vs. Volume fraction (φ). PZT particles were used in an Epotek 302-3M matrix. Structured composite is 1-3; unstructured is 0-3. (Image reprinted with permission of American Institute of Physics ©)

New research shows that greater piezoelectric properties of 1-3 composites can be created by using piezoelectric fibers instead of spherical particles (48). In one study, a 20% volume fraction of PZT

fibers in a Polyurethane matrix generated a d_{33} value of 350 pC/N (Figure 13), which is even higher than most piezoceramics. For comparison, a 20% volume fraction of PZT spherical particles in an epoxy matrix only had a d_{33} of 10 pC/N. To this point, spherical particles have been used in the research for the piezoelectric implant, but switching to fibers could be a logical next step to increase the electrical outputs of the composite.

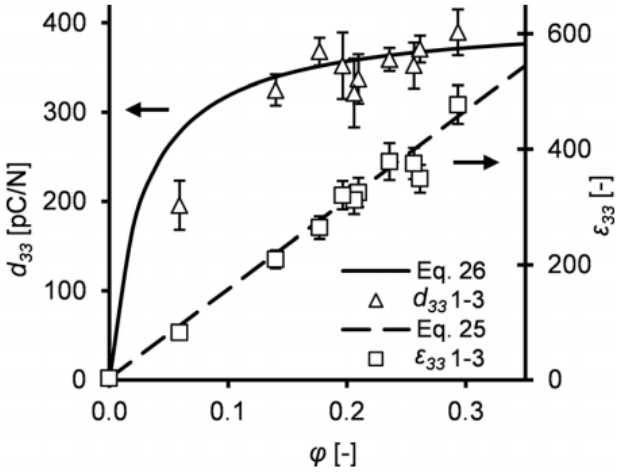

Figure 13. d_{33} and dielectric constants vs. volume fraction of 1-3 composites using PZT fibers in a Polyurethane matrix (Image reprinted with permission of American Institute of Physics ©)

Several methods exist for creating 1-3 composites. One manufacturing technique includes cutting a horizontal grid into the polymer and filling it with piezoelectric rods (46). Another involves covering parallel piezoelectric rods with a liquid pre-polymer, which would then harden (46) . An additional method involves threading piezoelectric fibers through a honeycomb support (49). These methods, however, are costly, time consuming, and labor intensive. More recently, a method for creating 1-3 composites using piezoelectric particles known as dielectrophoresis (DEP) has been developed, which simplifies manufacturing.

Dielectrophoresis (DEP)

In DEP, piezoelectric particles are mixed into a liquid pre-polymer. As the polymer begins to solidify, an AC field is passed over the composite. This causes the particles to polarize and exhibit a mutually attractive force as the particle's polarity switches back and forth in phase with the electric field (46, 50). To prevent the particles from migrating toward one of the poles, an AC field, rather than a DC field, must be used. As the frequency of the AC field is increased, the dipole-dipole interactions of the molecules begin to dominate other forces (50) and begin to attract and repel each other. The strength of these interactions is known to depend on the dielectric permittivities of the particles and pre-polymer, as well as the difference between them (46). Under suitable conditions, the particles will be drawn together by the dipole interactions and begin to line up in chains or columns parallel to the field (46, 50). When the polymer solidifies, these particles are locked in place forming a 1-3 composite (Figure 14).

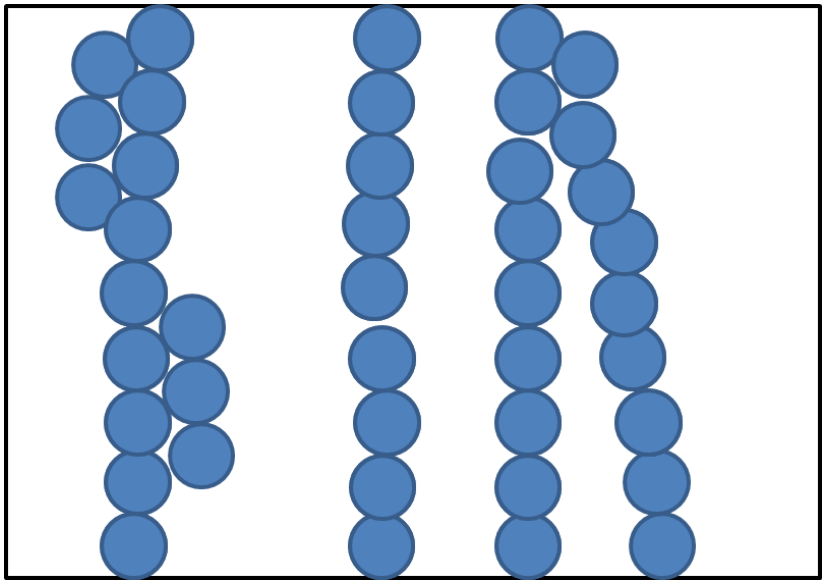

Figure 14. Typical DEP 1-3 composite structure. This model shows chain formation in the direction of the electric field. Some chains will begin to form thicker columns as other particles and chains join.

The electric fields (≈1 kV/mm) used in DEP are high enough to cause the particles to polarize with respect to the field, but not high enough to cause a change in the piezoelectric dipole moment.

Because of this, DEP only causes translation of the particles, not rotation and creates a chain aligned composite that is not poled (Figure 15a).

The composite must still be poled after solidification because although DEP aligns all the particles in parallel chains, the dipole of each individual particle faces a random direction. If a material created through DEP was not poled, when the material was compressed the electricity generated by each individual dipole would cancel each other out on average. Poling uses extremely high electric fields, around 10 kV/mm, to actually change the crystalline structure of the particles, which serves to align the piezoelectric dipole moments with the field. Poling causes the piezoelectric dipoles of the particles to align in the same direction, greatly increasing the piezoelectric properties of the composite in that direction.

DEP has some major limitations, however. The size and shape of current piezoelectric structures is greatly limited by the electric fields required for the poling process. To avoid the electricity shorting through the material, this limits the choices of materials to those with high dielectric constants. Even using these materials, the electric field required for poling is high enough that composites can only be made a few millimeters thick.

Even with its limitations, DEP can be used as the safe route for the piezoelectric spinal implant since it is a proven method for manufacturing piezoelectric composites (51-53). Design features that enable use of DEP manufacturing are described in Chapter V in the Piezoelectric Composite section.

Piezoelectrophoresis

Piezoelectrophoresis (PEP) is a novel manufacturing method for piezoelectric composites that is currently in development. PEP will address the primary limitations of DEP and allow for the creation of large, tough, piezoelectric composite materials. With PEP, there will be no need for the extremely high electric fields of the final poling step that significantly hinders DEP.

PEP revolves around the application of hydrostatic pressure to a piezoelectric composite through compression of the material as the polymer solidifies. The compression of the material will cause the piezoelectric particles to polarize in the direction of their piezoelectric dipole moment. Similar to DEP, these electric potentials will interact with those of surrounding particles, forming chains. Since the piezoelectric dipole moments of each particle could be facing any direction, these chains would therefore be randomly oriented. A 3-3 composite would be created, which would not display a strong net piezoelectric effect.

When the hydrostatic pressure is applied cyclically in phase with an externally applied AC field, however, the piezoelectric dipole moments can interact with the electric field. This causes a net torque on the particles, aligning the piezoelectric dipoles with the applied field, as seen in Figure 15b. Just as before, the interparticle forces then cause chain formation, but this time, it is aligned with the electric field. Thus, a 1-3 composite with a net piezoelectric behavior can be produced without the need to pole the material.

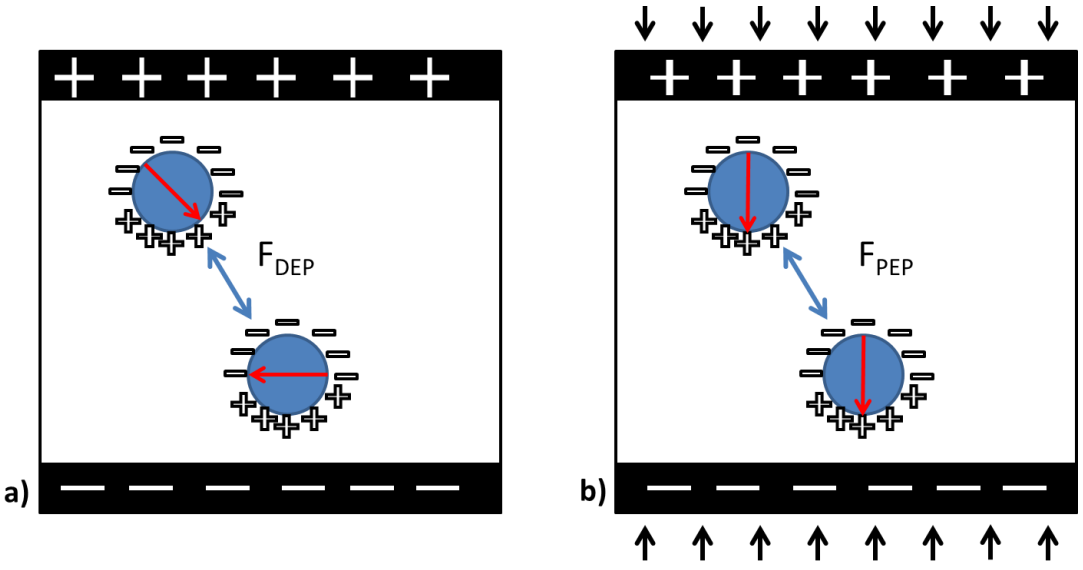

Figure 15. The interparticle forces on the still-liquid composite created by a) DEP and b) PEP. The red arrows are the piezoelectric dipole moments. The cyclical application of compression and electric field cause PEP to align the piezoelectric dipole moments of the particles, as well as align the particles themselves.

From theoretical models developed, the electric field necessary for this is over three orders of magnitude lower than that required for poling the composite in DEP, around 4 V/mm. Based on this, structures in excess of 2 m thick could theoretically be created.

IV. Specific Aims

The stages of the development and validation of the piezoelectric implant can be broken down into four sections:

- Development of Implant Design
- Power Analysis Using a Lumped Parameters Model
- Material Generation Research
- Proof of Concept Testing

The implant design and the power analysis are the primary focus of my master's thesis. These were used to drive the research and find trends that allow for the implant to generate a current density inside the therapeutic window. To help validate the theoretical analysis and implant design, preliminary data will be given for the material generation research and the proof of concept testing. At this point, the purpose of this data is not to strictly define the amount of current that can be generated, but to validate the theories generated by the implant design and theoretical power analysis.

The first stage was the development of the implant design. The piezoelectric composite will make up the majority of the implant, but it alone is not enough to deliver electricity to the fusion. A design for the implant was developed that utilizes the composite, as well as additional materials and circuitry to deliver a negative electric potential to the fusion area, while protecting the fusion from the positive electric potential.

The theoretical power analysis and material generation research occurred simultaneously and helped drive each other. The power analysis for piezoelectric composites was developed using a lumped parameters model based off of previous piezoceramic power generation models(54). Individual variables regarding material properties, shape of the implant, and the implant's environment were able to be isolated to determine each one's effect on power and current output.

Material generation research involved creating composite specimens through DEP and PEP, and is still ongoing. DEP was attempted first and has been successfully used to construct many structured composites. Recently, construction of composites using PEP has begun. PEP has yet to produce a poled piezoelectric composite, but refinements are still being made to the process. Some of the successfully poled DEP composites were then tested to analyze trends and compare with the power analysis results.

As a final proof of concept, tests were completed to see if one of the composites could partially recharge a battery. The piezoelectric composite underwent physiological loads and was successfully able to store energy on the battery.

V. Development of Implant Design

Basic Implant Design

The design of the implant revolves around the piezoelectric composite, but the composite alone is not enough to deliver electricity to the body. The overall implant design will include:

- The piezoelectric composite
- A rectifying circuit
- An insulated grounding wire
- An insulating layer
- A negative potential outer electrode

And possibly

- Storage circuitry

Piezoelectric Composite

There are two main layouts that will be examined for the piezoelectric composite: a layered composite and a thick composite.

Layered Composite

DEP has been identified as the safe route for the creation of the piezoelectric composite. It is already a proven manufacturing method (51-53), although it does have its limitations. Since the electric fields required to pole the material are extremely high, it would not be possible to create a composite of the necessary thickness for the implant. However, it could also be possible to create electrode configurations that allow for the creation of the entire layered composite at once (Figure 16).

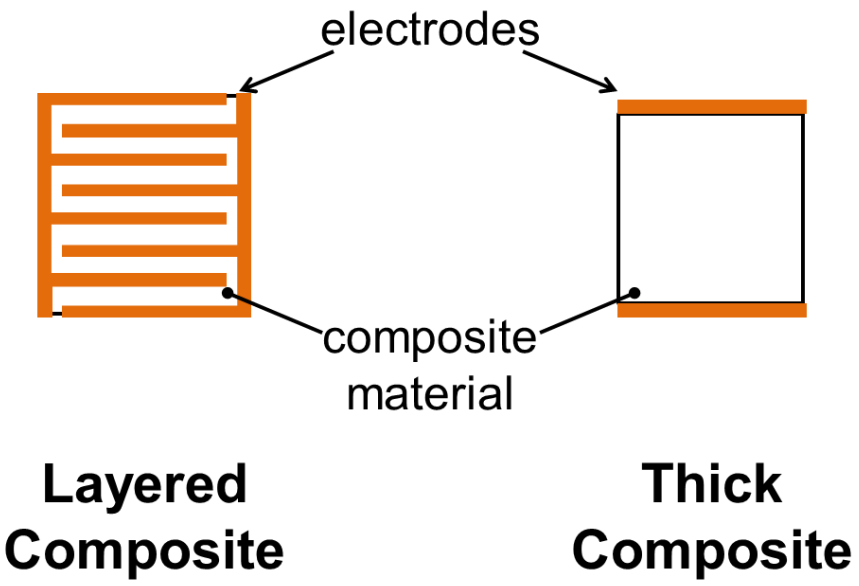

Figure 16. Layered composite vs. thick composite

This electrode configuration keeps the thickness of the composite between each pair of electrodes low enough that DEP could successfully be used to pole the material. In this configuration, the layers of the composite are mechanically in series, but electrically in parallel. For a simple prototype, it would be possible to create many small samples of the composite and layer them on top of each other to achieve the required thickness of the implant.

The layered approach does have some advantages over a single solid material. It can be accomplished using DEP, a method that has already been shown to work. Also, the peak power output for layered composites occurs at a lower resistance than for thick composites (43).

Thick Composite

If PEP is successful, a much thicker composite will be able to be produced. In this design, the composite is made of a single section with electrodes on each end. Should PEP prove successful, the thick composite would be much easier to manufacture, due to its simple design. In the lumped

parameter power generation analysis (Chapter VI), the effect of thickness on power and current generation will be determined.

Rectifying Circuit

Compression of the composite will generate electricity, but this electricity cannot be delivered straight to the patient. When the composite is compressed, it will generate an AC current, causing a negative potential at one end and a positive potential at the other, which will oscillate over time (Figure 17).

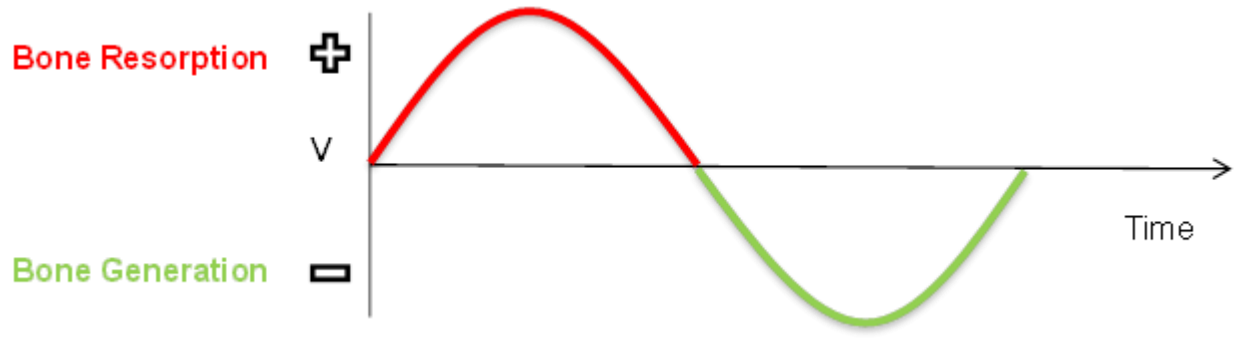

Figure 17. Unrectified output voltage

Since bone resorbs with a positive potential, some way must be found to remove it from the intervertebral space, while still delivering the negative, bone-growing potential to the fusion area. This cannot simply be done by exposing one electrode to the fusion area since the current delivered by the piezoelectric composite is AC and will oscillate between negative and positive.

The AC signal must therefore be converted into a DC signal that will have two outputs: one consistently positive and the other consistently negative. To accomplish this, a rectifying circuit will be used. A basic rectifying circuit is made of four diodes arranged as shown in Figure 18.

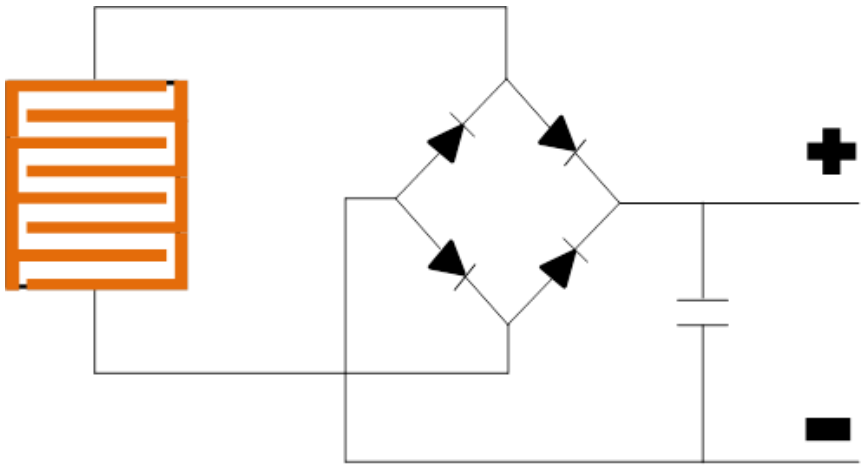

Figure 18. Composite with rectifying circuit

When the current at the top input to the rectifying circuit is positive and the bottom is negative, the current flows through the circuit as shown in Figure 19. When the opposite occurs, as in Figure 20, the sign of the DC output remains the same.

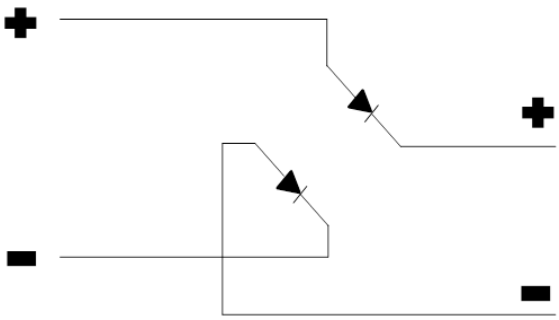

Figure 19. Rectifying circuit with positive input on top

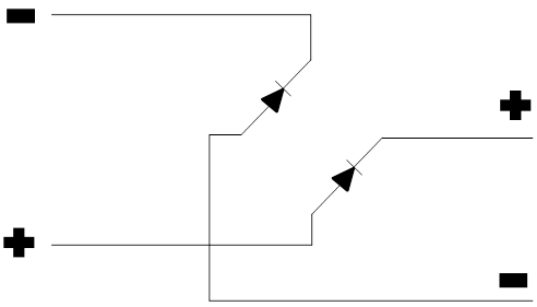

Figure 20. Rectifying circuit with positive input on bottom

This output, however, is not a steady DC current. Instead, the sign of the current remains constant, but the amplitude varies between its peak value and zero. To smooth the output, a capacitor can be added in parallel. This decreases the output voltage, but serves to smooth the final output (Figure 21).

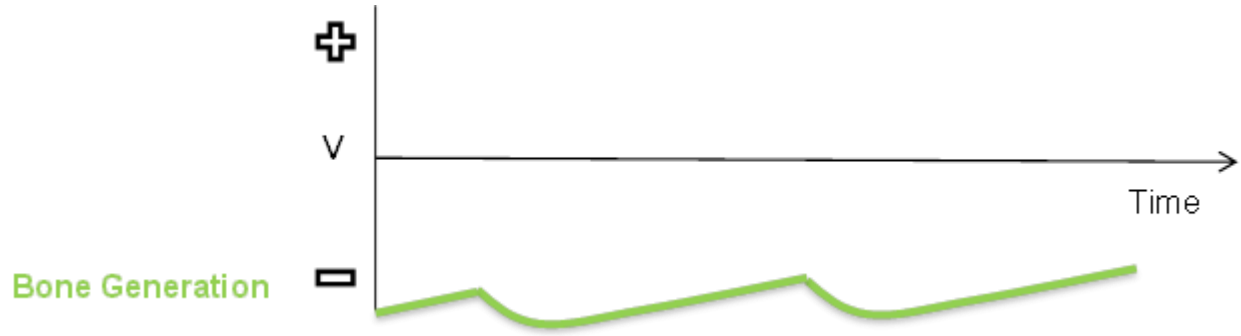

Figure 21. Rectifying circuit output voltage

Insulated Grounding Wire

The rectifying circuit will provide two output potentials: one constantly positive and the other constantly negative. Since the positive potential resorbs bone, it is necessary to protect the fusion area from it. To accomplish this, the positive wire leaving the rectifying circuit will be insulated and embedded in soft tissue outside of the intervertebral space. This effectively grounds the wire, allowing the positive charge to dissipate where it will cause no harm to the patient.

Insulating Layer

The electrodes on the piezoelectric composite must also be insulated to prevent a positive potential from affecting the fusion area. The whole implant will be covered in an insulating, biocompatible material, such as PEEK. Only the output wires from the rectifying circuit will be left uncovered.

Negative Potential Outer Electrode

The negative potential wire leaving the rectifying circuit will be attached to an outer electrode covering the insulating layer (Figure 22). The outer electrode does not necessarily cover the entire outer surface of the implant. Instead, the electrodes can be strategically located to provide stimulation to the parts of the fusion that will benefit most from the electrical stimulation. The primary electrode locations will be on the sides of the implant, so as to directly stimulate the autograft placed in and around the cage. The electrode will be made of titanium, which is used commercially for DC electrical stimulation (26). The overall area covered by the electrodes will be determined so as to deliver a current density of 25 $\mu A/cm^2$ to the fusion, which is the same as delivered by current DC electrical stimulation devices (29, 31).

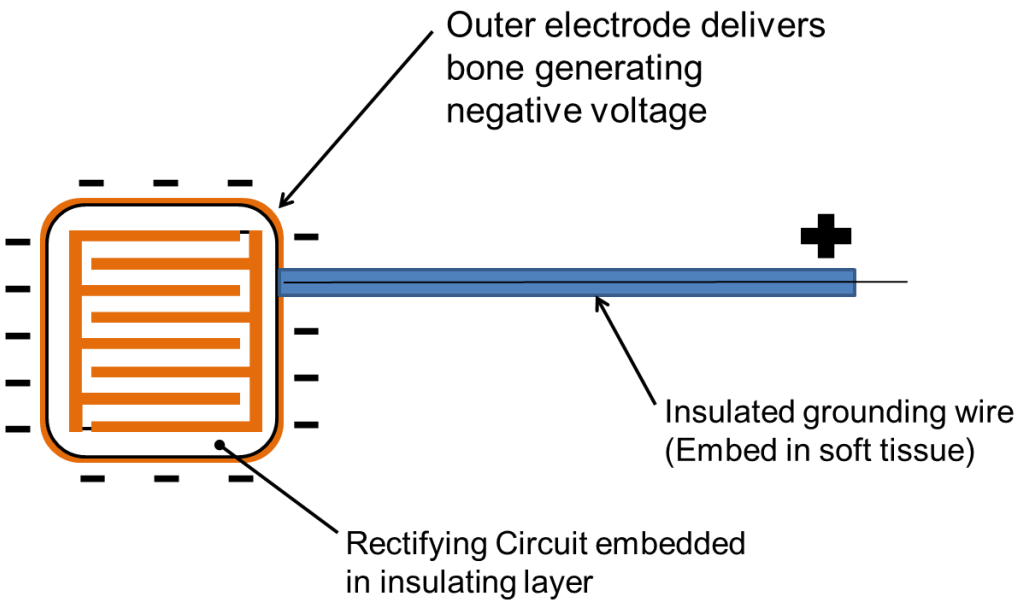

Figure 22. Overall implant design

Implant Geometry

The geometry will also be similar to that of the currently used fusion cages (Figure 3). Fusion cage shapes are similar between companies and complications are rare, so there is no need to

drastically change the geometry. It is also important that surgeons immediately feel comfortable with the piezoelectric implant. If the new cage is shaped similar to the previous implants, it should be easier for them to incorporate the piezoelectric implant into their surgical routine.

Delivery/Storage of the Generated Electricity

The design mentioned so far will be contained in each of the options listed. A small amount of current-limiting circuitry similar to what is already used in DC stimulators will also be included to ensure an appropriate amount of current density is delivered to the fusion.

Direct Stimulation of the bone

Ideally, the best option would be to deliver the current generated by the piezoelectric implant directly to the bone. In this case, the current generated would need to be great enough to be continuously delivered to the bone. Extra circuitry to store the energy, which would take up more room and could decrease efficiency, would not be necessary.

Store energy using a battery

If the piezoelectric element cannot continuously deliver enough power to the fusion, a storage circuit will need to be included. One option to store charge would be to use a small battery. A battery could be added to the circuit after the rectifying circuit (Figure 23).

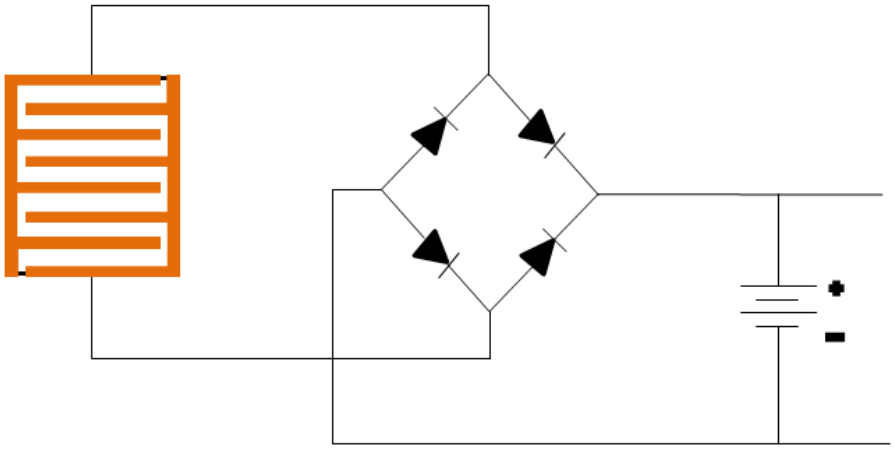

Figure 23. Composite, rectifying circuit, and battery setup

The rectifying circuit is still necessary in this design option because the battery needs a DC signal to constantly charge. The battery would deliver power to the fusion area and be recharged by the piezoelectric composite. To be feasible, the battery must be small. A rechargeable watch battery, for example, could be added to the implant without taking up a great amount of room.

The primary factor that determines the charge time for a rechargeable battery is the amount of current supplied to it (55), although a battery specific, minimum voltage must also be generated. Since the current is of primary importance in charging a battery, there are several circuitry methods that can be employed to increase this. For example, if the piezoelectric elements are connected in parallel, like in the layered composite, the current from each layer is additive. Another possible method to increase current is the incorporation of a Buck converter (Figure 24).

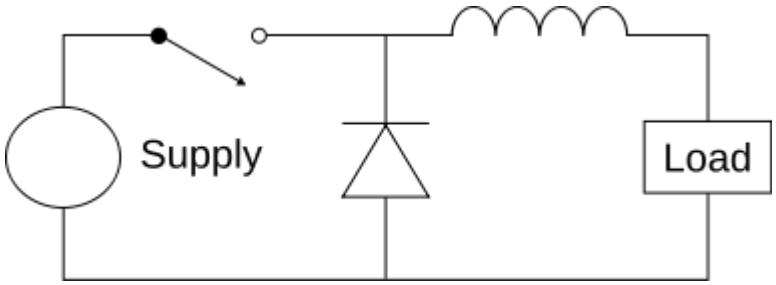

Figure 24. A Buck converter (Public Domain)

Buck converters are simple circuits designed to step down voltage while increasing current. The current behaves according to Equation 2, but becomes more inefficient as D decreases.

$$I_{out} = \frac{I_{in}}{D} \quad (2)$$

Output current

I_{in} – Current input
D – Duty cycle (fraction of time gate is closed)

Store energy using a capacitor

Energy could also be stored using a capacitor, although with the piezoelectric implant, it may not be the best solution. The frequency of the signal will be extremely low (≈1 Hz), so the impedance of the capacitor will be high (Eq 3).

$$Z_{cap} = \frac{1}{j\omega C} \quad (3)$$

Impedance of the capacitor
j – The imaginary number
ω – Frequency
C – Capacitance

This greatly limits the amount of charge that can be stored on the capacitor. The two ways to improve the amount of energy stored on the capacitor are to increase the frequency of the signal or to increase the capacitor size. Unfortunately, since the frequency will depend on the user's movements, it will be relatively low. The size of the capacitor can be increased, but to actually smooth the output voltage, the capacitor must be large enough that the output voltage is greatly decreased. Piezoelectric material studies have also shown that a storage circuit containing only a single capacitor is insufficient to power electronic devices without extra circuitry (55).

Primary Design Targets

There are three primary design targets that are necessary to meet for the piezoelectric implant. First, the implant must be able to deliver adequate current density to provide bone growth. The target for the implant is to deliver 25 $\mu A/cm^2$, although a current density as low as 1 $\mu A/cm^2$ could be acceptable (30). This value can be achieved by generating a current between 1-100 μA and tailoring the size of the electrodes to achieve the ideal current density. The current could either come directly from the piezoelectric implant, or from a small battery the piezoelectric implant is actively recharging. If the battery is being used to store the charge, the most important design target is the current supplied to the battery from the piezoelectric implant.

Second, the material must be mechanically strong. One of the major problems with piezoceramics is that they are extremely brittle. It is not acceptable to have a fusion cage that is weak and might break after implantation, even if it can generate the required current. The piezoelectric composite must be designed to have a high enough toughness to withstand high impacts and continue working properly.

Third, the implant must be of an appropriate size. It should be a similar shape as current fusion cages. It needs to be small enough to fit into the intervertebral space, but still large enough to maintain the correct space between the adjacent vertebrae. Fusion cages currently come in a variety of sizes ranging from 5-25 mm thick, and the piezoelectric cage should do the same.

Input Parameters

To accomplish these design targets, there are many variables that can be taken into account. Some will be able to be directly controlled by changes to the implant, but others are inherent to the environment experienced by the implant.

Implant Variables

These variables can be directly controlled, although there are realistic ranges for the variables that must be considered. Material properties that may influence power generation and implant strength are included in Table 1.

- Particle volume fraction

Particle volume fraction can range from 0-100%, but the design parameters narrow this down slightly. For the composite to show a measureable piezoelectric effect, the volume fraction should be at least 10%, although the piezoelectric properties of the composite will still be quite low. A higher volume fraction of the particles is desired because as the volume fraction increases, so will the piezoelectric properties of the composite. It is also important, however, for the matrix material of the composite to be able to provide a toughness not found in the ceramic particles. As the volume fraction of particles increases, the ceramic particles have a greater impact on the mechanical properties of the composite and the toughness imparted by the matrix is reduced. The manufacturing of the composite also gets more difficult as the volume fraction of the particles increases, limiting the feasible amount of particles that can be added. The matrix material currently used in the manufacturing process is a two-part epoxy, with which it would be difficult to create composites with volume fractions above 40%. The final implant is likely to use a matrix material that requires a high-temperature manufacturing processes, which would allow for much higher volume fractions to be used. The realistic range of particle volume fraction has been set at 10-80%.

- Particle d_{33}

The particle's d_{33} value plays an important role since it is a measure of the amount of charge generated per amount of force on by the material. A realistic range of values for ceramic particles will range between 50-500 pC/N.

- Particle and matrix dielectric constants

The dielectric constant, also known as relative permittivity, of a material is a measure of the resistance encountered when forming an electric field inside the material. Materials with high dielectric constants are good insulators and have a high polarizability. The dielectric constant for ceramic materials is in the range of 1000-10,000, while the range for polymers is in the range of 1-85.

- Particle and matrix Young's modulus

Young's modulus is a measure of the stiffness of a material. It is quite important for mechanical stability, but probably less so for electrical production. The Young's modulus examined for particles ranges from 20-200 GPa, and the Young's modulus for the polymer matrix ranges from 1-10 GPa.

- Implant cross-sectional area and thickness

Using either the layered or thick implant approach, it should be possible to make the implant the appropriate size for implantation. The cross-sectional area of a fusion cage is usually in the range of 300-600 mm^2, but to see the effect of small and large cross-sections, a range from 100-900 mm^2 will be examined. The thickness of the composite has a fairly small range. Most implants are between 5-25 mm thick, so values around that are needed to test for the thick implant. For the layered implant, the thickness of an individual layer can be even lower than 1 mm. An *n*-layered implant would act like *n* composites of small thickness that are mechanically in series, but electrically in parallel.

Implant Variables	Range
Particle Volume Fraction	10-80%
Particle d_{33}	50-500 pC/N
Particle Dielectric Constant	1000-10,000
Particle Young's Modulus	20-200 GPa
Particle Resistivity	$1\text{-}10^{17}$ Ω*cm
Matrix Dielectric Constant	1-85
Matrix Young's Modulus	1-10 GPa
Matrix Resistivity	$10^{9}\text{-}10^{17}$ Ω*cm
Composite Cross-sectional Area	100-900 mm^2
Composite Thickness	0.1-25 mm

Table 1. Realistic ranges of implant variables

Environment Variables

The environment variables largely cannot be controlled, but are inherent to the implant's use as a lumbar fusion cage. Realistic ranges of environmental variables that would affect the power generation capability of the implant are included in Table 2 and are as follows:

- Force on implant

The force on the implant is primarily controlled by the weight of the patient. The spine supports much of the weight of the upper body and much of this will be passed directly through the implant. The force on the implant will change depending on the activities performed by the user. In a common activity like walking, the force on the intervertebral disc in the lumbar region can range from 1.0 to 2.95 times body weight (56-59). With the inclusion of posterior instrumentation in a spinal fusion, the force on the implant itself is halved (60). In high impact situations, such as jumping or running, the force on the implant increases. Conversely, the force on the implant decreases during an activity like sleeping.

- Frequency

The frequency of compression on the implant will also depend on the activities performed by the patient. In normal situations, the frequency will not vary to a large degree. Most activities will occur with a frequency less than 5 Hz. Walking, for example, usually occurs at a frequency between 1.2 and 2 Hz (58). It would be possible to increase the frequency of implant compression by mechanically stimulating the patient using a high frequency, low amplitude stimulus; however, this would require patient compliance, which is something that is best to avoid.

- Electrical resistance of the bone

The electrical resistance of bone is another variable that is dependent on the environment. Peer-reviewed literature is actually quite sparse on this. According to the leading manufacturer of DC electrical stimulation devices, however, the resistance of bone ranges between 0 and 40 kΩ (29).

Environmental Variables	Realistic Range
Force on Implant	300-1500 N
Frequency of Compression	.3-5 Hz
Resistance of Bone	0-40 kΩ

Table 2. Realistic ranges of environmental variables

Safety and Efficacy Analysis

When designing a medical implant, the top priority is that it will be safe for the patient to have embedded in their body. Early in the design phase, it is helpful to brainstorm about what could go wrong to help steer the design down paths that will limit any danger to the patient. The importance of a certain failure mode is determined based on its severity, likelihood of occurrence, ease of detection. At this point in the development of the implant, only the severity and occurrence have being determined. Both

categories are ranked from 1-10, with 10 being the most severe or most likely to occur. A score is then determined by multiplying the numbers together to determine the biggest safety risk.

Failure Mode and Effects Analysis

FUNCTION	DEFAULT	SEVERITY		OCCURRENCE	
Part Name Part/ Function	Potential Failure Mode	Potential Effect(s) of Failure	SEV	Potential Cause(s) of Failure	OCC
Rectifier circuit	Short circuit in rectifier circuit	Electricity is not delivered to the fusion	3	A path for electricity is formed, bypassing several diodes	1
		Electricity is half-wave rectified, delivering half the power to the fusion	2	A path for electricity is formed, bypassing one diode	1
	Rectification is unsuccessful	A pulsed signal is delivered to the storage circuit, causing inefficient storage of energy	2	Part of the diode bridge breaks (diode breaks or wire breaks)	2
		Signal could be half wave rectified, resulting in decreased power	2	Diode breaks, creating an open circuit	2
Storage circuit	Short circuit in storage circuit	Electricity is not delivered to the fusion	3	A path for electricity is formed, bypassing the battery	1
	Battery discharges an excess of charge	A high amount of charge is released causing bone and tissue necrosis	7	Circuitry limiting the current output of the implant breaks	2
	Battery or capacitor does not store charge	A pulsed signal is delivered to the bone, causing a lower bone growth rate	2	Battery becomes disconnected	2
Delivery circuit	Short circuit in delivery circuit	Electricity is not delivered to the fusion	3	A path for electricity is formed, bypassing the fusion	1
	Positive wire migrates	Possible irritation or damage to nerves or cauda equina resulting in pain or muscle contraction	8	Wire not secured in the soft tissue	3
				Wire too long- could move around, irritating nerves	1
		Bone resorption or necrosis occurs when wire contacts bone or posterior instrumentation	7	Wire not secured in the soft tissue	4
	Positive wire breaks	Possible irritation or damage to nerves or cauda equina resulting in pain or muscle contraction	8	Wire gets kinked, which leads to a break or exposed wire	3
				Wire comes detached at its connection to the implant- occurance depends on	2
		Bone resorption or necrosis occurs when wire contacts bone or posterior instrumentation	7	Wire gets kinked, which leads to a break or exposed wire	3
				Wire comes detached at its connection to the implant- occurance depends on	2
	Delivery system doesn't deliver p	Doesn't stimulate bone growth	3	A path for electricity is formed, bypassing the positive wire and the	1
	Delivery system instantaneous power transfer	Shock the patient (pain, muscle contraction)	7	Circuitry limiting the current output of the implant breaks	2

Composite	Composite is not successfully structured (still 0-3)	A reduced amount of electricity is delivered	2	DEP or PEP is unsuccessful	1
	Implant stiffness is too high	Implant causes damage to endplates/endplate subsidence	7	Poor material selection	1
		Implant causes stress shielding (local bone resorption)	7		
	Composite cracks	Patient exposed to microparticles if insulating shell cracks too (similar effects as wear particles)	8	Fatigue life too low	2
		Could lead to fracture	6		
		Reduced power generation	2		
Insulating shell	Wear particles are created	Immune response which can eat away at local tissue	6	Implant not properly implanted, causing excess friction between implant and bone	2
		Osteolysis	6		
		Local chronic buildup of particles, causing tissue necrosis	6		
		Systemic chronic buildup of particles, causing tissue necrosis	7		
	Insulating shell cracks	Patient exposed to microparticles (similar effects as wear particles)	8	Sudden spike in stress (car accident, gun shot, knifing, police baton)	2
	Poor osseointegration	Depends partially on the exposed surface area of the insulating shell and the osseointegration of the outer electrodes	4	Poor material selection	1
Outer electrodes	Wear particles are created	Immune response which can eat away at local tissue	7	Implant not properly implanted, causing excess friction between implant and bone	2
		Osteolysis	7		
		Local chronic buildup of particles, causing tissue necrosis	7		
		Systemic chronic buildup of particles, causing tissue necrosis	8		
	Electrodes short circuit to other hardware (posterior instrumentation)	Hardware becomes negatively charged, generating bone growth around it	1	Implant loosens and moves too close to other ha	1
	Outer electrodes crack	Leads to wear particles	7	Sudden spike in stress	2
	Poor osseointegration	Depends partially on the surface area of the electrodes and the osseointegration of the exposed insulating shell	4	Poor material selection	1
Piezoelectric particles	Particles depolarize	Implant loses piezoelectric properties and does not generate electricity	2	Extreme implant heating, such as autoclaving	4
	Particle vibration	Possible weakening of implant	3	Possibly from MRIs, microwaves, or x-rays	2
Overall implant	Implant fractures	Patient exposed to microparticles	8	Sudden spike in stress (car accident, gun shot, knifing, police baton)	2
		Nerves get pinched (pain)	9		
		Collapsed disc height	9		
	Implant migrates	Implant pinches nerves, causing local and systemic pain	9	Implant placed improperly during surgery	2
				Surface of implant has inadequate friction properties	1
		Disc height collapses due to implant migration, causing local and systemic pain	9	Implant placed improperly during surgery	2
				Surface of implant has inadequate friction properties	1
	Implant continues generating electricity after fusion	Long term nerve irritation	8	Implant still being stressed after fusion (stress shielding)	2
		Potential ectopic bone formation	6		

Table 3. Failure Mode and Effects Analysis

Although there are many possible safety issues with the implant, most of them have an extremely low occurrence. Based on the safety analysis (Table 3), the most important design consideration should be the insulated grounding wire. The wire must be able to easily and safely be inserted in soft tissue. The wire will have to travel from the intervertebral space to nearby soft tissue without aggravating the nerves in the vicinity of the intervertebral space. The wire needs to be able to be easily and painlessly attached to the soft tissue, to prevent it from migrating and possibly causing serious problems. However, a design for the wire's end should be able to be created to prevent the wire from migrating after implantation.

The biocompatibility of the materials is another important safety factor. The matrix material, insulating layer, and electrodes will be easily created out of materials that are regularly used in the body. The particles used in the composite, however, are more difficult to create out of biocompatible materials. Many of the piezoceramic materials with the highest piezoelectric properties are lead based, like PZT, which would cause tissue necrosis if exposed to the body. To avoid this serious issue, particles with better biocompatibility, such as $BaTiO_3$, should be used. If these particles were not able to generate the required electricity to stimulate bone growth, less biocompatible materials could be used only if it could be proven that the insulating layer separating the composite from the body would not crack, even under high impact stresses.

One safety concern that is often mentioned is whether the implant will continue to generate bone growth after the vertebrae have successfully fused together. As the bones fuse together, however, the bone itself will begin to take some of the force of the upper body; the implant will no longer be supporting the weight all by itself. This will cause the implant to undergo less stress and generate less electricity. The electricity should be low enough to be unable to pass through the circuitry, such as the diodes, and electricity will stop being applied to the fusion. Even if a small amount of electricity was still

being generated, other spinal fusion DC devices have not shown negative side effects of continued stimulation.

MRI compatibility is another common concern for the piezoelectric implant, especially if a battery is included. Current DC stimulation devices, which incorporate lithium batteries, can have MRI scans taken of them as long as precautions are taken (61). If the piezoelectric implant needed a battery, it would be a smaller battery of the same type, so MRI scans should also be okay, as long as precautions are taken. If a battery is not used, however, then the MRI should not cause problems with the implant. The majority of piezoelectric materials, including PZT, have been found to be safe to use in an MRI (62).

Most of the failure modes with circuitry are minor. The occurrence for them is low because the circuitry will be embedded in the insulating layer, protecting the components from harm. The severity of these is usually low, as well; the worst case scenario being that no electricity is delivered to the fusion. Although it is important that the device stimulates bone growth, the negative consequences of these problems are relatively low. Most of the other failure modes can be avoided with proper material selection. Choosing materials with appropriate biocompatibility, fatigue life, and stiffness, as well as enough toughness to survive a sudden spike in stress will prevent most of the problems from occurring.

The bottom line is that the piezoelectric fusion cage will not face many safety issues that have not already been surmounted by currently used fusion cages or DC stimulators. The wire and biocompatibility are the biggest concerns, but should be able to be made safe for the patient based on design and material selection. Overall, the piezoelectric fusion cage should be considered safe for implantation.

VI. Power Analysis Using a Lumped Parameters Model

To guide the creation of the piezoelectric composite, a lumped parameters model of the composite was developed. Lumped parameter models have already been used in research to successfully predict power generation from piezoceramic materials (43, 54, 63). To date, little work has been documented on piezoelectric composites using lumped parameters models for power analysis.

Since this project is focused on the design of an implant, time is of the essence. Therefore, it is more important to use this lumped parameters model to find trends in the data that help improve the power output, rather than to quantitatively predict the exact power output. For the preliminary research, values in the same order of magnitude of the experimental results will be acceptable. After experimental results are obtained, further optimization of the code can be completed to more accurately predict the electrical outputs. Keeping this in mind, realistic ranges of material, geometric, and environmental variables were examined to see each of their effect on the power, voltage, and current output of the composite.

Methods

Lumped Parameters Model

The lumped parameter model for the piezoelectric composite was based off of work done by Platt et al. (43, 54). Platt created a lumped parameters model which accurately predicted peak power output for a ceramic piezoelectric element. The model developed for the piezoelectric composite is shown in Figure 25.

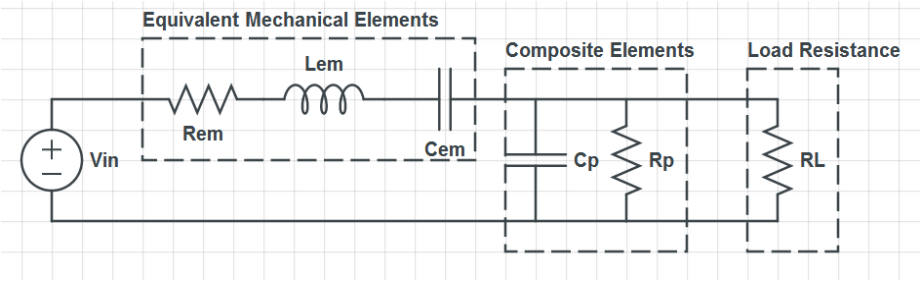

Figure 25. Lumped parameters model for power analysis of a piezoelectric composite

Each of the elements of the lumped parameters model is based off of a combination of material, geometric, and environmental variables. Vin, for example, is based partially on the d_{33} of the piezoelectric material and the force applied. The Equivalent Mechanical Elements are determined based on the mass, damping, and stiffness of the material (Rem, Lem, Cem). The Composite Elements represent the capacitance (Cp) and resistance (Rp) of the piezoelectric material. The Load Resistance (RL) is the electrical resistance of the object to which the electricity is being delivered.

Several key changes were made from Platt et al.'s work to develop the model for a piezoelectric composite, although only one element was added to the lumped parameters model. Ceramics act almost completely as a capacitive element, which is shown in Figure 25 as Cp. Polymers, on the other hand, act almost completely as a resistive element. A composite of the two materials, therefore, will have properties of both. To model this, a resistor, Rp, was placed in parallel with Cp (Figure 25), giving the current alternate pathways through the material.

Other adjustments had to be made to the material properties of the piezoelectric material. The lumped parameters model for the piezoceramic relied on material properties such as the ceramic's dielectric constant, piezoelectric charge coefficient, and Young's modulus. Since the composite is a combination of materials, the overall value of these parameters will depend on the properties of the particles and polymer matrix, as well as the particle volume fraction. Every element of the lumped parameters model relies on at least one of these material properties.

The equations used to calculate the composite's dielectric constant, piezoelectric charge coefficient, Young's modulus, and resistivity are based on 0-3 composites (Eq 4-7). Similar 1-3 composite equations exist, but some rely on a term for the ratio of particle size to interparticle spacing, which cannot be determined without experimental data. Since the lumped parameters model is being used to guide the initial development of the composite, this value is not yet known. The 0-3 equations will provide a base reading of the voltage, current, and power, which will be lower than that actually produced by the 1-3 composite.

$$\varepsilon_{0-3} = \varepsilon_1 \left(1 + \frac{n\Psi(\varepsilon_2 - \varepsilon_1)}{n\varepsilon_1 + (\varepsilon_2 - \varepsilon_1)(1-\Psi)}\right) \quad (4)$$

Dielectric constant of a 0-3 composite (52, 64-66)

ε_1 – Dielectric constant of the matrix
ε_2 – Dielectric constant of the particles
n – Inverse depolarization factor
Ψ – Particle volume fraction

$$d_{33_{0-3}} = \left(\frac{n\,\Psi\varepsilon_{0-3}}{n\varepsilon_{0-3} + (\varepsilon_2 - \varepsilon_{0-3})}\right) d_{33_2} \quad (5)$$

Piezoelectric charge coefficient of a 0-3 composite (66-70)

$\varepsilon_{0\text{-}3}$ – Dielectric constant of the 0-3 composite
ε_2 – Dielectric constant of the particles
d_{33_2} – Piezoelectric particle charge constant
n – Inverse depolarization factor

$$E_C = E_1\left(1 + \frac{3\left(\frac{E_2}{E_1}-1\right)\Psi}{\left(\frac{E_2}{E_1}+2\right)-\left(\frac{E_2}{E_1}-1\right)\Psi}\right) \quad (6)$$

Young's modulus of a 0-3 composite(71)

E_1 – Young's modulus of the particles
E_2 – Young's modulus of the matrix
Ψ– Particle volume fraction

$$\rho_C = \rho_1\left(1 + \frac{3\left(\frac{\rho_2}{\rho_1}-1\right)\Psi}{\left(\frac{\rho_2}{\rho_1}+2\right)-\left(\frac{\rho_2}{\rho_1}-1\right)\Psi}\right) \quad (7)$$

Resistivity of a 0-3 composite(71)

ρ_1 – Resistivity of the particles
ρ_2 – Resistivity of the matrix
Ψ– Particle volume fraction

Using the lumped parameters model will help determine which variables have the greatest impact on the power, voltage, and current output of the composite. The results will specifically help guide material selection and geometry of the implant.

Material Selection

Two different materials were investigated for the piezoelectric particles: PZT and $BaTiO_3$. $BaTiO_3$ would be considered a possible option because it is considered to be biocompatible. In fact, a few small rods of it are often embedded in current fusion cages so the polymer cage can be visible on x-rays. PZT is the most commonly used piezoelectric material (72) and has some of the highest piezoelectric properties of any material. PZT has an advantage over $BaTiO_3$ because it has a higher d_{33} coefficient and higher Curie temperature; however, PZT is a lead-based ceramic and is not considered to be biocompatible.

Many different matrix materials were tested as well, including epoxy, PEEK, Polyurethane, PVDF, PVDF-TrFE-CFE, and PMMA mixed with carbon black. A two-part epoxy (Epotek 302-3M, from Epoxy Technology Inc., Billerica, MA, USA) was tested due to its previous use in DEP and because it could easily cure at room temperature. The first composite specimens created in lab would be made out of Epotek 302-3M, so it was important to have for comparison. Polyurethane was tested due its use in previous work (48) and its ease of use in manufacturing. PEEK was selected to be tested due to its common use in spinal cages. PVDF, PVDF-TrFE-CFE, and PMMA mixed with carbon black were all selected based on early power analysis results, and had properties that hinted at promising results. The material properties used in the lumped parameters model are shown in Table 4.

Material	Young's Modulus (GPa)	Dielectric Constant	Resistivity (Ω*cm)	d_{33} (pC/N)
PZT	63	1350	10^{15}	300
$BaTiO_3$	67	1000	10^{10}	120
Epotek 302-3M	1.7	3.3	10^{13}	NA
PEEK	3.6	3.3	$4.9*10^{16}$	NA
Polyurethane	1.65	3.2	10^{14}	NA
PVDF	2.0	8.5	$1.5*10^{14}$	NA
PVDF-TrFE-CFE	.45	50	$9.9*10^{13}$	NA
PMMA and .11%VF Carbon Black	2.5	60	10^{10}	NA
PMMA and .3%VF Carbon Black	2.5	85	$3.33*10^{7}$	NA

Table 4. Material properties for particle and matrix materials. Young's Modulus, dielectric constant, resistivity, and d_{33} are used in the lumped parameters model.

To accurately compare the effects of the different input variables on power, current, and voltage, all variables not being tested will be set at the values shown in Table 5. These values are not extremes, but are relatively in the middle of the range of values tested. Each test will be conducted over

a wide range of load resistances, since the value of the load resistance greatly affects the output values of each input variable. The results for the current are of primary importance, since it factors directly into the amount of current density delivered to the fusion (target ≈25 $\mu A/cm^2$).

	Lumped Parameter Variables	Value
Particle Variables	Particle Volume Fraction	30%
	Particle d_{33}	300 pC/N
	Particle Dielectric Constant	1350
	Particle Young's Modulus	63 GPa
	Particle Resistivity	10^{15} Ω*cm
Matrix Variables	Matrix Dielectric Constant	8.5
	Matrix Young's Modulus	2 GPa
	Matrix Resistivity	$1.5*10^{14}$ Ω*cm
Size Variables	Composite Cross-sectional Area	400 mm^2
	Composite Thickness	20 mm
Environment Variables	Force	500 N
	Frequency of Compression	1 Hz

Table 5. Values for variables for the lumped parameter model tests. The value for each variable is held constant unless it is the specific variable being tested.

Results and Discussion

The power analysis using the lumped parameter model provided substantial information to help guide the creation of the piezoelectric composite. In this analysis, individual variables were examined to see the impact they had on power, voltage, and current. Using this information as a guide, specific materials were tested due to their use in lab, their use in spinal cages, or their useful material properties.

The results are divided between an analysis of the individual variables and a comparison of specific materials. The individual variables tested can be broken down into particle properties, matrix properties, implant geometry, and environmental variables.

Variable Analysis

Load Resistance

Figures 26-28 show the change in power, voltage, and current over a range of load resistances.

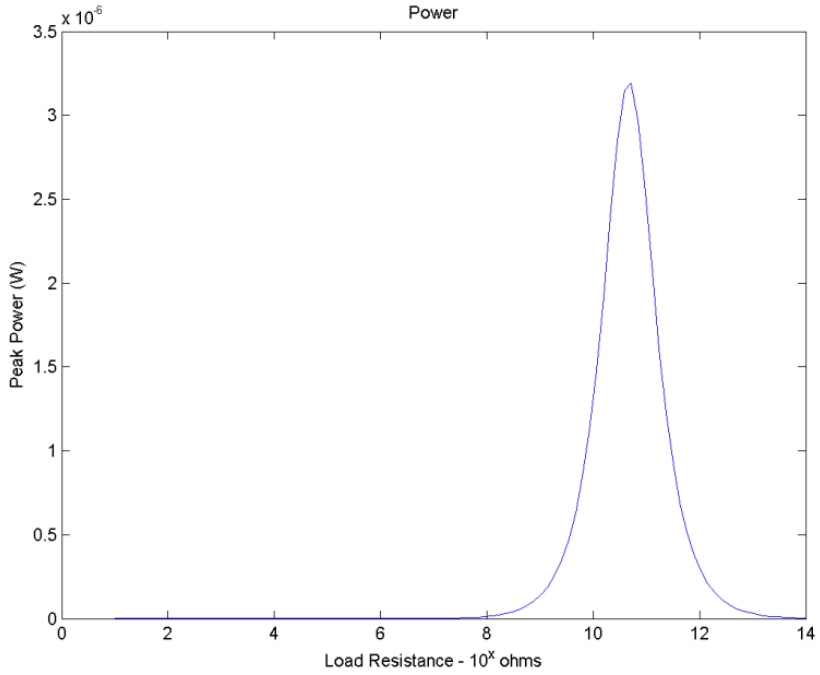

Figure 26. Power vs. Load Resistance

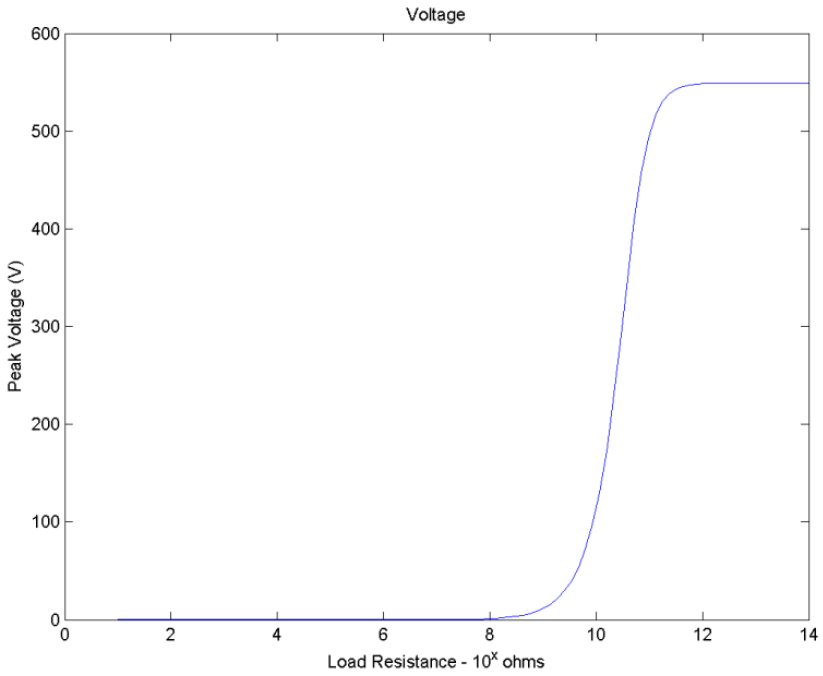

Figure 27. Voltage vs. Load Resistance

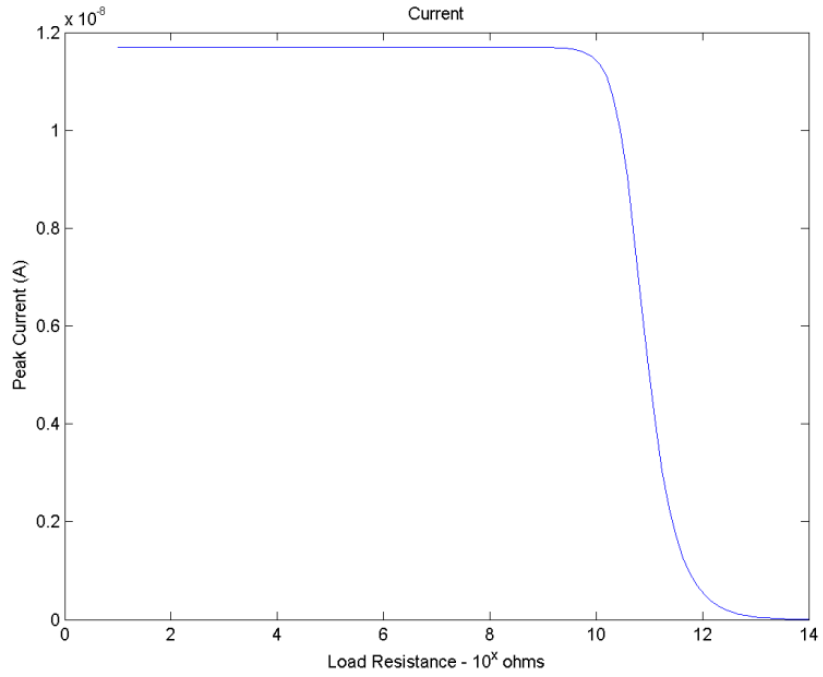

Figure 28. Current vs. Load Resistance

Load resistance has the greatest impact of the input parameters on the output variables. As can be seen in Figure 26, the power peaks at a load resistance around $10^{10.5}$ Ω. This follows a similar trend seen in Platt et al.'s work on piezoceramics (43, 54). A difference between Platt's piezoceramic models and the piezoelectric composite model is the resistance that the peak power occurs. The piezoceramic model's power peaks at $10^{8.5}$ Ω, which is two orders magnitude lower than that of the piezoelectric composite. Voltage stays low at small load resistances, but increases around 10^{8} Ω, before plateauing around $10^{10.5}$ Ω (Figure 27). Current shows the opposite trend. Current is constantly at its peak value from 10 Ω to $10^{10.5}$ Ω before dropping (Figure 28). The resistance of bone ranges between 0-40 kΩ, which is in the region of maximum current. This means it is not necessary to add large resistors in series with the bone to achieve the desired current.

Existing DC stimulation devices deliver 60 μA of current to the fusion, which is over three orders of magnitude over the peak current for this composite (Figure 28). However, changes to the materials and the implant geometry should allow for the generation of more current.

The value that the power peaks at can change depending on the input variables selected. The load resistance also can greatly change the relationship between the other input variables and power, voltage, and current. For this reason, each input variable will be shown over a range of load resistances.

Particle Volume Fraction

Figures 29-31 show the change in power, voltage, and current over a range of volume fractions and load resistances.

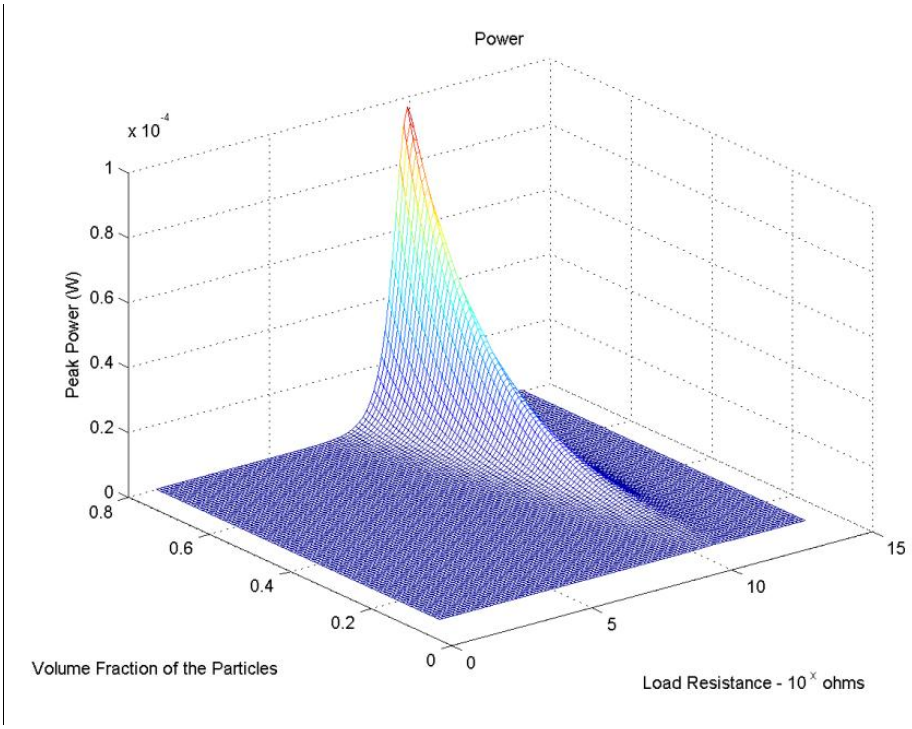

Figure 29. Volume Fraction and Load Resistance vs. Power

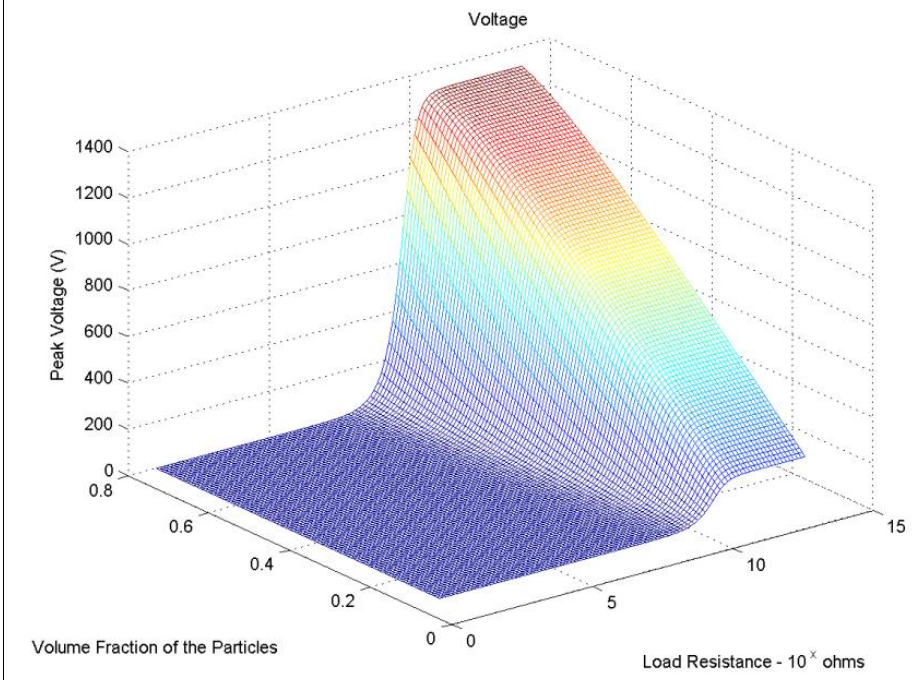

Figure 30. Volume Fraction and Load Resistance vs. Voltage

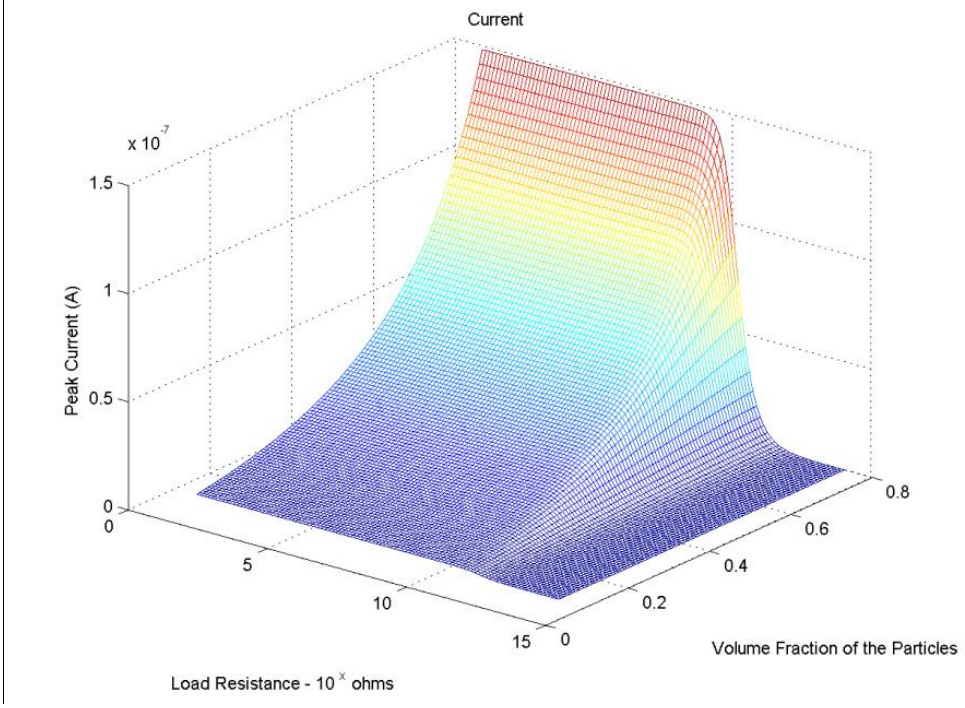

Figure 31. Volume Fraction and Load Resistance vs. Current

The volume fraction of the piezoelectric particles understandably plays a large role in the amount of power, current, and voltage output. The piezoelectric particles are the part of the composite that generate electricity, so the higher percentage used, the higher the electrical outputs. The values of the output variables at 10% volume fraction are almost negligible compared to those at 80% volume fraction. Power and current increase in an exponential fashion: gradually at first, but more rapidly at higher volume fractions. Over this range, power roughly doubles for every 10% increase in volume fraction (Figure 29). Voltage, on the other hand, has a much more steady increase (Figure 30). Current has a four times increase in output from a 30% volume fraction to a 70% volume fraction (Figure 31). Increasing the volume fraction of particles would be an easy way to increase the current generated by the piezoelectric composite.

Particle d_{33} Coefficient

Figures 32-34 show the change in power, voltage, and current over a range of particle d_{33} coefficients and load resistances.

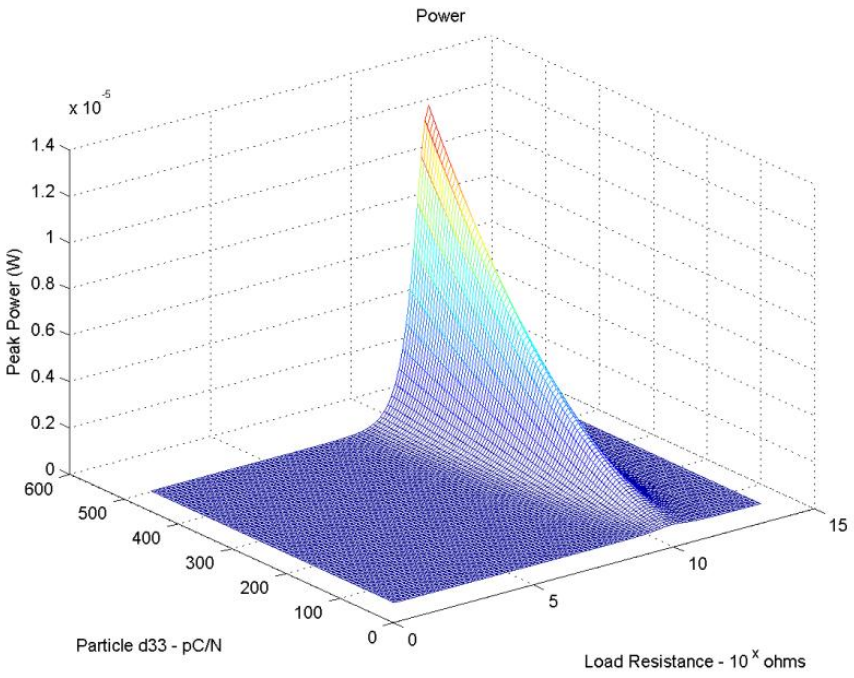

Figure 32. Particle d_{33} and Load Resistance vs. Power

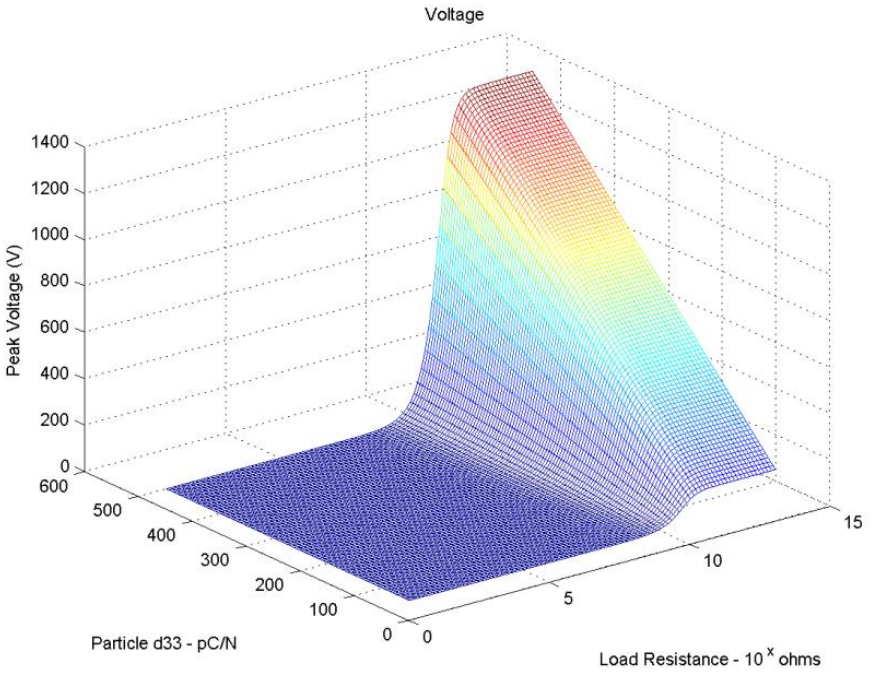

Figure 33. Particle d_{33} and Load Resistance vs. Voltage

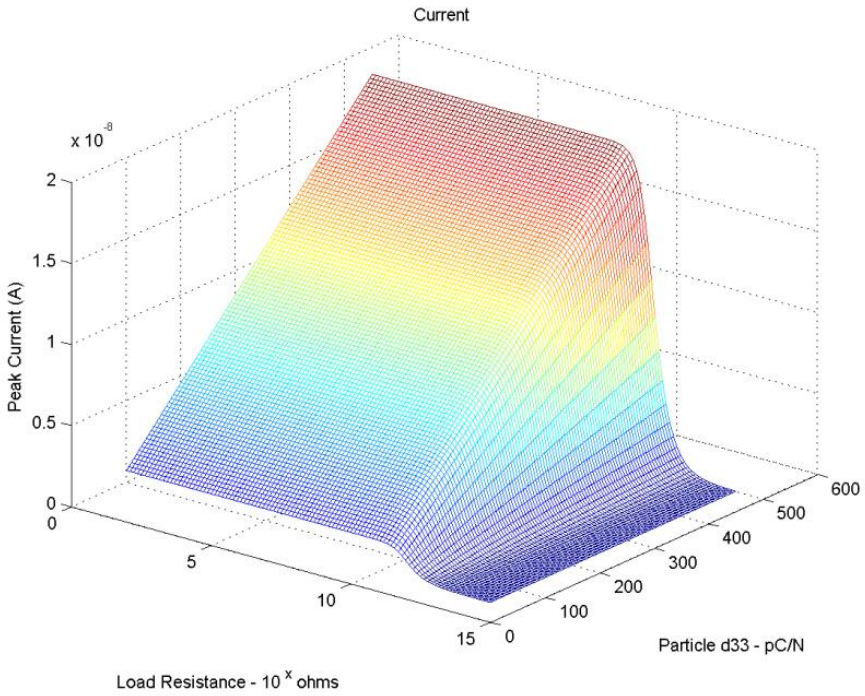

Figure 34. Particle d_{33} and Load Resistance vs. Current

The piezoelectric particles' d_{33} coefficient shows a positive impact on the electrical output variables. Voltage and current have close to a linear relationship with the d_{33} coefficient (Figure 33, 34). Power, however, has more of a parabolic relationship with the d_{33} coefficient (Figure 32). The electrical output's positive correlation with the d_{33} value is expected, since the d_{33} coefficient is a measure of how much charge is generated per force applied. PZT's d_{33} value is 300 pC/N, which is one of the highest values among piezoelectric materials. This, when compared to $BaTiO_3$'s 120 pC/N d_{33} value, means PZT should generate greater electrical outputs.

Particle Dielectric Constant

Figures 35-37 show the change in power, voltage, and current over a range of particle dielectric constants and load resistances.

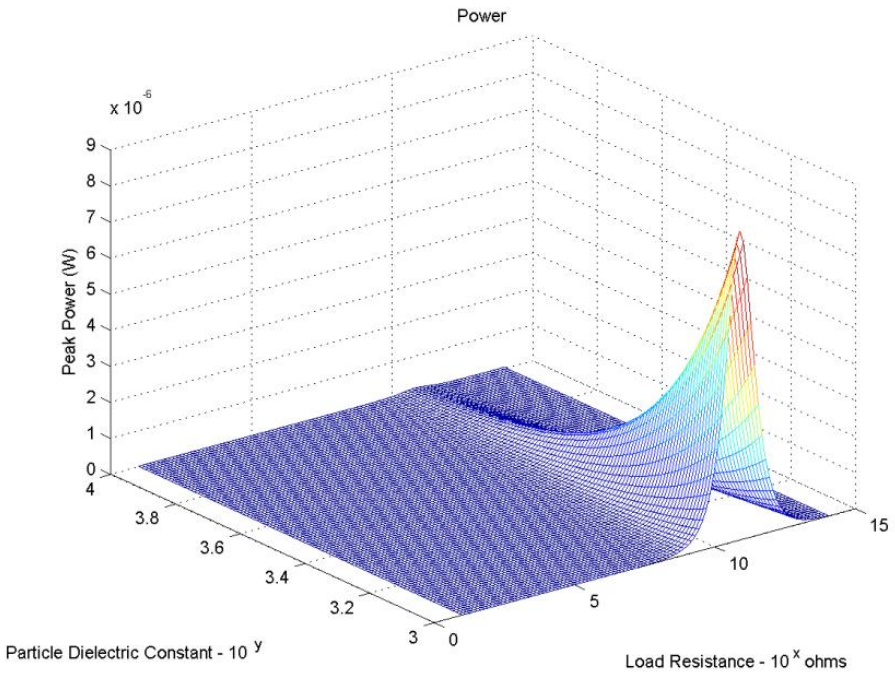

Figure 35. Particle Dielectric Constant and Load Resistance vs. Power

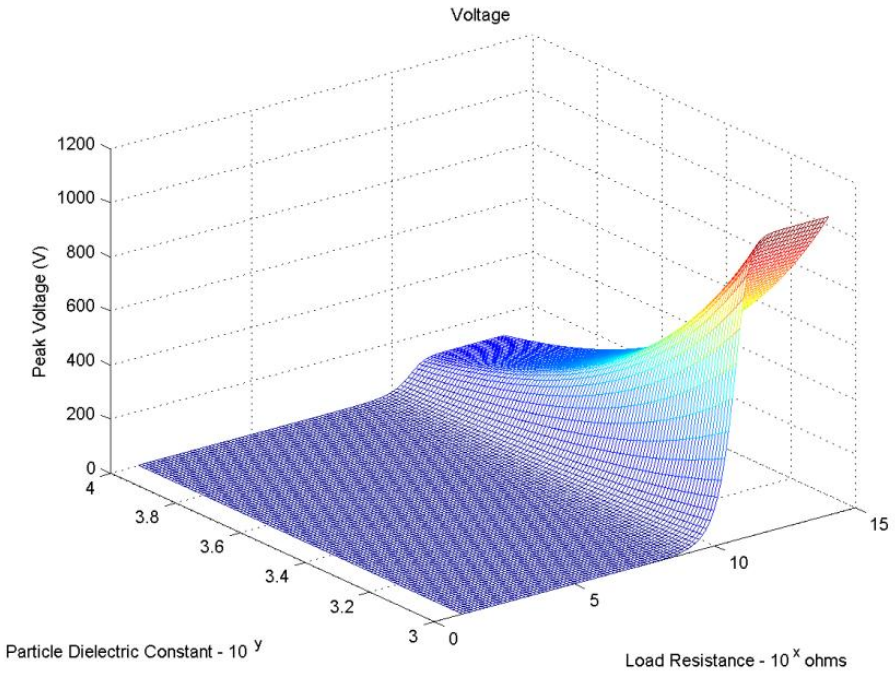

Figure 36. Particle Dielectric Constant and Load Resistance vs. Voltage

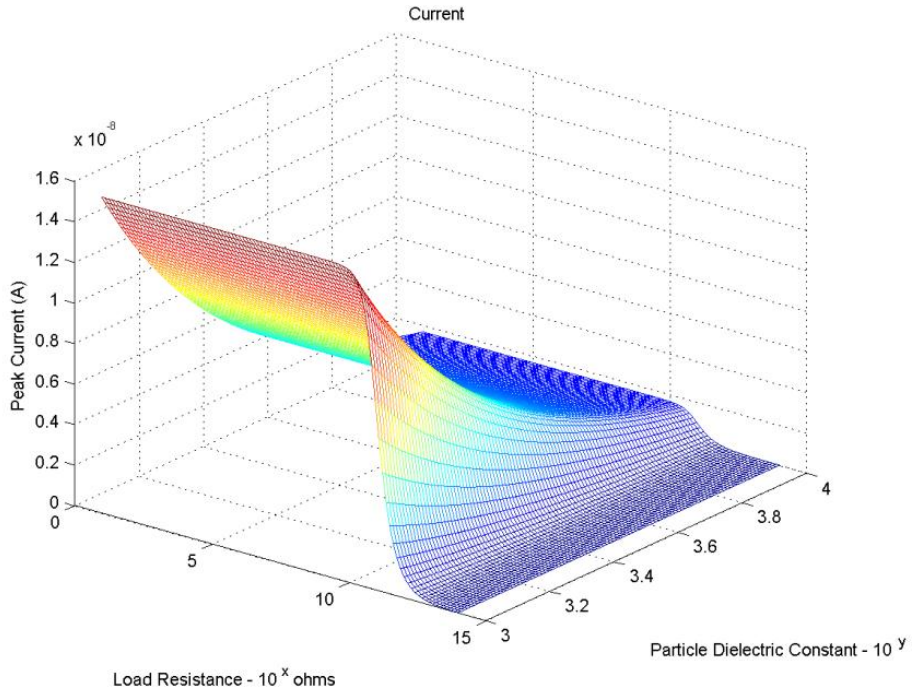

Figure 37. Particle Dielectric Constant and Load Resistance vs. Current

The electrical outputs of the piezoelectric material have a negative correlation with the particle's dielectric constant (Figure 35-37). The effect of the particle's dielectric constant is greater at

lower values, but it still does not have as big of an impact as the d_{33} coefficient (Figures 32-34). The d_{33} coefficient and the dielectric constant are the only two particle material properties that have an impact on this theoretical power analysis. Therefore, to maximize current generation a particle material with a high d_{33} coefficient and low dielectric constant should be chosen, with a priority on the d_{33} coefficient.

Matrix Dielectric Constant

Figures 38-40 show the change in power, voltage, and current over a range of matrix dielectric constant and load resistances. Also shown are the changes in power, voltage, and current over a range of matrix dielectric constants for specific load resistances.

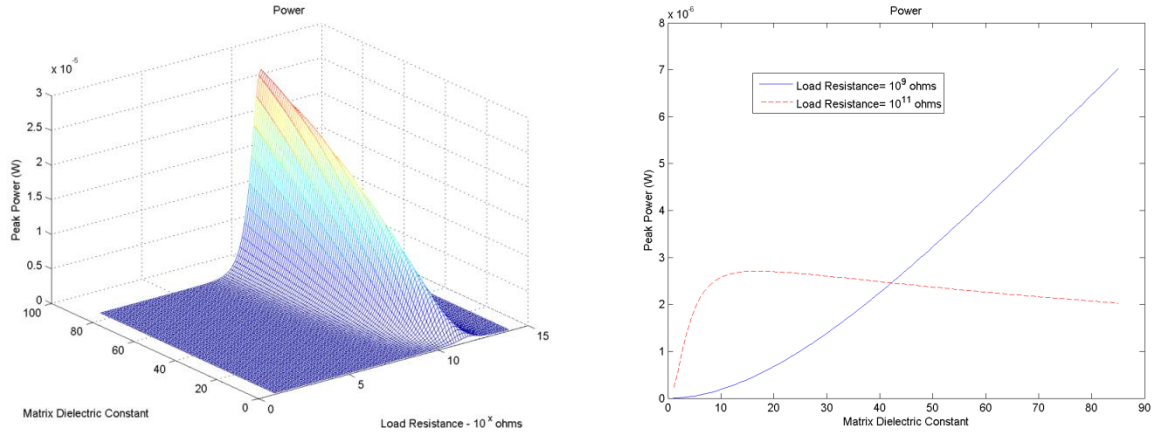

Figure 38. Matrix Dielectric Constant vs. Power

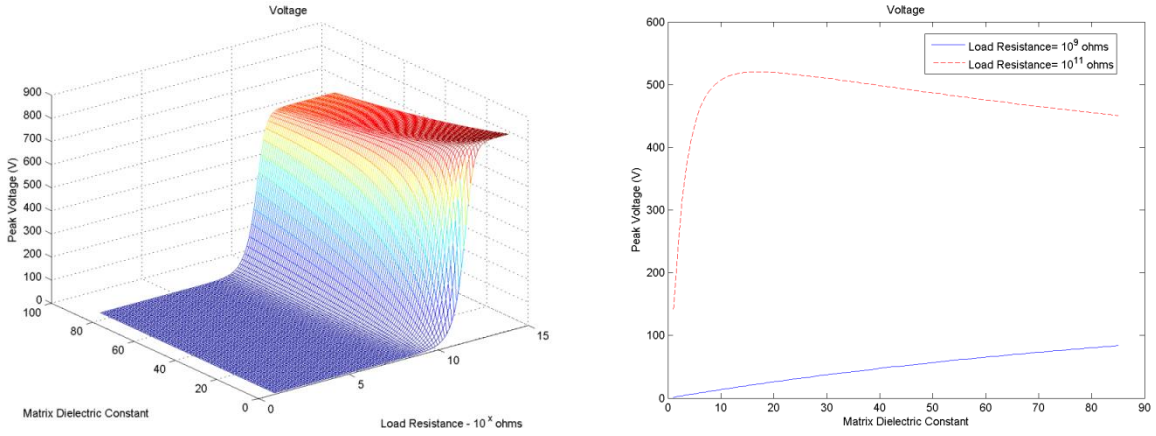

Figure 39. Matrix Dielectric Constant vs. Voltage

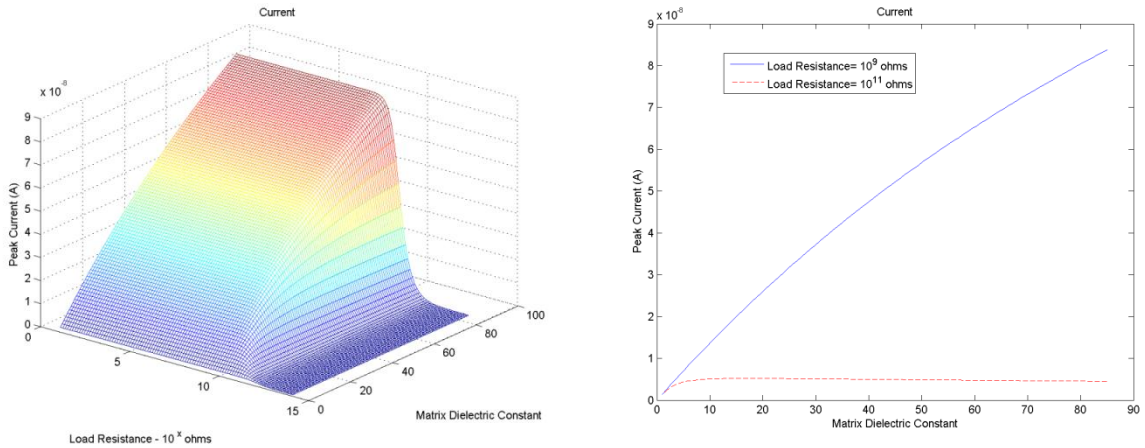

Figure 40. Matrix Dielectric Constant vs. Current

The dielectric constant of the matrix material has a complex relationship with the output electrical measurements. In general, as the matrix dielectric constant increases, power, voltage, and current increases. The nature of the relationship between matrix dielectric constant and electrical outputs changes, however, as the load resistance varies. As the dielectric constant increases, the resistance where maximum power output occurs shifts to a lower resistance (Figure 38). For resistances under the resistance of maximum power output, power constantly increases with increasing matrix dielectric constant. For higher load resistances, the power plateaus and even decreases slightly as dielectric constant increases. Voltage, at low load resistances, increases with dielectric constant (Figure 39). That trend reverses, however, at high load resistances. Current is positively affected by an increased matrix dielectric constant at low load resistances, but is negatively affected at high load resistances (Figure 40). Since maximum current occurs at the low resistances, choosing a material with a high dielectric constant will increase the current output.

Matrix Resistivity

Figures 41-43 show the change in power, voltage, and current over a range of matrix resistivities and load resistances.

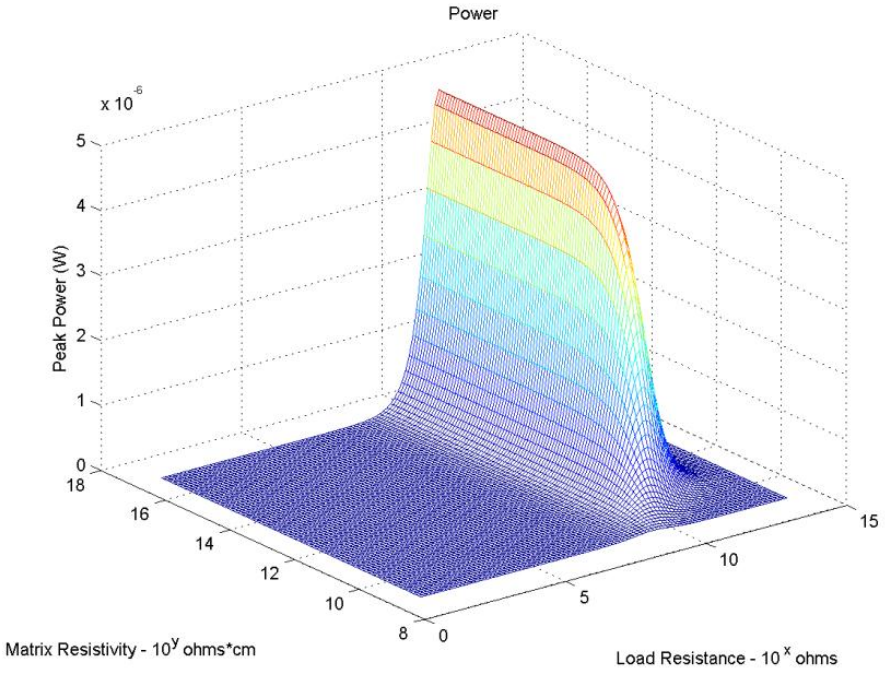

Figure 41. Matrix Resistivity and Load Resistance vs. Power

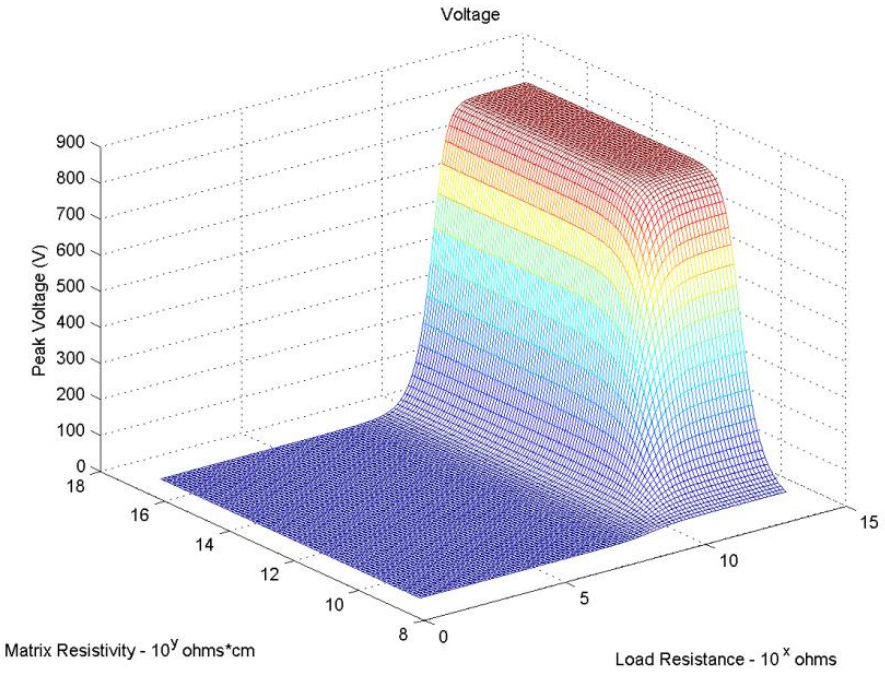

Figure 42. Matrix Resistivity and Load Resistance vs. Voltage

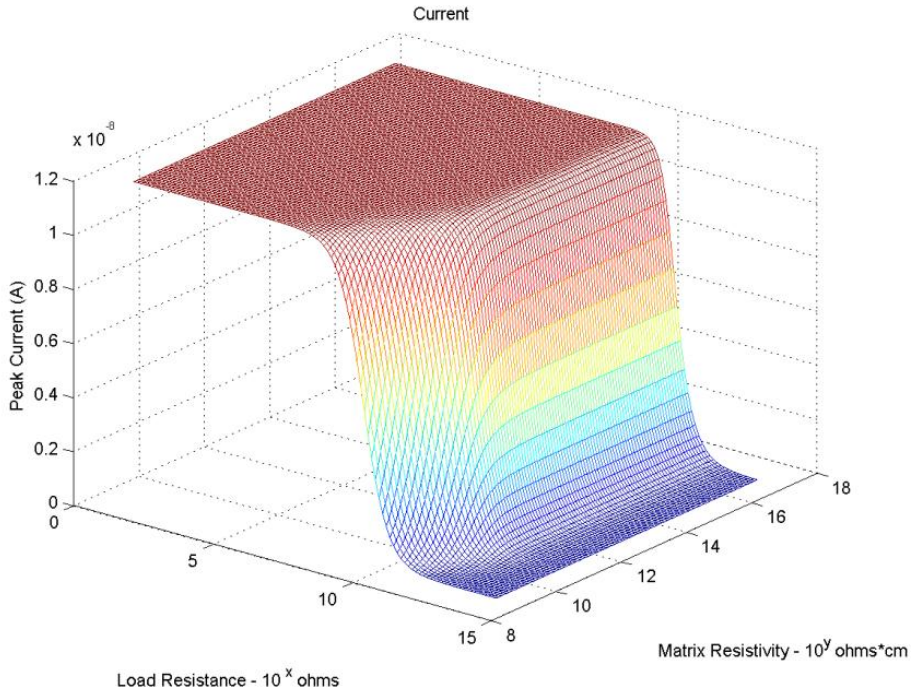

Figure 43. Matrix Resistivity and Load Resistance vs. Current

For the range of resistivities for polymers, the matrix resistivity acts almost as an on/off switch. This is apparent in Figure 41. The power is at a constant maximum, until the resistivity drops below 10^{11}

Ω*cm, when the power drops to near zero. Voltage has a similar reaction to changes in resistivity (Figure 42). A resistivity above 10^{12} Ω*cm generates maximum voltage, but for resistivities below that, the value of voltage drops to near zero. Current is mostly unaffected by resistivity over this range, but the drop in current begins to occur at lower load resistances for resistivities under 10^{11} Ω*cm (Figure 43). Of the matrix material properties, only dielectric constant and matrix resistivity had an effect on the electrical outputs. To maximize the current generated, choosing a matrix with a high dielectric constant is the top priority. The matrix resistivity does not have much effect specifically on the current, although low values will produce almost no power or voltage.

Specimen Cross-sectional Area

Figures 44-46 show the change in power, voltage, and current over a range of cross-sectional areas and load resistances.

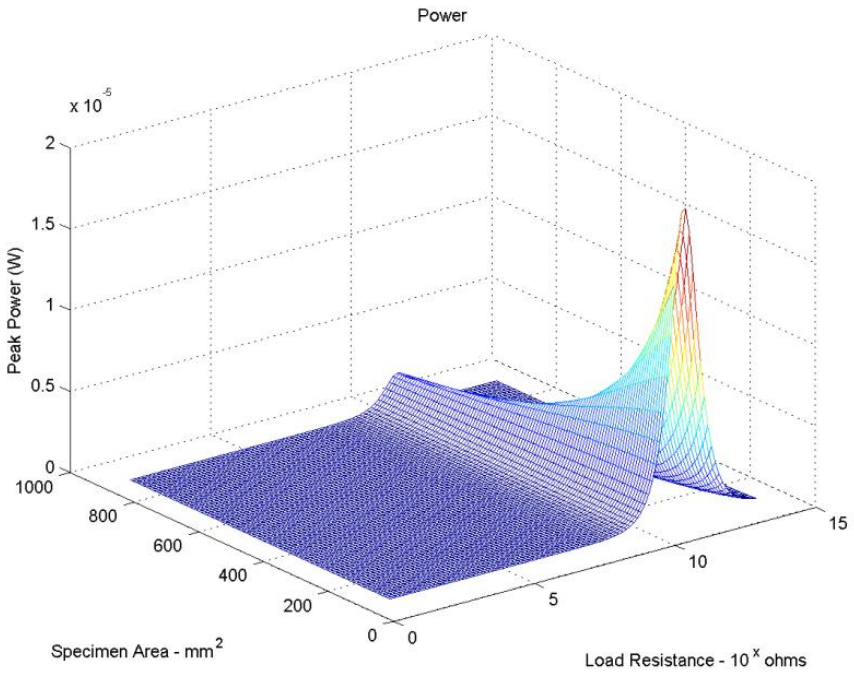

Figure 44. Cross-sectional Area and Load Resistance vs. Power

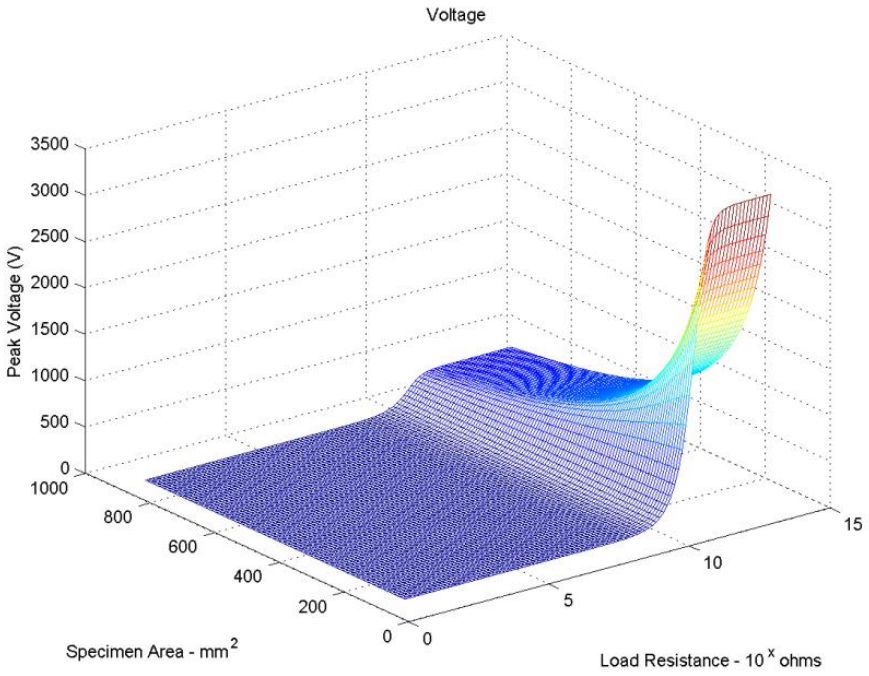

Figure 45. Cross-sectional Area and Load Resistance vs. Voltage

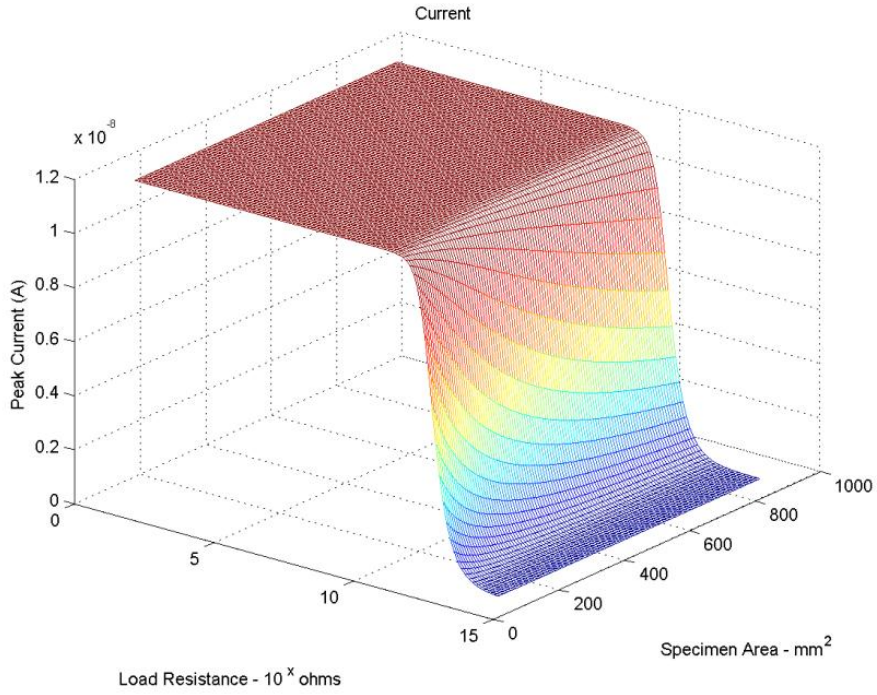

Figure 46. Cross-sectional Area and Load Resistance vs. Current

In general, as the area of the specimen decreases, the power and voltage created by the material increases (Figure 44, 45). The change is gradual at high cross-sectional areas, but increases

faster at smaller areas. Current is not affected by specimen area at low load resistances (Figure 46). It is only affected at high resistances where the current decreases with increasing cross-sectional area.

At least part of the reason the decrease in area increases the power is because of the increase in stress experienced by the material. Therefore, the power or current generated cannot be doubled or tripled by using two or three small areas of material. The force each would experience would be divided among the total area.

Specimen Thickness

Figures 47-49 show the change in power, voltage, and current over a range of thicknesses and load resistances. Also shown are the changes in power, voltage, and current over a range of thicknesses for specific load resistances.

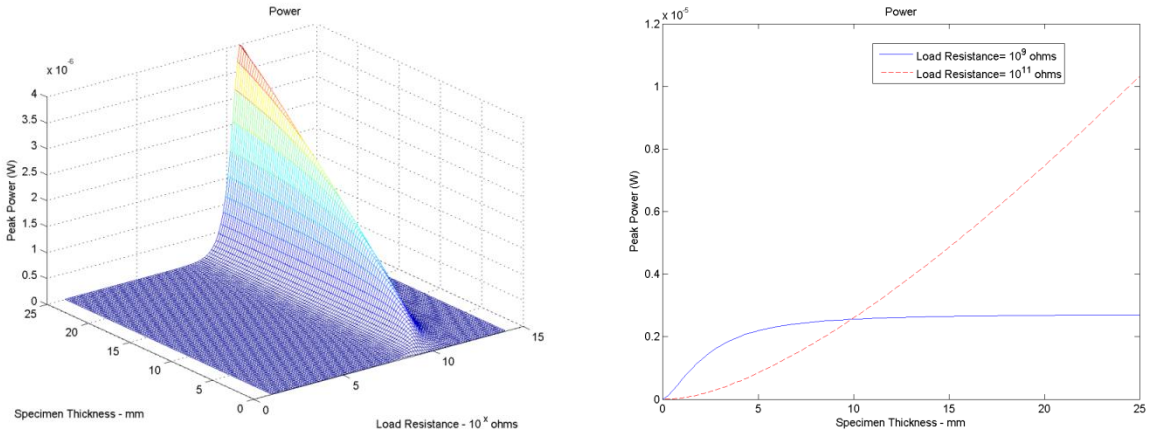

Figure 47. Thickness vs. Power

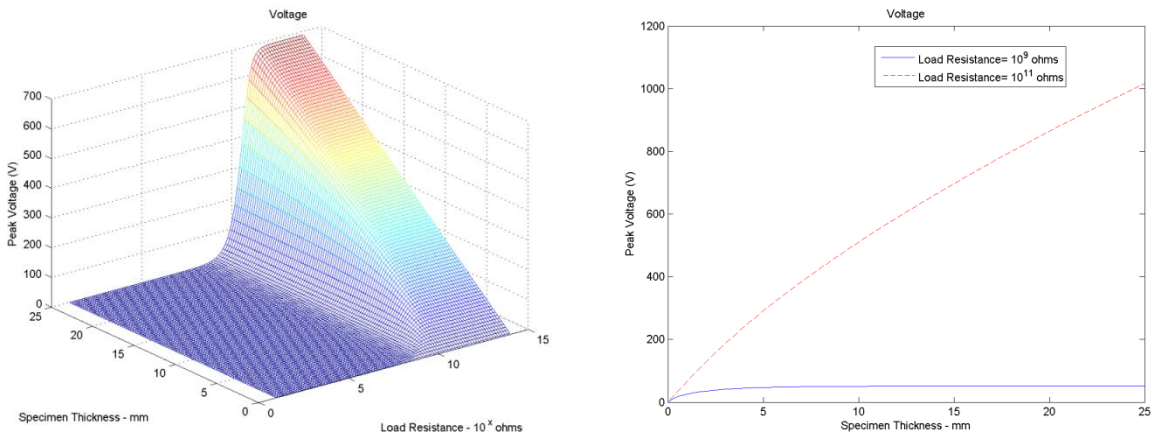

Figure 48. Thickness vs. Voltage

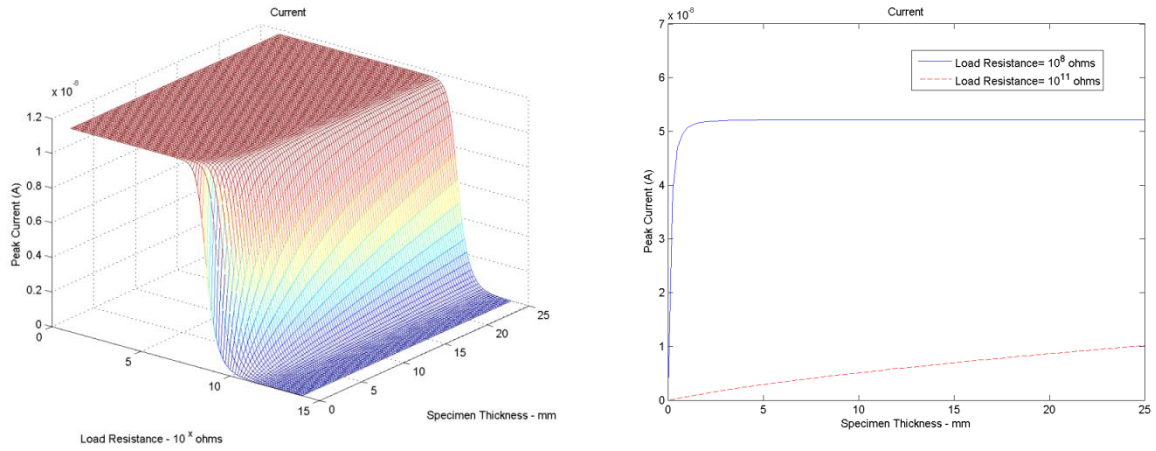

Figure 49. Thickness vs. Current

Material thickness is another variable that provides complex results. At higher resistances, the power and voltage consistently increase with increases in thickness (Figure 47, 48). Just below the load resistance that gives peak power, the power and voltage values increase with thickness, but only over a small range. Current shows little change with thickness, especially at low load resistances (Figure 49). At higher resistances, current shows an increase with material thickness.

Unlike using multiple small cross-sectional areas, using multiple small thicknesses could be a feasible way to increase current output. The layered composite design (Figure 16) would provide these small thicknesses and allow for a large increase in current. If these layers are wired in parallel, the current will be additive. If the implant had five layers, for example, it would result in a five time increase in current over a similarly sized thick composite.

Force

Figures 50-52 show the change in power, voltage, and current over a range of force and load resistances.

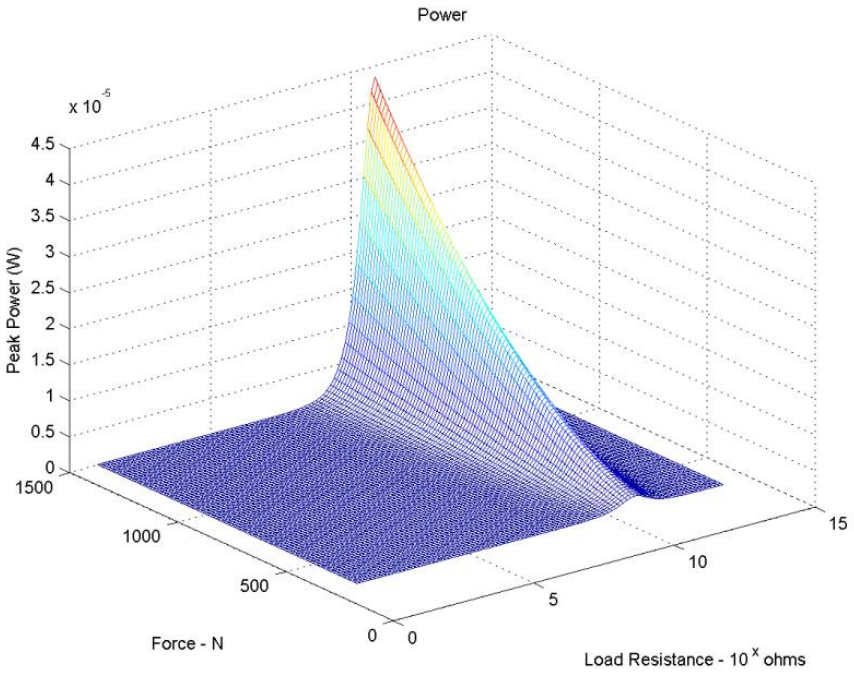

Figure 50. Force and Load Resistance vs. Power

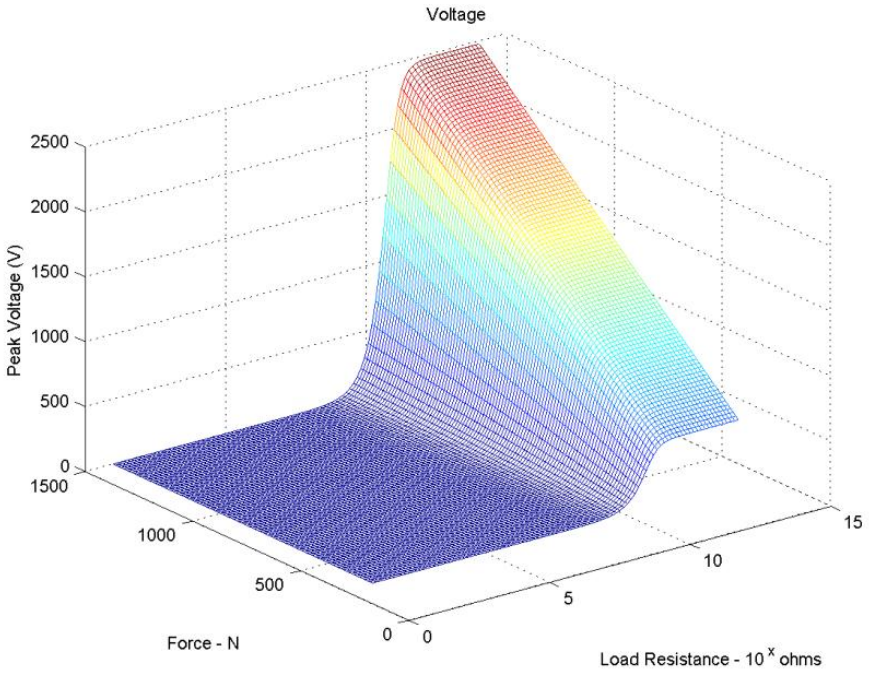

Figure 51. Force and Load Resistance vs. Voltage

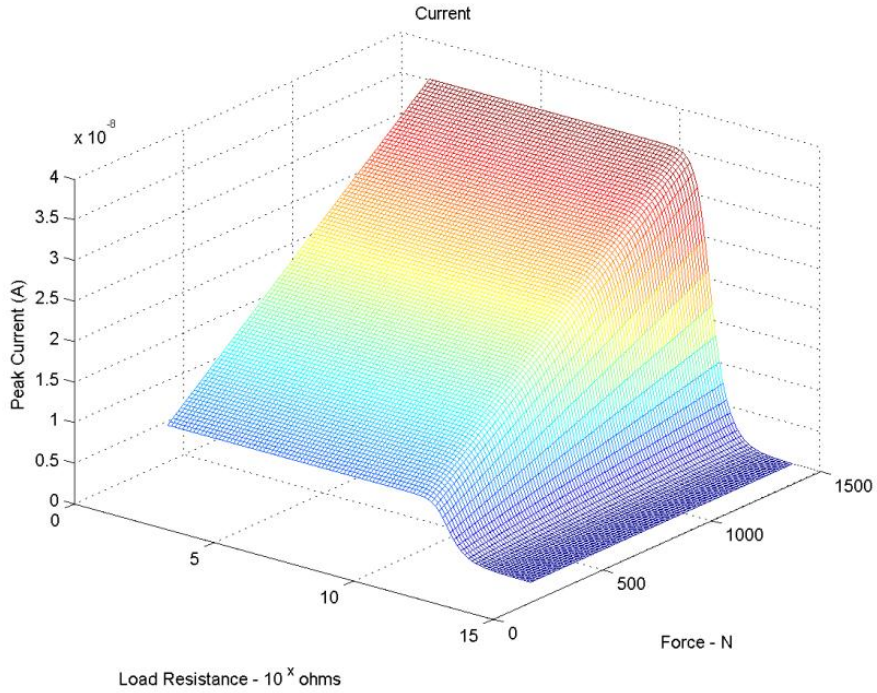

Figure 52. Force and Load Resistance vs. Current

Force shows a positive linear relationship with current and voltage (Figure 50-52). As force increases, so do each of the output variables. Since power is equal to the multiplication of current and

voltage, it has an even greater increase. This positive correlation is expected because based on the d_{33} coefficient, the higher the input force, the greater amount of charge created. Force has the greatest influence on the output variables at low resistances for current, at high resistances for voltage, and near the resistances for peak power output for power.

Much of the force being applied to the fusion cage relies on the weight of the patient's upper body and the intensity of the person's activity. These results suggest that obese patients, who are in the difficult-to-fuse population, will generate more current than a person who is lightweight. In addition, people who perform high impact activities (e.g. running) would have increased rates of success due to the greater amount of force placed on the implant, although back pain would probably limit such activities. These results also mean that the piezoelectric fusion cage is going to be more successful at lower levels in the spine. There may not be much difference between the levels in the lumbar spine, but compared to the cervical spine, there would be a larger difference. The lumbar spine supports much of the weight of the upper body, whereas the cervical spine only supports part of the weight of the head and neck. The current generated would be affected by the difference in load bearing in the two locations.

Compression Frequency

Figures 53-55 show the change in power, voltage, and current over a range of compression frequencies and load resistances. Also shown are the changes in power, voltage, and current over a range of compression frequencies for specific load resistances.

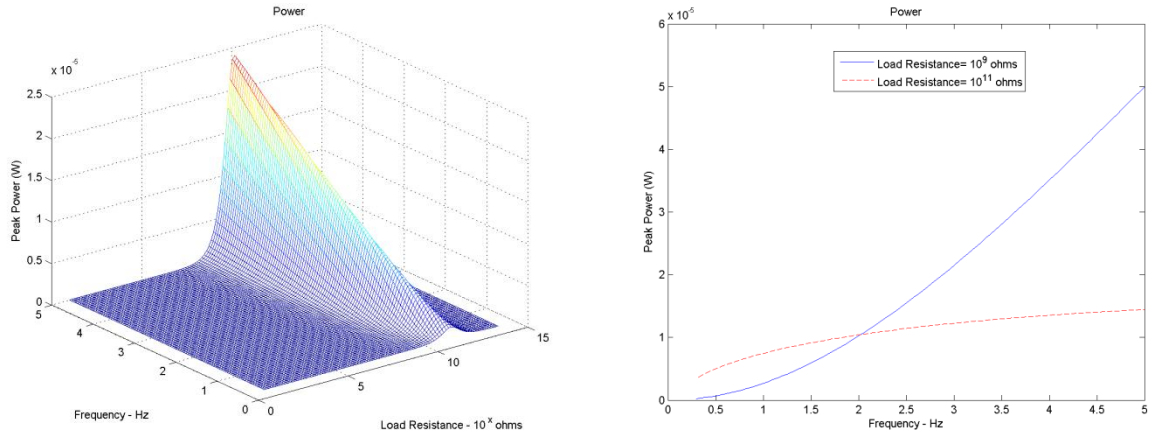

Figure 53. Frequency vs. Power

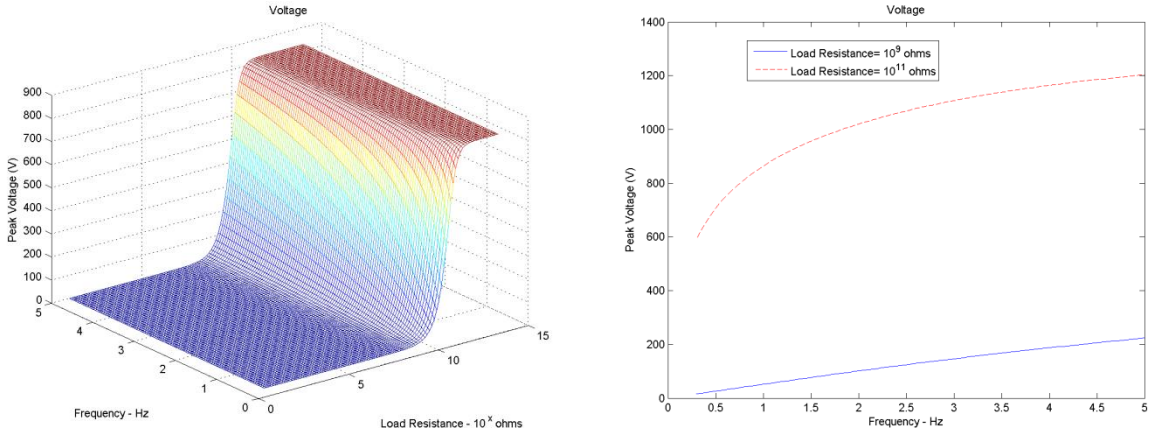

Figure 54. Frequency vs. Voltage

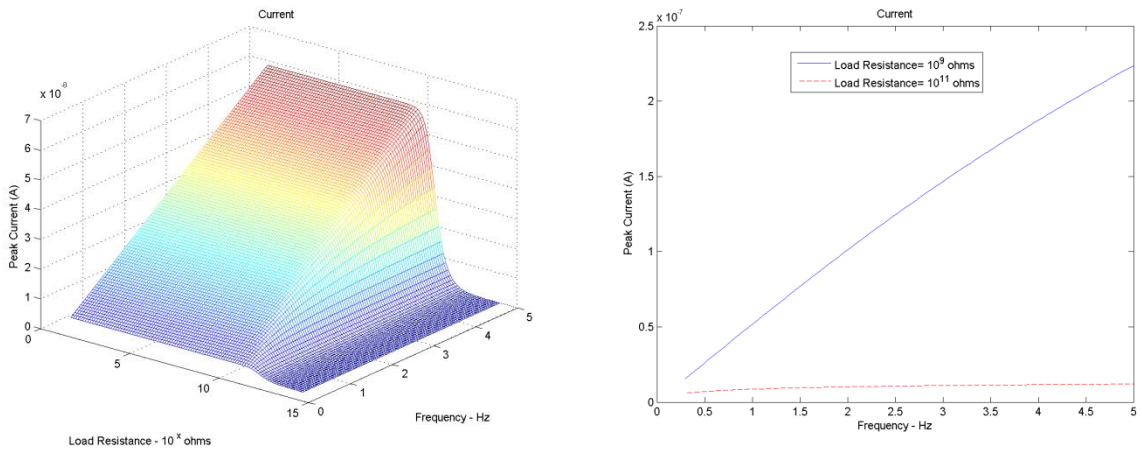

Figure 55. Frequency vs. Current

Frequency of the applied load has a positive correlation on the electrical outputs (Figure 53-55). At resistances below the resistance for maximum power, increases in frequency increase the power and current. Above that resistance, however, the changes in frequency have little effect on the two electrical outputs. Voltage only shows a positive correlation with frequency for values between 10^9 Ω to 10^{12} Ω. The maximum voltage is not affected by changes in frequency.

The value of this variable will be low for this application. People who just had spine surgery are going to be in pain for weeks after surgery, so high impact, high frequency activities are unlikely. Sprinting, for example, would generate a high amount of current since it applies both high frequency and high force to the implant, but would probably be much too painful for the patient for some time. For awhile after surgery, walking is probably one of the most intense activities that can be expected to be performed. Also, as can also be seen on Figure 53-55, it is important to have some frequency to the force being applied. Just resting or laying down will not generate much, if any, electricity because the frequency is so low.

Variables with Lower Level Effects

The Young's modulus for both the particles and matrix showed virtually no change (<1%) in electrical outputs over the realistic ranges for the moduli. This is not unexpected since the Young's

modulus is a mechanical property of the material, rather than an electrical one. The resistivity of the particles also showed virtually no change in power, voltage, and current outputs.

Material Comparison

Matrix Material

Figures 56-58 show the change in power, voltage, and current over a range of load resistances for different matrix materials.

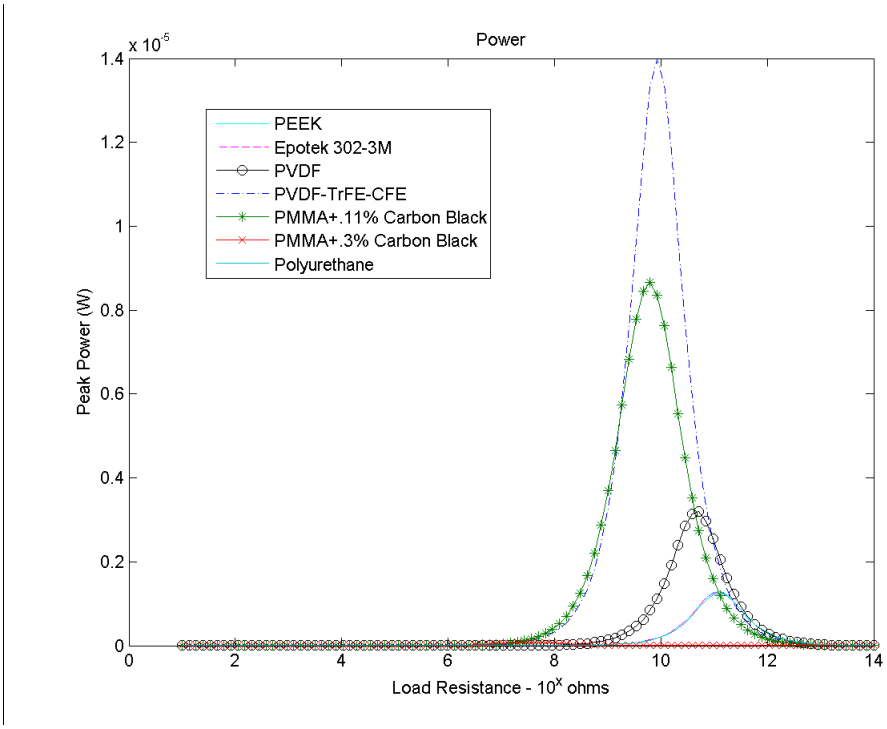

Figure 56. Comparison of power generated by different matrix materials over a range of load resistances

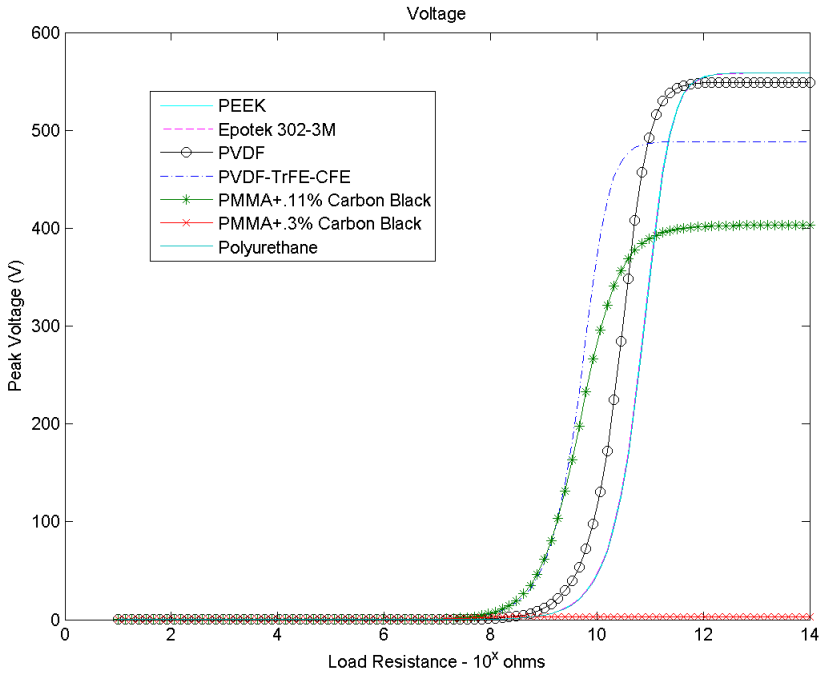

Figure 57. Comparison of voltage generated by different matrix materials over a range of load resistances

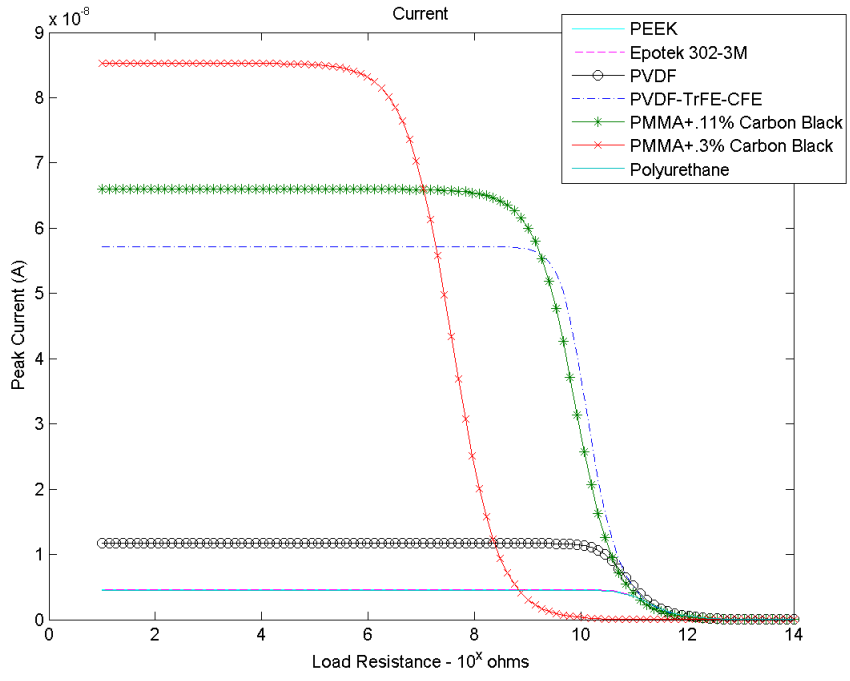

Figure 58. Comparison of current generated by different matrix materials over a range of load resistances

The analysis of different matrix materials generated useful results (Figure 56-58). To deliver a current density in the therapeutic window, matrix materials that deliver the greatest amount of current are superior. From the materials simulated, this means that PMMA with .3% carbon black is the best matrix, with PMMA with .11% carbon black and PVDF-TrFE-CFE also showing high current values (Figure 58). Epotek 302-3M, PEEK, and polyurethane all have extremely similar results, practically overlayed on each other on the graphs. The electrical outputs generated by them are low compared to the other materials. The maximum current generated by PMMA with .3% carbon black is 17 times greater than the maximum current generated by Epotek 302-3M, the material used in the experimental testing.

These results can be best understood from examining the individual variable analysis. The only variables that changed for each matrix material were the dielectric constant, resistivity, and Young's modulus. An increase in the matrix's dielectric constant greatly increased the power and current output, while Young's modulus showed virtually no effect (<1%) on the electrical outputs. The resistivity of the matrix showed little effect on the current, but once the resistivity drops below 10^{12} Ω*cm, the power drops to near zero. PMMA with .3% carbon black has a high dielectric constant, but low resistivity, giving it the highest current, but the lowest power of all seven materials. PVDF-TrFE-CFE has a high dielectric constant and a high resistivity, giving it both a high power and high current output compared to the other materials. PMMA with .11% carbon black is similar to PVDF-TrFE-CFE in that it shows both a high power and current. PEEK, polyurethane, and Epotek 302-3M show similar, but low results since they have the same low dielectric constant and a resistivity well above 10^{12} Ω*cm.

Particle Material

Figures 59-61 show the change in power, voltage, and current over a range of load resistances for different particle materials.

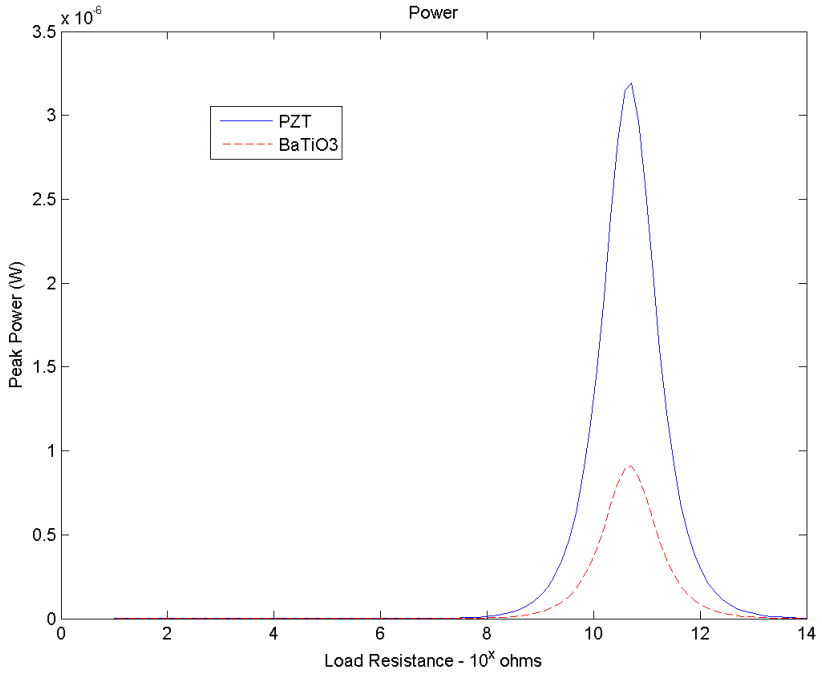

Figure 59. Comparison of power generated by different particle materials over a range of load resistances

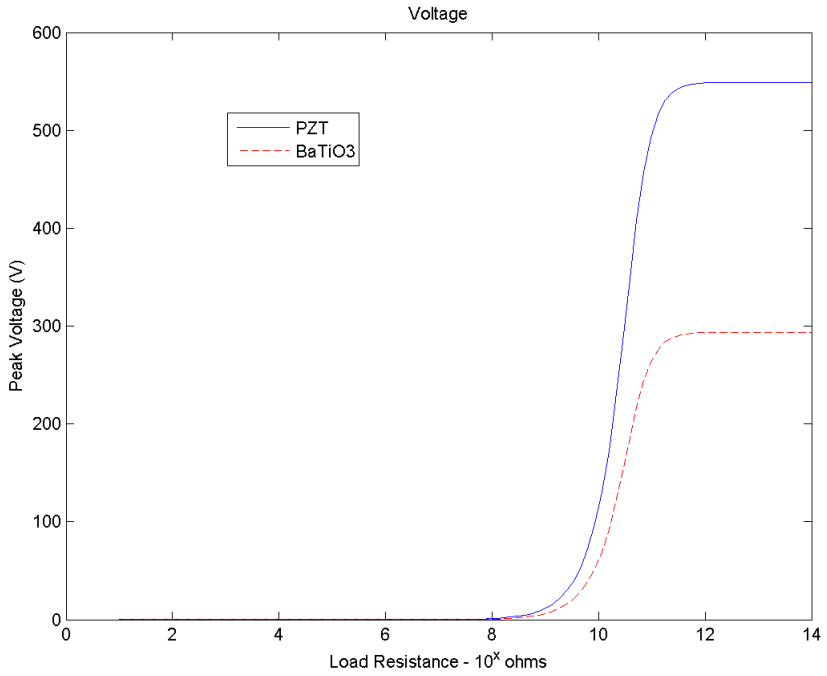

Figure 60. Comparison of voltage generated by different particle materials over a range of load resistances

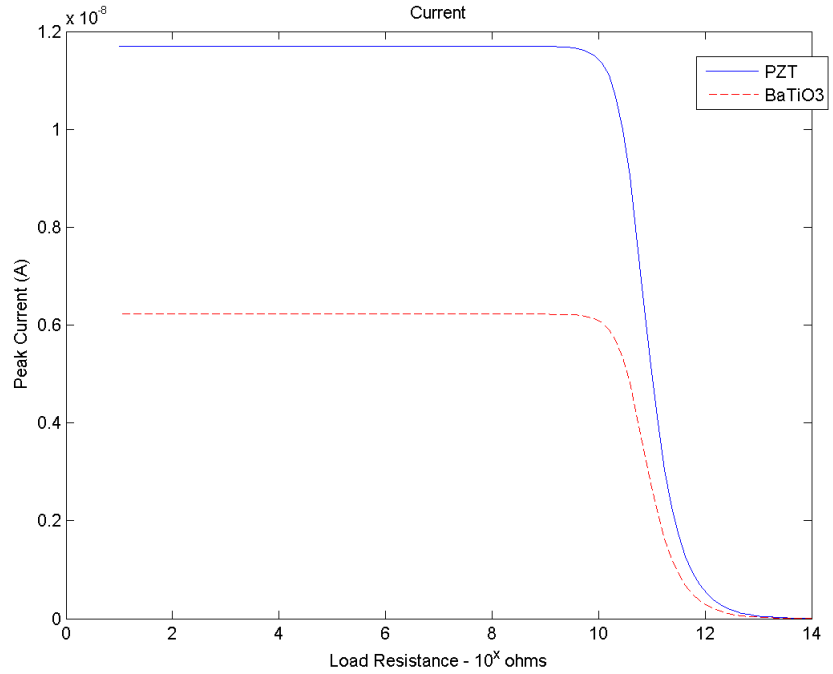

Figure 61. Comparison of current generated by different particle materials over a range of load resistances

From these figures, PZT shows better electrical outputs than $BaTiO_3$ (Figure 59-61). PZT shows nearly triple the power and about double the voltage and current as $BaTiO_3$. The main factor in this is

PZT's higher d_{33} value. $BaTiO_3$ has a lower dielectric constant that PZT, which should improve its electrical outputs, but it is not enough to compensate for a d_{33} value that is less than half that of PZT. Although PZT is not considered biocompatible, the implant design has the piezoelectric composite embedded in an insulating layer of biocompatible material (Figure 22). Choosing a strong, biocompatible material for the insulating layer, such as PEEK, will prevent the PZT particles from coming into contact with the body, making PZT the better option than $BaTiO_3$. However, if the appropriate current density can be generated with $BaTiO_3$, it would be preferable due to its biocompatibilty.

The lumped parameters model can also be applied to the recent paper on piezoelectric fibers (48) to predict the theoretical increase in current due to the aspect ratio of the particles. Using the values supplied by van den Ende, et al. (47, 48)(Table 6), the lumped parameters model predicted a 34.4 times increase over the spherical particles. According to the lumped parameters model, the material choices of polyurethane and Epotek 302-3M will produce almost identical electrical outputs, so the increase should be unaffected by matrix material (Figure 56-58). Since the papers supply only the composite values for d_{33} and dielectric constant and not the values for the particles or matrix, these resutls cannot be directly compared to the other theoretical values; however, when compared to each other, the results suggest an increase in properties with the PZT fibers.

Particle Type	Volume Fraction	Matrix Material	Composite d_{33} (pC/N)	Composite Dielectric Constant	Theoretical Max Current (A)	Increase over Spheres
PZT Fibers	20%	Polyurethane	350	300	$1.1*10^{-6}$	34.4x
PZT Spheres	20%	Epotek 302-3M	10	18	$3.2*10^{-8}$	NA

Table 6. Properties and theoretical current produced by materials used by van den Ende, et al. (47, 48)

VII. Material Generation Research

Piezoelectric composites specimens were developed concurrently with the power analysis. Since DEP is a manufacturing method that has been proven to work, the material generation research began using it to structure the composites. When DEP reached the stage where it could be used to successfully create composites and could be used to create the fusion cage, PEP was attempted.

DEP

Many of the possible matrix materials that would be used in the actual implant require high (> 175^{o}C) temperatures. As of now, the manufacturing setup does not have the equipment to process materials at elevated temperature while cyclically compressing it and/or passing an AC current through it. For proof of concept testing, a two part epoxy (Epotek 302-3M, from Epoxy Technology Inc., Billerica, MA, USA) can be used to form a matrix material at room temperature. Epotek 302-3M was chosen because of its low conductivity, its ease of use, and its previous use in DEP research (51). Compared to other epoxies, Epotek 302-3M has a high viscosity which helps to prevent sedimentation of the particles as the mixture solidifies(51).

Piezoelectric composites were created through the following steps:

- Part A and B of the epoxy were placed under a vacuum and heated for one hour
- Particles were mixed into Part A, and everything was vacuumed and heated for an hour
- Part A and B were mixed vigorously for 3 minutes, vacuumed for two minutes to remove any final air bubbles, and injected using a syringe into the assembled jig

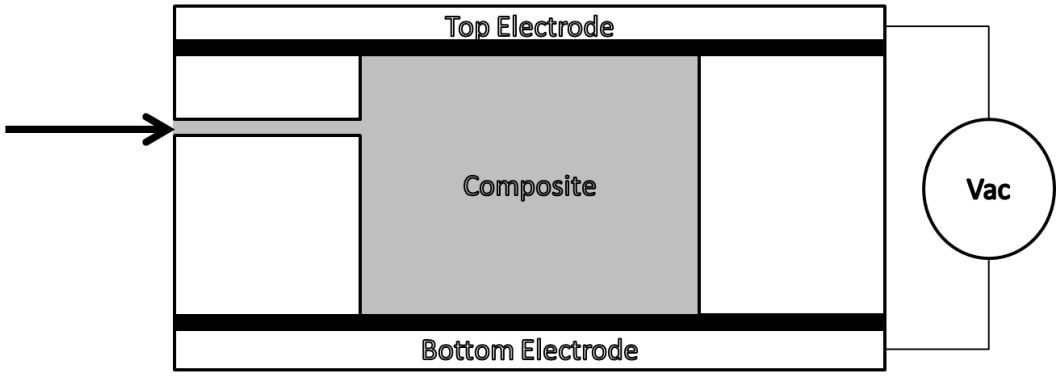

Figure 62. Schematic of the DEP setup

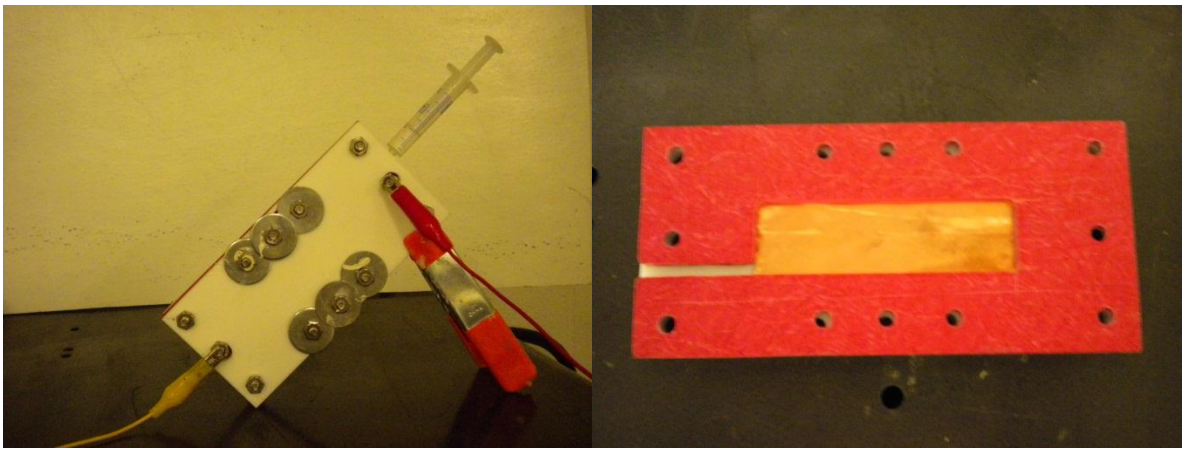

Figure 63. The DEP manufacturing setup and an inside view of the DEP jig

DEP was then performed on the curing composite by passing a 1 kV/mm electric field at 1 kHz through the thickness of the composite for three hours (Figure 62, 63). At that point, the composite had gelled, and was left in the jig overnight to completely solidify. Copper electrodes were attached to each side during the solidification of the composite (Figure 63). The electrodes covered the majority of the composites, but were trimmed back slightly from the edge to prevent electricity from shorting around the composite during the poling process. Through this process, composites measuring 78 mm by 23 mm by 3.5 mm were created, which were then divided into four specimens measuring 19.5 mm by 23 mm by 3.5 mm (Figure 64).

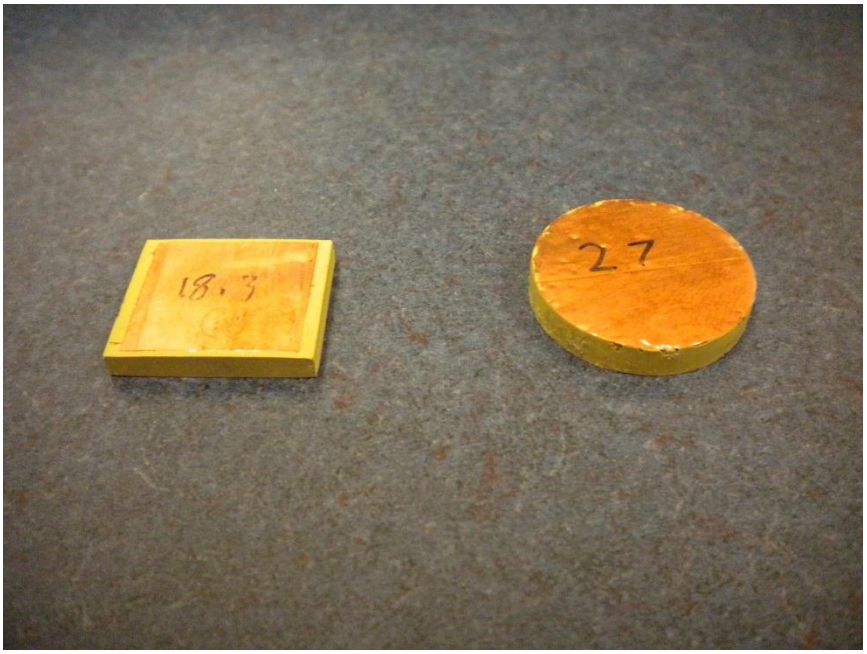

Figure 64. DEP specimen (18.3) and PEP specimen (27)

Two of the main problems encountered early in DEP research were bubbles in the composites and the molds not completely filling. If the bubbles were too prevalent, the material would often short during poling, making it impossible to get up to the poling voltage necessary to orient the particles' dipole moments. In order to eliminate bubbles, the materials were heated and degassed after every step to get as much air out as possible. Part A and B, the syringes, and the jig were all heated to 60^{o}C, which caused the mixture of A and B to be less viscous and easier to inject into the jig.

After the specimens were created, they also had to be poled. As mentioned previously, the limiting factor of DEP is the high electric fields required to pole the materials. Each DEP specimen was poled by applying a DC electric field of 10 kV/mm for 30 min. For the larger DEP specimens, this required a poling voltage of 37 kV. The specimens were tested an hour later. Many of the thinner specimens with air bubbles had problems of electricity shorting directly through the composite, burning a hole through the material. As the process was refined, the amount of air bubbles was reduced, and the electricity shorting through the material ceased to be a problem.

PEP

The manufacturing method of PEP is similar to DEP, but requires that the composite be compressed in phase with the electric field while the material solidifies (Figure 65).

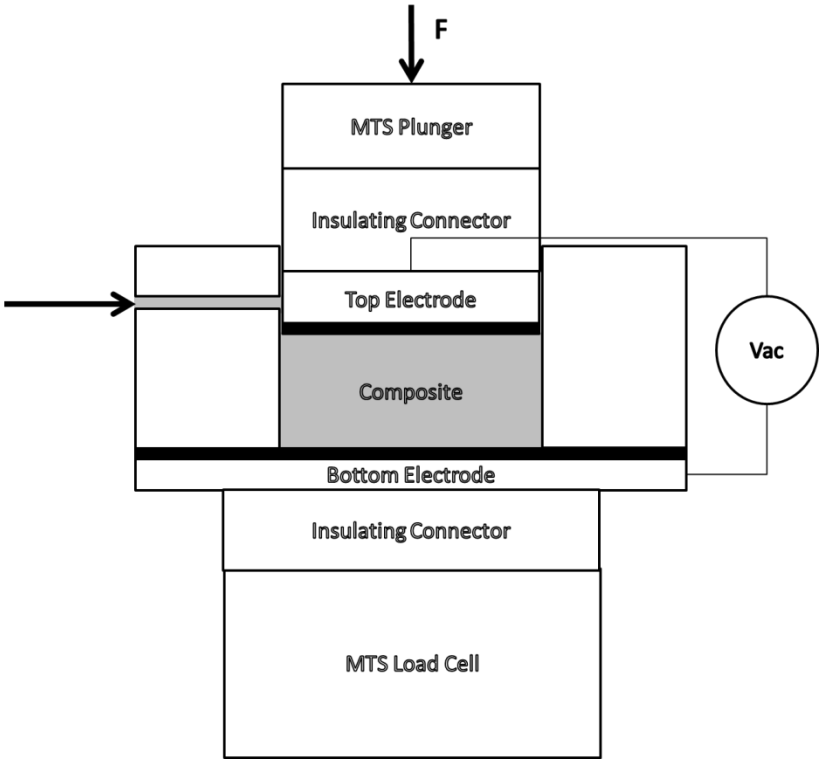

Figure 65. Schematic of the PEP setup

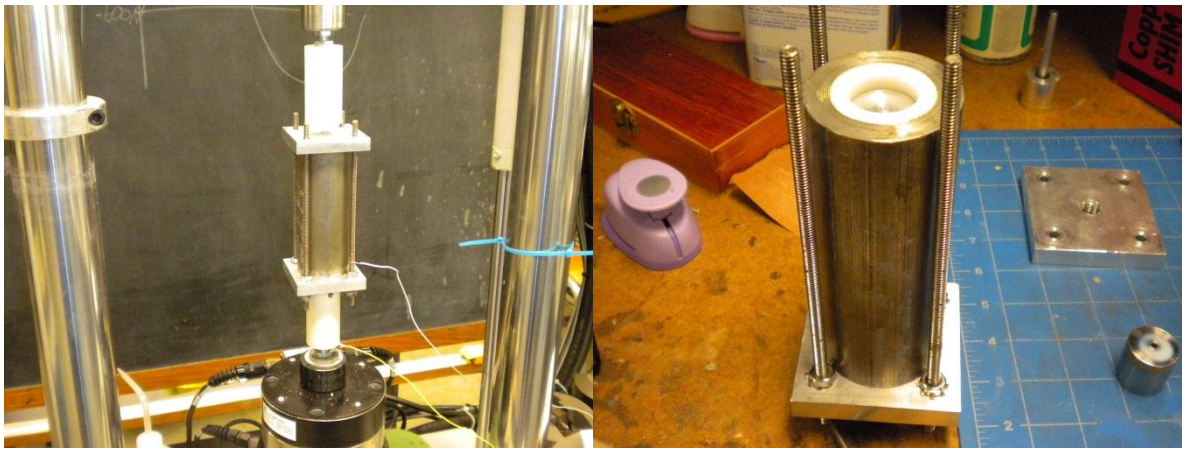

Figure 66. The PEP manufacturing setup and an inside view of the PEP jig

In PEP, the jig is placed into the MTS 858 Mini Bionix II with the top off to allow for injection of the composite (Figure 66). The composite is prepared the same way as in DEP. The composite is then injected into the watertight inner chamber. The bottom plunger of the jig is brought up until both the top and bottom plungers are in contact with the curing composite and a preload of 600 N is applied. A voltage with an amplitude of 500 V is then cyclically applied at a frequency between 10-50 Hz. The MTS 858 Mini Bionix II is then brought into phase with the electric field, and compresses the composite cyclically with an amplitude of 400 N. To this point, PEP has been unable to create poled piezoelectric specimens. Research into this manufacturing method is still young, however, and solutions are being sought.

Experimental Power Analysis

Experimental Test Setup

A power analysis was conducted on the composite specimens by compressing them cyclically with a mean compressive force of 600 N and an amplitude of 500 N to mimic physiological loading. The tests were conducted at 1, 5, and 10 Hz. Data were collected continuously during the 15 cycles that were completed at each resistance and frequency. The MTS 858 Mini Bionix II was used to apply compression and measure the voltage across a collection of 18 different load resistances, ranging from 2 MΩ to 5 TΩ. A simple setup was used to measure the voltage (Figure 67).

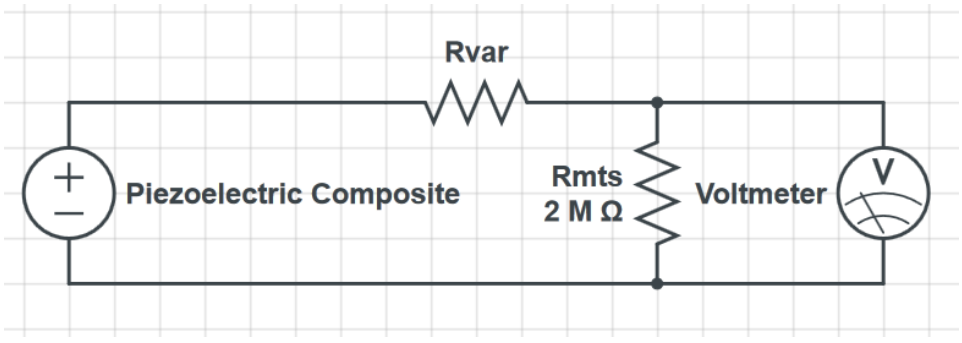

Figure 67. Test setup for experimental power analysis

From these tests, the voltage, power, and current curves could be determined. Four different composites were tested. From the experimental power analysis, the effects of composite structure, volume fraction, compression frequency, and heat treatment could be compared. The test results were also compared to the theoretical results from the lumped parameters model. The data for each composite is shown in Table 7. The thickness and cross-sectional area of each specimen was roughly the same. The PZT particles used in this experiment had a layer of binding agent on the surface of the particles. To see if this caused a change in the power generated by the composite, the particles used in Composite 1 were heated to 700 ^{o}C for one hour to burn off the binding agent. Second batches of Composite 3 and 4 were created to show a measure of repeatability in the electrical outputs.

	Particle Material	Matrix Material	Volume Fraction	Composite Structure	Structure Method	Particles Heat Treated	Number of Batches	Total Specimens
Composite 1	PZT	Epotek 302-3M	30%	1-3	DEP	Yes	1	4
Composite 2	PZT	Epotek 302-3M	30%	1-3	DEP	No	1	4
Composite 3	PZT	Epotek 302-3M	20%	1-3	DEP	No	2	5
Composite 4	PZT	Epotek 302-3M	20%	0-3	None	No	2	5

Table 7. Properties of the composites tested

Experimental Test Results

From the power analysis results for each composite, the peak voltage, power, and current were determined. The results for each individual specimen were averaged to calculate the result for the different composites. On Figure 68-84, the standard deviation for each point has been plotted as error bars. Unless specifically stated otherwise, all results shown occurred with a compressive frequency of 1 Hz.

Composite Structure

For the Composite Structure comparison, Composites 3 and 4 were analyzed. Figures 68-70 show the change in power, voltage, and current over a range of load resistances for 1-3 and 0-3 composites.

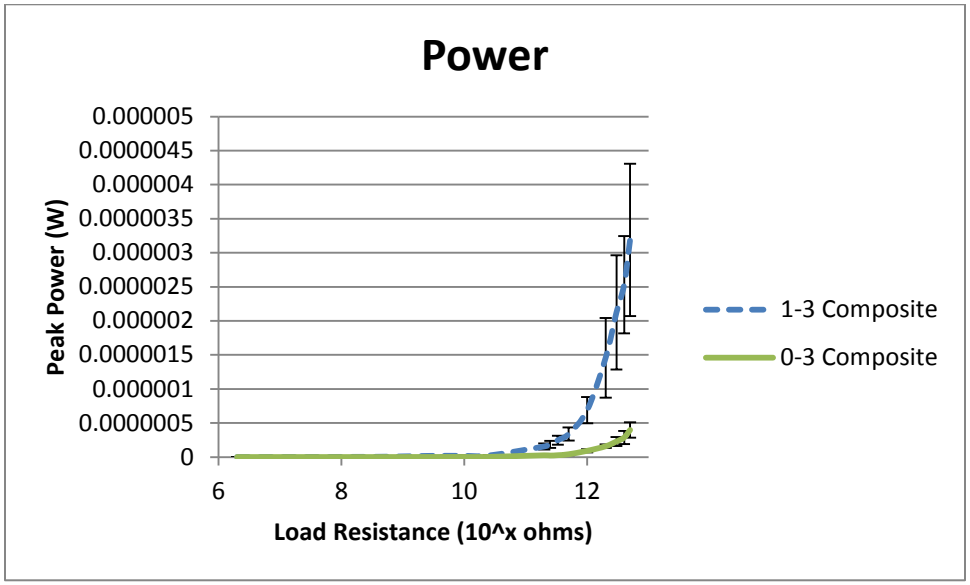

Figure 68. Composite Structure Comparison. Peak Power vs. Load Resistance for Composites 3 and 4

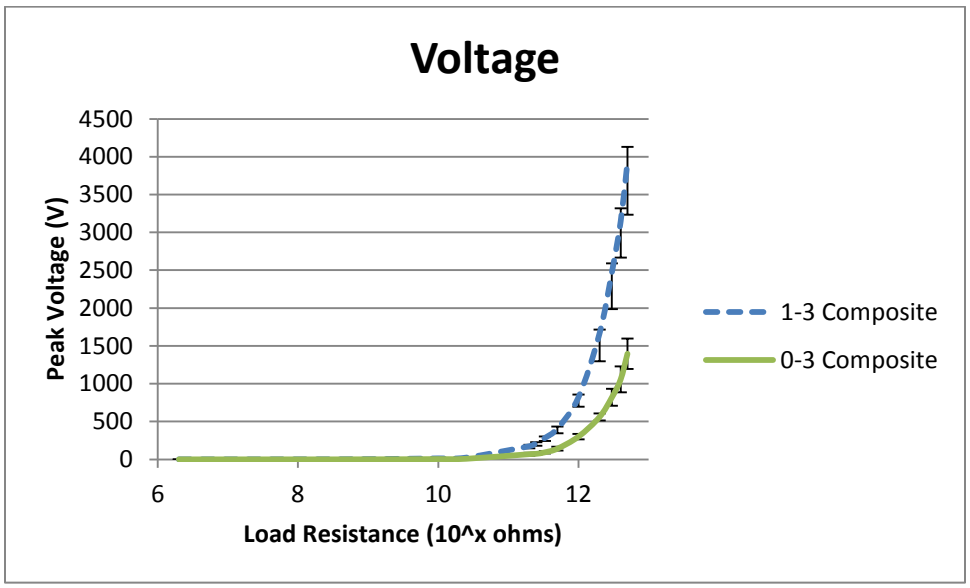

Figure 69. Composite Structure Comparison. Peak Voltage vs. Load Resistance for Composites 3 and 4

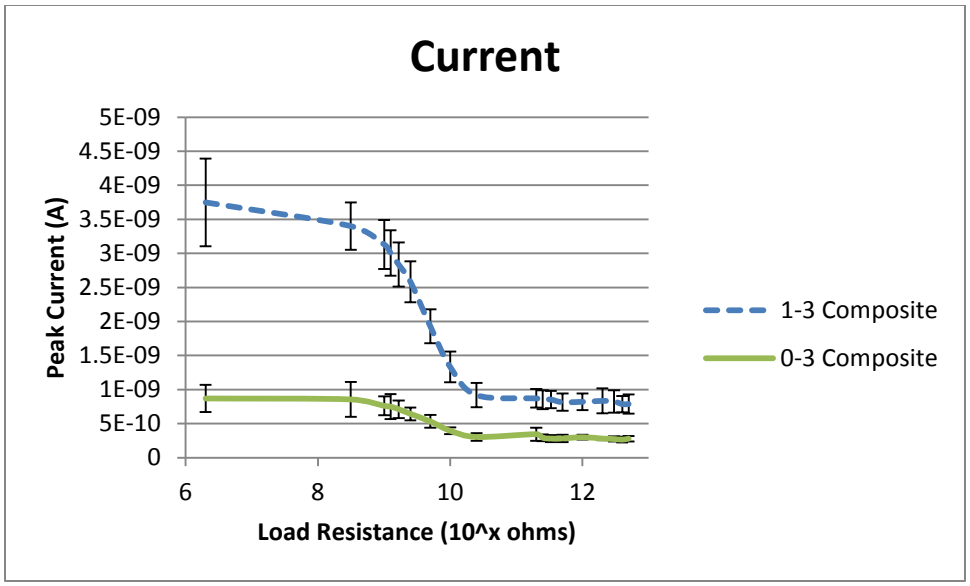

Figure 70. Composite Structure Comparison. Peak Current vs. Load Resistance for Composites 3 and 4

As shown in Figures 68-70, the 1-3 composite shows greater electrical outputs than the unstructured 0-3 composite. The 1-3 composite generated 8.02 times the 0-3 results for maximum power (Figure 68). The difference for voltage was less, with the 1-3 composite generating 2.82 times the voltage (Figure 69). The maximum current for 1-3 was 4.31 times that of the 0-3 composite (Figure 70).

These results were expected, especially since Composites 3 and 4 both were only 20% volume fraction composites. As shown in Figure 11, the difference in properties between 0-3 and 1-3 composites is accentuated at low volume fractions. Still, this is proof that DEP was able to successfully structure the composite and is a viable way to increase the piezoelectric properties of the composite during manufacturing.

To show repeatability between different batches of the same composite, two batches of Composite 3 and 4 were created. Composite 3 had four specimens in the first batch and one in the second. Composite 4 had three specimens in the first batch and two in the second. The results for the electrical outputs were similar between batches for either composite. Although the sample size is still

low overall, the results were able to show a measure of repeatability, leading to improved confidence in the electrical output values.

Volume Fraction

For the Volume Fraction comparison, Composites 2 and 3 were analyzed. Figures 71-73 show the change in power, voltage, and current over a range of load resistances for 20% and 30% volume fraction composites.

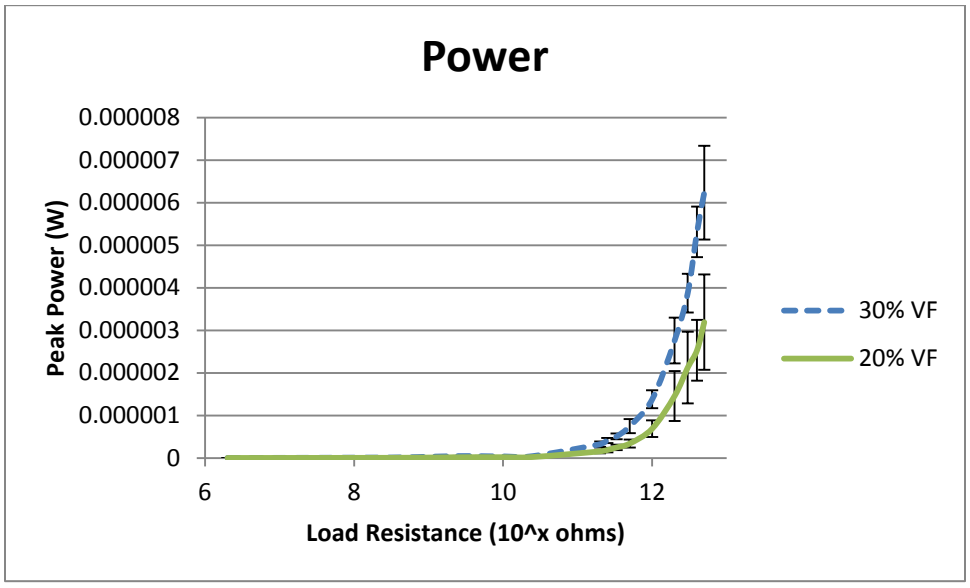

Figure 71. Volume Fraction Comparison. Peak Power vs. Load Resistance for Composites 2 and 3

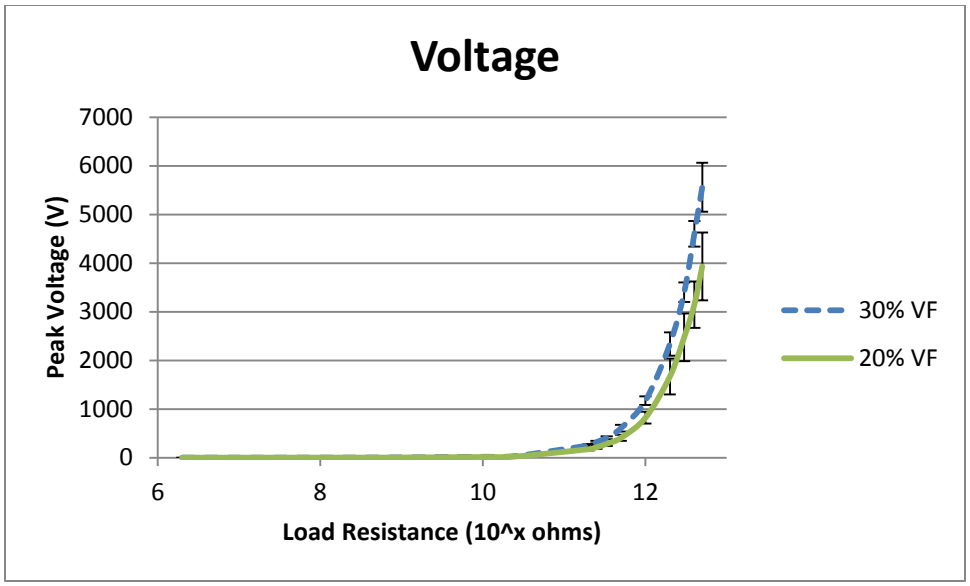

Figure 72. Volume Fraction Comparison. Peak Voltage vs. Load Resistance for Composites 2 and 3

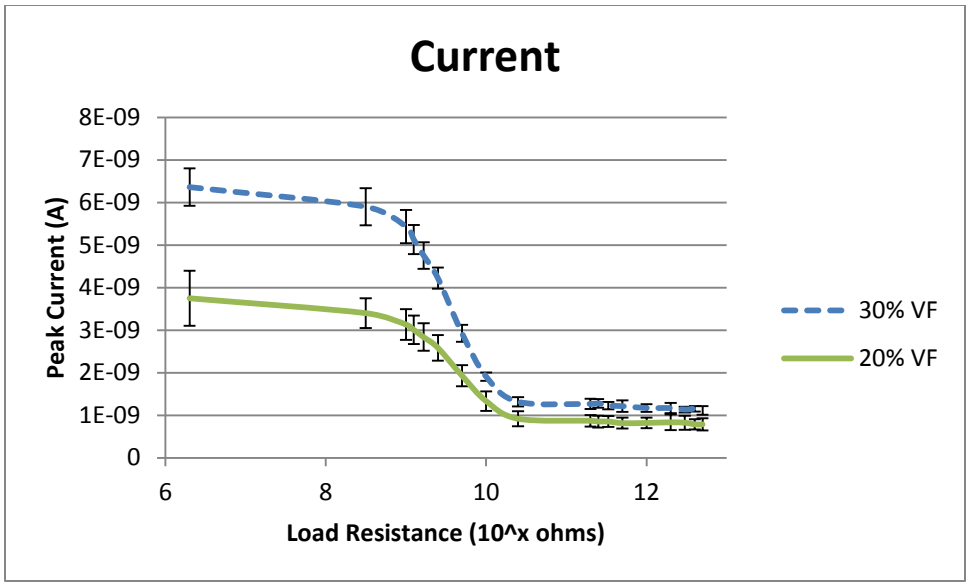

Figure 73. Volume Fraction Comparison. Peak Current vs. Load Resistance for Composites 2 and 3

As shown in Figures 71-73, the comparison between the two particle volume fractions was as anticipated. The maximum power is 1.95 times greater for the 30% volume fraction composite as compared to the 20% volume fraction. The increase in voltage, however, is smaller at only 1.41 times greater (Figure 71, 72). The maximum current for the 30% volume fraction composite is 1.70 times greater than the 20% volume fraction composite (Figure 73). The theoretical model for power

generation suggests that the maximum current will increase at an even faster rate as volume fraction increases, until it reaches a point where manufacturing becomes impossible (Figure 31). Based off of the experimental results and the theoretical model, increasing the volume fraction of the particles should increase the amount of current available to deliver to the patient.

Compression Frequency

For the Compression Frequency comparison, Composite 2 was analyzed. Figures 74-76 show the change in power, voltage, and current over a range of load resistances for 1, 5, and 10 Hz.

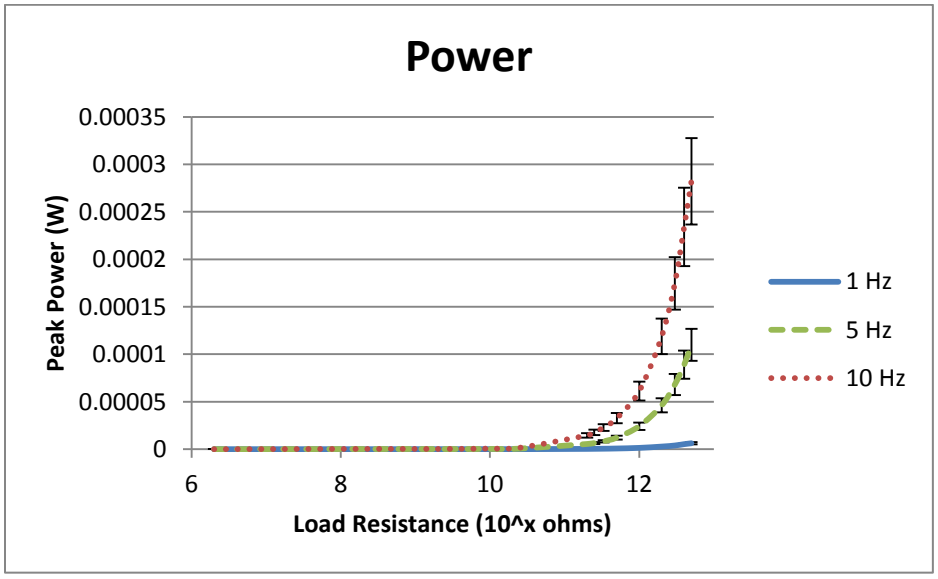

Figure 74. Compression Frequency Comparison. Peak Power vs. Load Resistance for Composite 2

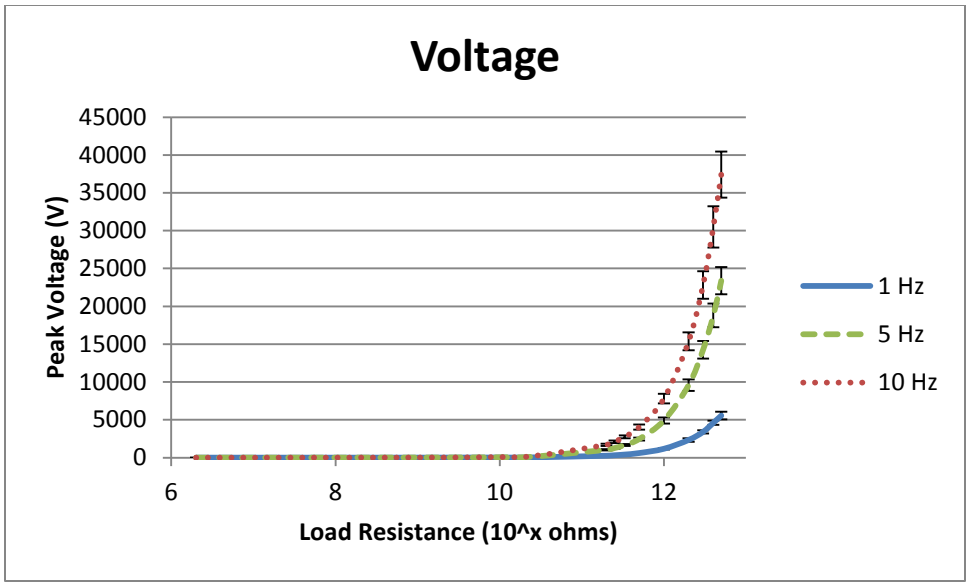

Figure 75. Compression Frequency Comparison. Peak Voltage vs. Load Resistance for Composite 2

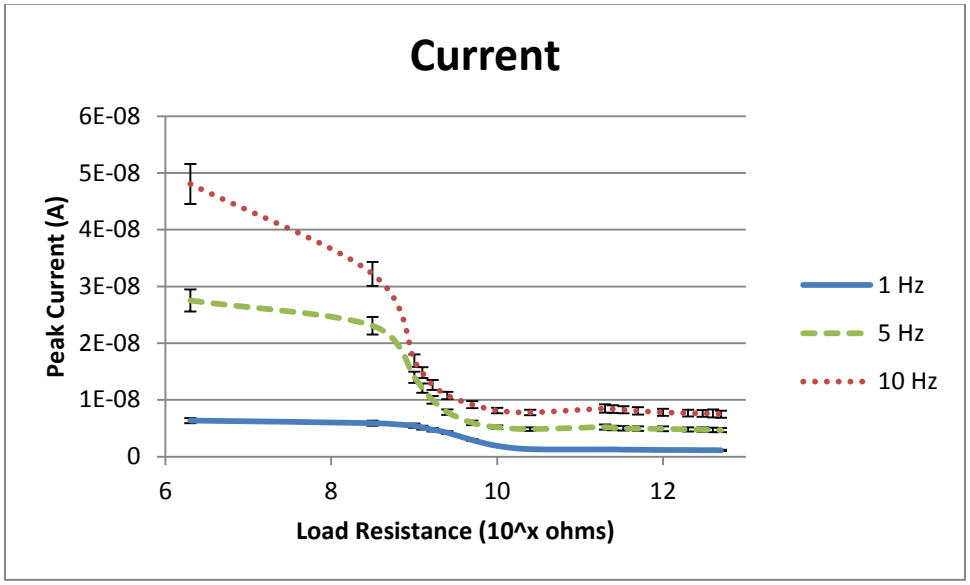

Figure 76. Compression Frequency Comparison. Peak Current vs. Load Resistance for Composite 2

The results for the effect of compression frequency followed the expected trend based on piezoelectric theory. As frequency increased, so did the electrical outputs. For power and voltage, the increase was greater between 1 and 5 Hz than 5 and 10 Hz (Figure 74, 75). Power showed a 17.7 times increase between 1 and 5 Hz and a 2.56 times increase between 5 and 10 Hz. The increase for voltage

was less, with a 4.21 times increase between 1 and 5 Hz and a 1.60 times increase between 5 and 10 Hz. Current displayed an increase of 4.32 times between the maximum current of 1 and 5 Hz, and an increase of 1.75 times between 5 and 10 Hz (Figure 76). One difference between the frequencies occurs at the maximum current outputs. Whereas the current at 1 Hz has a flat region at low resistances, 10 Hz decreases more quickly. Part of this could be due to the resistances that were chosen for testing. The resistances chosen were concentrated in the theoretical transition region, where power theoretically peaks and current decreases. Experimentally, however, the current begins to change earlier than expected, especially for 10 Hz. Further testing will need to be done to quantify where the transition begins for the 10 Hz tests. These results show that if the patient was to engage in an activity with a higher frequency than a slow walk, the amount of current generated could be increased.

Heat Treatment

For the Heat Treatment comparison, Composites 1 and 2 were analyzed. Figures 77-79 show the change in power, voltage, and current over a range of load resistances for composites with heat treated and non-heat treated particles.

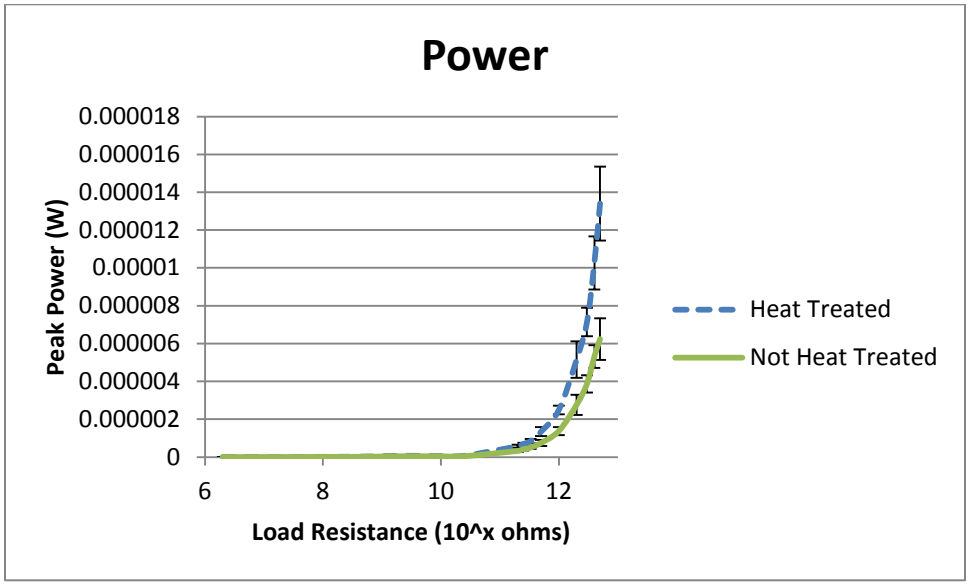

Figure 77. Heat Treatment Comparison. Peak Power vs. Load Resistance for Composites 1 and 2

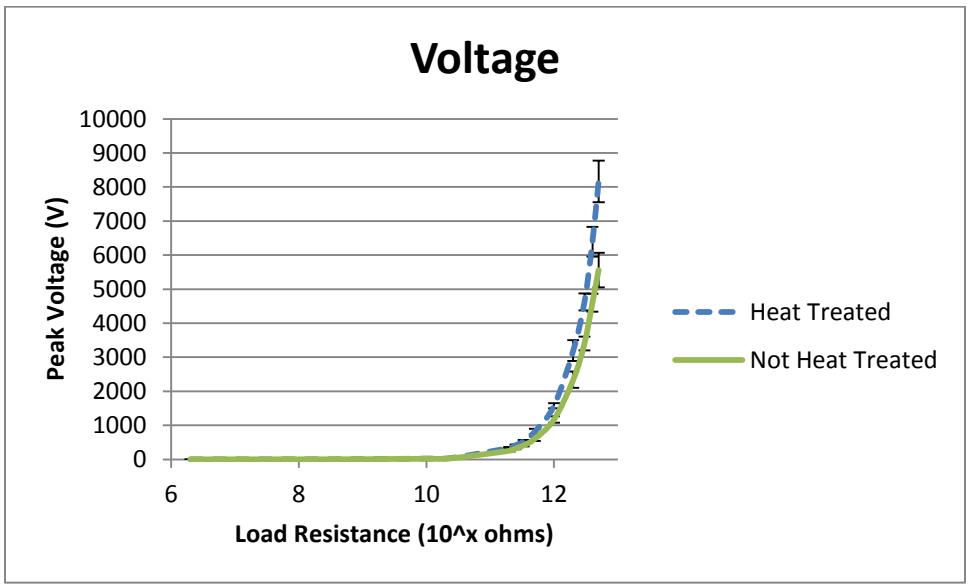

Figure 78. Heat Treatment Comparison. Peak Voltage vs. Load Resistance for Composites 1 and 2

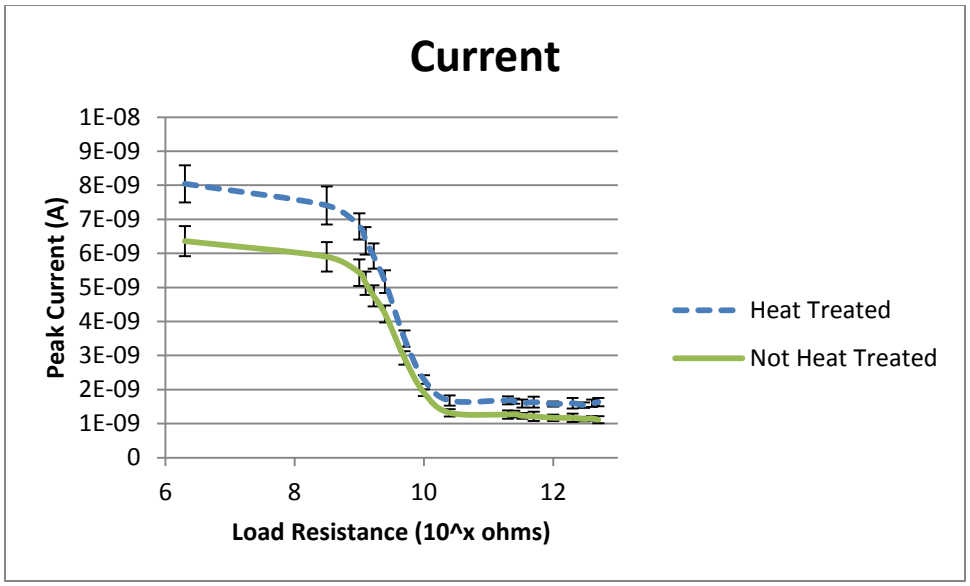

Figure 79. Heat Treatment Comparison. Peak Current vs. Load Resistance for Composites 1 and 2

Heat treatment of the particles had a lesser effect on the electrical outputs than the other factors that were compared. The heat treated composite displayed higher results for all the electrical outputs than the non-heat treated specimen (Figure 77-79). Maximum power for the heat treated samples was 2.15 times greater and the maximum voltage was 1.47 times greater than the non-heated treated particle composites. The current displayed was 1.26 times greater for the heat treated samples. Simply choosing particles without the binding agent should provide the increase in electrical outputs seen here. Since the sample size of Composite 1 and 2 is small (1 batch, n=4), however, it is difficult to tell for sure that the heat treated particles improve the current output. More specimens would need to be created to validate this trend.

Experimental vs. Theoretical Results

For the Experimental vs. Theoretical Results section, Composites 2 and 3 were compared to the results predicted by the lumped parameters model. The results for voltage, power, and current are shown for Composite 2 (Figure 80-83). Only current results were shown for Composite 3 (Figure 84). As noted previously, 0-3 composite equations were used for the theoretical model, so the theoretical model should produce lower electrical outputs than the experimental results.

Unfortunately, many of the input values used in the theoretical model cannot be measured using available lab equipment. The dielectric constant of the matrix and the d_{33} coefficient, dielectric constant, resistivity and Young's modulus of the particles could not be directly measured. Therefore, the values used for these inputs are literature values, rather than experimentally measured values. Due to this, results will be considered successful if the theoretical and experimental results are in the same order of magnitude and follow the similar trends.

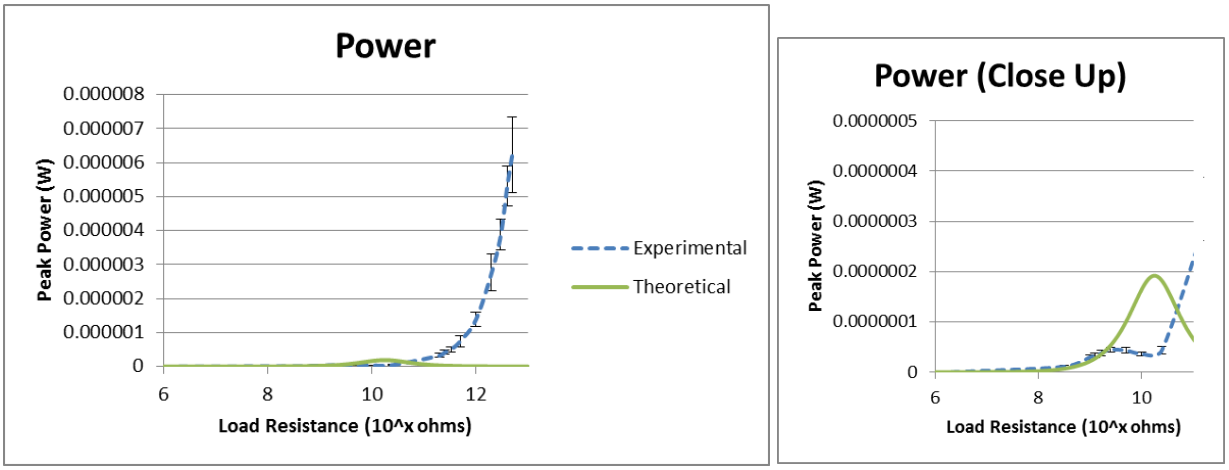

Figure 80. Experimental vs. Theoretical Results for Composite 2. Peak Power vs. Load Resistance

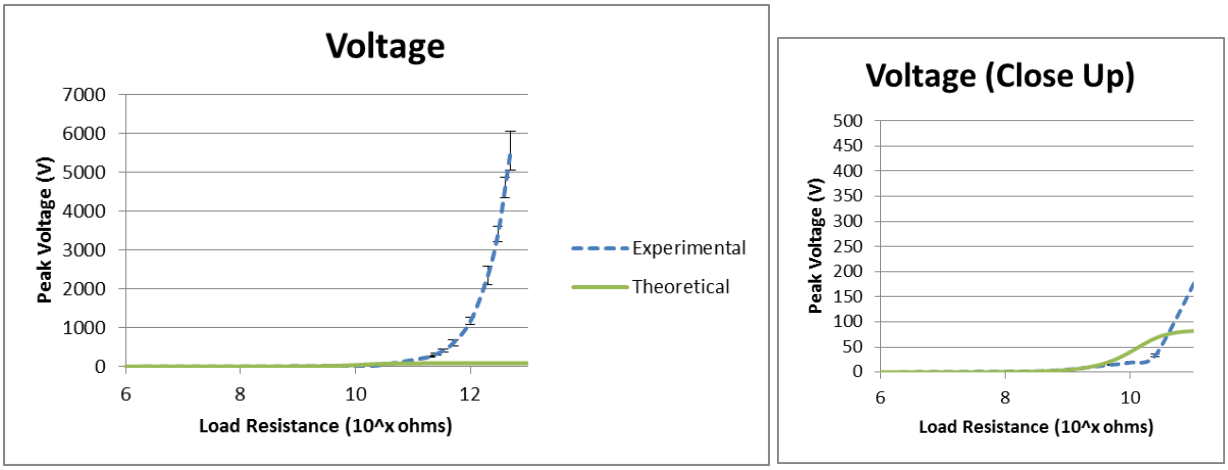

Figure 81. Experimental vs. Theoretical Results for Composite 2. Peak Voltage vs. Load Resistance

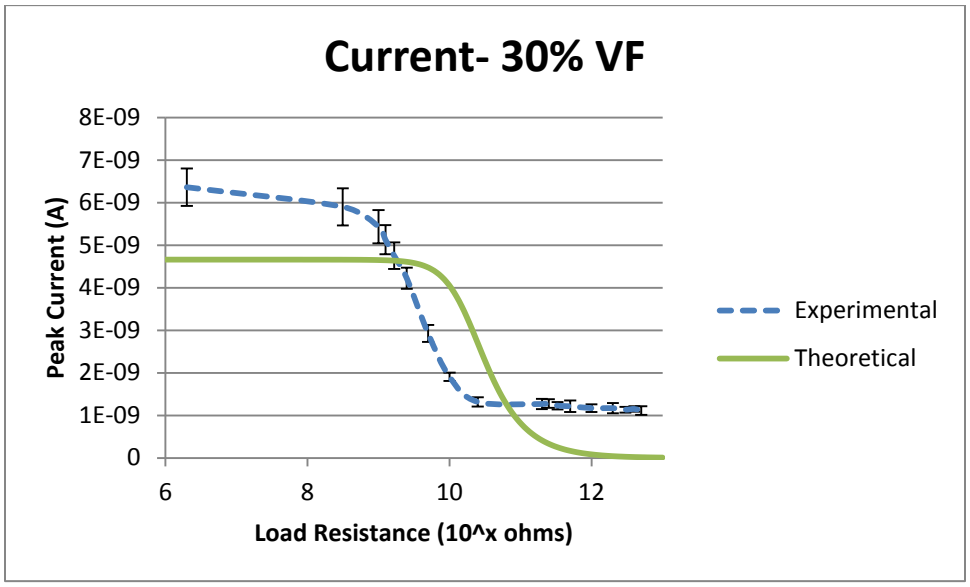

Figure 82. Experimental vs. Theoretical Results for Composite 2. Peak Current vs. Load Resistance

As can be seen in Figure 80 and Figure 81, voltage and power show greater values at high resistances than those originally predicted with the theoretical model. Experimentally, the power and voltage continue to rise, even as the resistance reaches 5 TΩ. Theoretically, the voltage should plateau at high resistances and the power should peak and decrease. It is possible that 5 TΩ was not a high

enough resistance for these to occur. At lower resistances, from 10^6 Ω to $10^{9.5}$ Ω, the theoretical models for voltage and power are closer in value (Figure 80 and 81 close ups).

The experimental values for current are closer to what was theoretically predicted than the voltage and power results (Figure 82). The experimental values for current are within an order of magnitude and follow a similar trend as the theoretical model. These results are acceptable for preliminary research, considering that 0-3 composite equations were used and many of the input parameters used were taken from literature. Experimentally, the maximum current is higher than what was predicted with the lumped parameters model. The maximum current produced was 26.7% greater the theoretical prediction. It was expected that the theoretical values would be lower since the composite terms used in the lumped parameters model were based off of 0-3 composites. Just like predicted, the current remained level over low resistances, but dropped off as the resistance increased with the change within 20% of the theoretical model. Based on this comparison, the lumped parameters model should be able to predict the output current of the piezoelectric composite within an order of magnitude. Further optimization of the lumped parameters model will allow for more accurate predictions for these values.

There are a few possibilities that would help account for the disparity between the voltage and power graphs. Five 1 TΩ resistors were used to create the upper resistances in this test, all of which have a tolerance range of +0%, -20%. The equipment available, however, cannot measure resistances of that magnitude, meaning the actual values of the resistors are not validated. If the values of the resistors were actually lower than 1 TΩ, the experimental values presented would overestimate the electrical outputs at high resistances. It is also possible that since the value of resistances being used are extremely high, the electricity may actually be shorting across other circuitry and bypassing the large resistance. This could possibly occur between rows used on the breadboard. If the electricity was able to

find a path with less resistance, it would cause the experimental electrical outputs to be overestimated, as well. This is at least partially supported by the close up of Figure 80, where the experimental values begin to decrease $10^{9.5}$ Ω, before increasing more rapidly at $10^{10.5}$ Ω. However, since maximum current is of primary interest and occurs at load resistances below $10^{9.5}$ Ω, the model should be able to be used with confidence to find trends in current generation.

Experimental and theoretical current outputs for different parameters are compared in Figures 83 and 84. Figure 83 shows the current generated by Composite 2 for different compression frequencies. At 5 Hz, the maximum current measured was 15.3% greater than the theoretical prediction. At 10 Hz, the experimental current values began to decrease at lower resistances than theoretically predicted, but the maximum current was only 3.1% greater than the theoretical prediction. From this data, it can be shown that the theoretical model accurately predicts the change in maximum current as the compressive frequency increases.

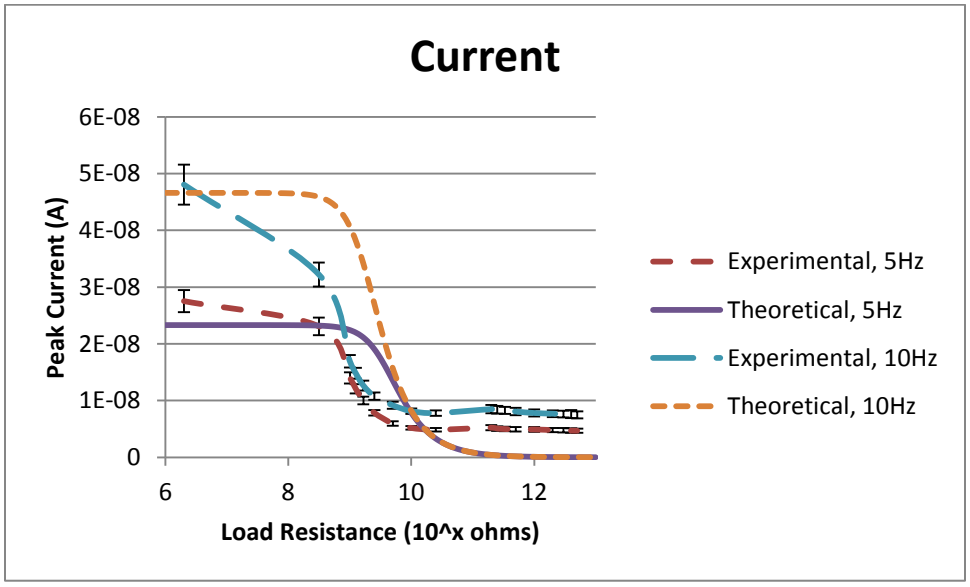

Figure 83. Experimental vs. Theoretical Results for Composite 2. Peak Current vs. Load Resistance at 5 and 10 Hz

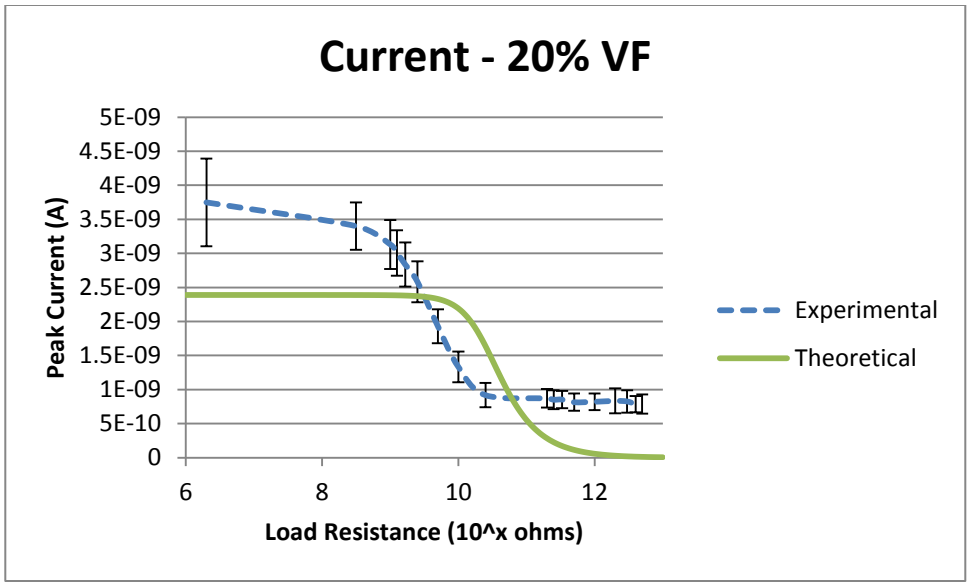

Figure 84. Experimental vs. Theoretical Results for Composite 3. Peak Current vs. Load Resistance for a 20% volume fraction composite

The maximum current generated for the 20% volume fraction composite was 36.3% greater than the theoretical prediction, which is not as close as previous comparisons, but is still within an order of magnitude (Figure 84). Since 0-3 composite equations were used, however, the theoretical values are expected to be lower than the experimental results. The difference between 0-3 and 1-3 composites is greatest at low volume fractions (Figure 11), which would explain why the results in Figure 84 do not compare as well as the other comparisons (Figures 82, 83). Based on the overall theoretical and experimental comparison, the theoretical model should be able to predict the maximum current within an order of magnitude and identify trends in the maximum current generated by the piezoelectric composite.

VIII. Proof of Concept Testing

Battery Recharge Tests

Since the composites manufactured using DEP can successfully generate electricity, the layered design for the implant is feasible. PEP has yet to create successful specimens, but the research is still ongoing. For a preliminary proof of concept, one of the specimens from Composite 2 (30% VF PZT and Epotek- 302-3M) was cyclically compressed using the MTS 858 Mini Bionix II and used to store energy on a small lithium-ion battery in a similar setup to what could actually be used on the implant (Figure 85). Based off of the experimental results, a 1 GΩ resistance was placed in series with the battery to raise the voltage generated by the piezoelectric composite higher than the voltage drop of the diodes, allowing electricity to pass through. Before charging, the battery was drained until it read 0 V. Similar to the experimental power analysis (Chapter VII), the composite specimen was poled for 30 min at 10 kV/mm and was tested an hour after the poling process finished. The composite was compressed with an amplitude of 500 N at 1 Hz to mimic physiological loading. The experimental setup is shown in Figure 86.

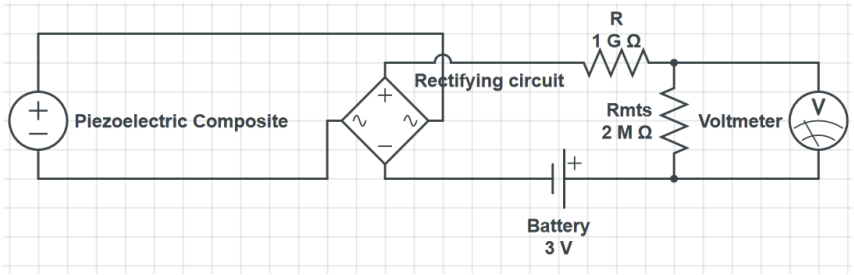

Figure 85. Layout of the battery charging tests

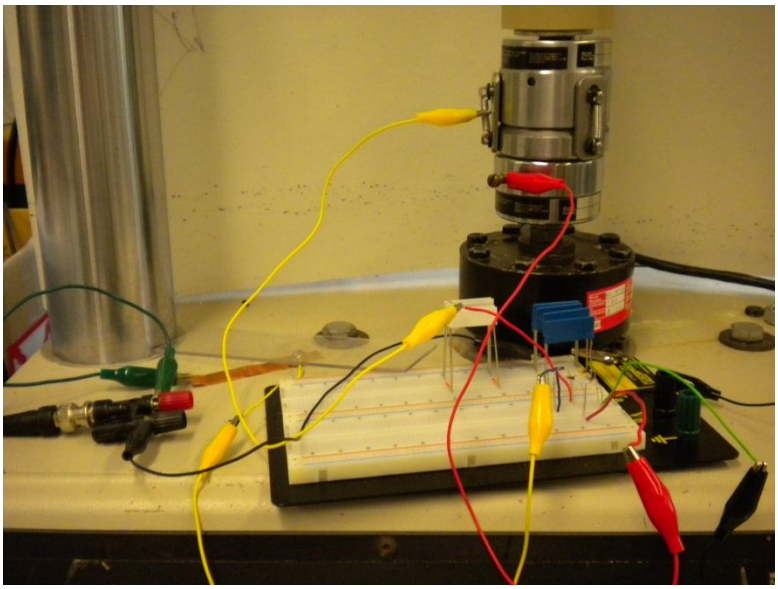

Figure 86. Picture of battery charging setup. The piezoelectric composite is compressed in the MTS shown in the upper right.

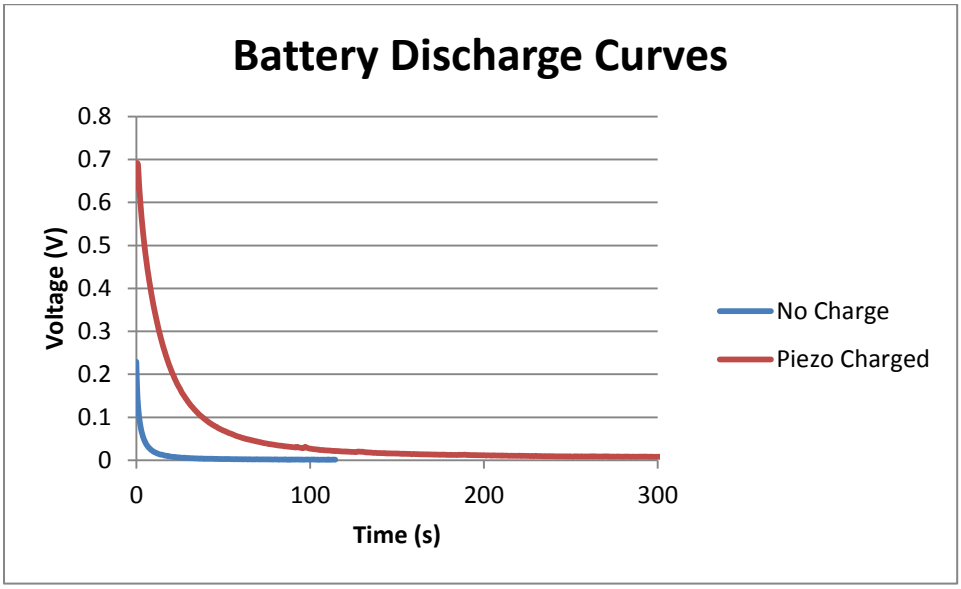

Figure 87. Battery discharge curves 5 hours after draining the battery. The No Charge line was not piezoelectrically charged. The piezoelectric composite was compressed for 5 hours for the Piezo Charged line.

The overall results for charging the battery are promising. After the test had been run for five hours, the battery was attached to a circuit with a total resistance of 46 kΩ, which simulated the body's natural resistance. The discharge curves are shown in Figure 87. As can be seen, the piezoelectric material was able to store a relatively small amount of energy on the battery (74 μ J). The "No Charge" line in Figure 87 depicts the battery's output voltage five hours after being completely drained. The

battery showed some recovery over the time period, although it was small compared to the energy stored by the piezoelectric composite. Two tests using the piezoelectric composite and two with no electrical stimulation were completed. The battery charged with the piezoelectric composite had an average total charge stored of 441.73 µC after five hours (Table 8). The battery that was not charged showed an average amount of 20.02 µC stored over the same time period.

Test	Charge Stored (µC)	Energy Stored (µ J)
Piezo Charged	440±100	74±11
No Charge	20±2	1.0±.3

Table 8. Battery discharge test data

Since the charge time for a rechargeable battery depends on the amount of current supplied to it (55), parameters for the implant will be chosen based on the power analysis that generate the highest current. Even though the amount of charge stored on the battery was low (Table 8) using the specimen from Composite 2 (30% PZT, Epotek 302-3M), improvements can be made for the actual implant. One method of increasing the current output of the piezoelectric cage would be to select materials with specific properties. According to Figure 58, a 17 times increase in current could be achieved by using PMMA with .3% Carbon Black instead of Epotek 302-3M as the matrix material (Figure 58). Much of this increase comes from PMMA and Carbon Black's high dielectric constant. The volume fraction of the particles could also be increased to improve current generation. An increase to a 70% volume fraction would quadruple the current output (Figure 31). Another increase in current could come from incorporation of the layered composite in the implant design. Assuming the implant is approximately 20 mm thick, it could be realistic to create an implant with ten layers. The power analysis indicates that this would lead to an additional 10 times increase in current (See Chapter VI). Another way to increase the current would be to improve the circuitry on the implant, perhaps by adding a Buck converter. A Buck converter could realistically increase the current from the piezoelectric composite by five to ten times. A final improvement to the composite could be to use piezoelectric fibers instead of spherical particles. As

shown in recent research, these fibers have dramatically raised the piezoelectric coefficients of the composite (Figure 13). At low volume fractions (<20%), this could lead to a 34.4 times increase in current output, according to the theoretical power analysis. At the moment, it is unknown how much this number is affected by large volume fractions (>50%), since the paper only tested up to 30% volume fractions (48).

Taking these improvements together, a low volume fraction composite could provide up to a 58,400 times increase in current over existing composites. Composite 1 (30% heat treated PZT) has delivered the highest current measured to this point: 8.04 nA at 1 Hz. Applying the theoretical increase to this current, the result is a peak current of 470 μA and an average current of 332 μA, which is 5.5 times greater than the 60 μA delivered by existing DC stimulation devices. This means that the piezoelectric fusion cage could continuously supply electricity to the fusion and have a larger electrode surface area than the DC stimulation devices.

IX. Conclusion

Through this research it has been determined that a piezoelectric spinal fusion cage is a feasible method to deliver electrical stimulation to spinal fusions. An initial design for the fusion cage was developed, containing a piezoelectric composite, a rectifying circuit, an insulated wire, an insulating layer, and an outer electrode. A power analysis using a lumped parameters model was completed to help guide material creation and implant design. Through this, it was determined that a layered composite and an increase in particle volume fraction would increase the performance of the design. PMMA with .3% Carbon black was determined to provide the highest current output of any of the matrix materials tested. Of the piezoelectric particles tested, PZT showed the higher electrical properties.

When the composites were created using DEP, the results followed trends that were expected. Higher volume fraction, a 1-3 structure, higher compression frequency, and heat treatment of the particles all increased the electrical outputs. The theoretical model accurately predicted the current output, and the voltage and power outputs at low resistances. The voltage and power at high resistances were greater than expected. PEP to this point has been unable to produce a poled piezoelectric specimen, but the research is still young and is ongoing. Proof of concept testing showed promising results because the composite was able to store electricity on a small cell battery. From the theoretical model and experimental results, it has been determined that by utilizing improved materials, circuitry, and the layered composite design, the current generated from the piezoelectric composite could theoretically be as high as 332 μA. This could be used to continuously supply an appropriate current density to the fusion, stimulating bone growth and speeding the fusion of the vertebrae.

Future Work

Tests to this point have focused on the creation of the composite and the determination of its ability to generate electricity. Now that experimental results have been obtained, improvements to the

theoretical power analysis can be made to more accurately model the generation of electricity, which should allow for a more accurate maximum current prediction. The next step is to validate several of the methods to improve current generation. A prototype made of three layered specimens will soon be made to verify that it results in a three time increase in current over a single specimen. Composites incorporating PZT fibers will be created, to verify the increase in piezoelectric properties that are expected. New matrix materials will also be tested, although this will take more time. Many of the matrix materials have high melting points (>175 ^{o}C), which the current setup is not equipped to handle while simultaneously performing DEP or PEP. Once the composite with the final materials is created, its material properties will have to be characterized before it could be implanted in the body. The composite will need to undergo fatigue tests and wear tests to make sure the implant will not fail under physiological loads. Based on the materials selected for the composite there should not be any issues with these tests, but it must still be verified.

After an appropriate current density (≈25 μA/cm^2) can be generated, the next step will be to begin animal testing. *In vitro* testing would be difficult and is not recommended, since the implant would have to be cyclically loaded under physiological loading conditions in a bioreactor. Such a setup would be expensive and difficult to create. Therefore, the next step will be animal testing. Small animals would not prove a good model for this research because much of the current generated by the implant depends on the amount of force exerted on the implant. Larger animals, such as goats, should be used. Eight goats would be implanted with the piezoelectric implant, with two being harvested every two months. DC electrical stimulation has shown average fusion times of around four months (26), so this test should show the implant's ability to stimulate bone growth, as well as show that the implant remains safe, even after the vertebrae have fused.

Future Material Uses

The uses of the new piezoelectric composite aren't just limited to spinal fusion implants. From the lumped parameters model, it can be shown that there are many ways to improve power output that would be impossible based on the physiological restrictions for the spinal cage. Size of the composite is the first clear limitation imposed by the restrictions of the intervertebral space. According to theoretical calculations, PEP could create piezoelectric structures larger than 2 meters thick, giving us the ability to create large, load bearing structures that could be used as sensors or power harvesters on a greater scale.

Other limitations for use in the body include the compressive frequency and force. High frequencies and forces that could be attained by machines are impossible with the human body. If the composite was used in tires on a car, for example, the frequency as well as force would be much greater, increasing current output. As the lumped parameter model shows, current generation increases extremely quickly as frequency and force increase (Figure 52, 55). However, although frequency and force are limited inside the body, they still help provide enough current to stimulate an increase in bone growth, making the piezoelectric fusion cage possible.

Closing Statements

The piezoelectric spinal fusion cage shows great promise. It fills a large need in the medical community due to the low success rates of current spinal fusion methods. Unlike other bone growth adjuncts, the piezoelectric cage is inexpensive, doesn't involve extra instrumentation, and doesn't require major patient compliance. The new implant will simply replace the old fusion cage used in the surgery and utilize the patient's own movements to help stimulate bone growth. Based on theoretical models and early experimental results, the piezoelectric implant should generate enough current

density to improve the rate of bone growth. If the piezoelectric fusion cage should become the standard for spinal fusions, it could significantly increase the success rate of a major surgical procedure.

X. References

1. NINDS. National Institute of Neurological Disorders and Stroke: Low Back Pain Fact Sheet 2011. Available from: http://www.ninds.nih.gov/disorders/backpain/detail_backpain.htm.
2. Bridwell K, Sedgewick T, O'Brien M. Degenerative spondylolisthesis. Journal of spinal disorders. 1993;6(6):461-72.
3. McGuire R, Amundson G. The use of primary internal fixation in spondylolisthesis. Spine. 1993;18(12):1662.
4. West III J, Bradford D, Ogilvie J. Results of spinal arthrodesis with pedicle screw-plate fixation. J Bone Joint Surg Am. 1991;73(8):1179-84.
5. Zdeblick TA. A prospective, randomized study of lumbar fusion. Preliminary results. Spine. 1993;18(8):983.
6. KANE WJ. Direct current electrical bone growth stimulation for spinal fusion. Spine. 1988;13(3):363.
7. Martini F TM, Tallitsch R. Human Anatomy, Sixth Edition. Sixth Edition ed. San Francisco: Pearson Education, Inc.; 2009.
8. WebMD. Upper and Middle Back Pain - Overview 2010. Available from: http://www.webmd.com/back-pain/tc/upper-and-middle-back-pain-overview.
9. Plumberger M. CY-L, Ma Y., Girardi F.P., Mazumdar M., Memtsoudis S.G. National in-hospital morbidity and mortality trends after lumbar fusion surgery between 1998 and 2008. The Journal of Bone and Joint Surgery. 2012;94-B:359-64.
10. Blumenthal SL, Ohnmeiss DD. Intervertebral cages for degenerative spinal diseases* 1. The Spine Journal. 2003;3(4):301-9.
11. Deyo RA, Gray DT, Kreuter W, Mirza S, Martin BI. United States trends in lumbar fusion surgery for degenerative conditions. Spine. 2005;30(12):1441.
12. HCUPnet. National and regional estimates on hospital use for all patients from the HCUP Nationwide Inpatient Sample (NIS) 2009. Available from: http://hcupnet.ahrq.gov/HCUPnet.jsp?Id=D87D477963C59C55&Form=SelCROSSTAB&JS=Y&Action=%3E%3ENext%3E%3E&_Oneway=Yes.
13. Carragee EJ, Hurwitz EL, Weiner BK. A critical review of recombinant human bone morphogenetic protein-2 trials in spinal surgery: emerging safety concerns and lessons learned. The Spine Journal. 2011;11(6):471-91.
14. Jorgenson SS, Lowe TG, France J, Sabin J. A prospective analysis of autograft versus allograft in posterolateral lumbar fusion in the same patient. A minimum of 1-year follow-up in 144 patients. Spine. 1994;19(18):2048.
15. An HS, Lynch K, Toth J. Prospective comparison of autograft vs. allograft for adult posterolateral lumbar spine fusion: differences among freeze-dried, frozen, and mixed grafts. Journal of spinal disorders. 1995;8(2):131.
16. Stanley SK, Barker JR, Jamrich ER, Odom Jr JA. Transforaminal lumbar interbody fusion: evolution and application. Contemporary Spine Surgery. 2005;6(6):1.
17. Brislin B, Vaccaro AR. Advances in posterior lumbar interbody fusion. The Orthopedic clinics of North America. 2002;33(2):367.
18. Zdeblick TA, Phillips FM. Interbody cage devices. Spine. 2003;28(15S):S2.
19. Gan JC, Glazer PA. Electrical stimulation therapies for spinal fusions: current concepts. European Spine Journal. 2006;15(9):1301-11.

20. Hsu WK, Wang JC. The use of bone morphogenetic protein in spine fusion. The Spine Journal. 2008;8(3):419-25.
21. Burkus JK, Heim SE, Gornet MF, Zdeblick TA. Is INFUSE bone graft superior to autograft bone? An integrated analysis of clinical trials using the LT-CAGE lumbar tapered fusion device. Journal of spinal disorders & techniques. 2003;16(2):113.
22. Glassman SD, Carreon L, Djurasovic M, Campbell MJ, Puno RM, Johnson JR, et al. Posterolateral lumbar spine fusion with INFUSE bone graft. The Spine Journal. 2007;7(1):44-9.
23. Epstein NE. Pros, cons, and costs of INFUSE in spinal surgery. Surgical neurology international. 2011;2.
24. Kahanovitz N. Electrical stimulation of spinal fusion: a scientific and clinical update. The spine journal: official journal of the North American Spine Society. 2002;2(2):145.
25. Park J, Kenner G. Effect of Electrical Stimulation on the Tensile Strength of the Porous Implant and Bone Interfac. Artificial Cells, Blood Substitutes and Biotechnology. 1975;3(2):233-43.
26. Simon J, Simon B. Electrical Bone Stimulation. Musculoskeletal Tissue Regeneration. 2008:259-87.
27. France JC, Norman TL, Santrock RD, McGrath B, Simon BJ. The efficacy of direct current stimulation for lumbar intertransverse process fusions in an animal model. Spine. 2001;26(9):1002.
28. GLAZER PA, GLAZER LC. ELECTRICITY: THE HISTORY AND SCIENCE OF BONE GROWTH STIMULATION FOR SPINAL FUSION.
29. Biomet. Implantable Spinal Fusion Stimulators Physician's Manual & Full Prescribing Information SpF PLUS-Mini, SpF - XL IIb 2009. Available from: http://www.biomet.com/spine/getFile.cfm?id=2889&rt=inline.
30. Simon BJ, Schwardt JD. Direct current stimulation of spinal interbody fixation device. Google Patents; 2001.
31. Schwardt JD, Jankowski GB. Preformed extendable mesh cathode for implantable bone growth stimulator. Google Patents; 2000.
32. Fredericks DC, Smucker J, Petersen EB, Bobst JA, Gan JC, Simon BJ, et al. Effects of direct current electrical stimulation on gene expression of osteopromotive factors in a posterolateral spinal fusion model. Spine. 2007;32(2):174.
33. Meril AJ. Direct current stimulation of allograft in anterior and posterior lumbar interbody fusions. Spine. 1994;19(21):2393.
34. Kucharzyk DW. A controlled prospective outcome study of implantable electrical stimulation with spinal instrumentation in a high-risk spinal fusion population. Spine. 1999;24(5):465.
35. Tejano NA, Puno R, Ignacio JMF. The use of implantable direct current stimulation in multilevel spinal fusion without instrumentation: a prospective clinical and radiographic evaluation with long-term follow-up. Spine. 1996;21(16):1904.
36. Rogozinski A, Rogozinski C. Efficacy of implanted bone growth stimulation in instrumented lumbosacral spinal fusion. Spine. 1996;21(21):2479.
37. Cundy P, Paterson D. A ten-year review of treatment of delayed union and nonunion with an implanted bone growth stimulator. Clinical orthopaedics and related research. 1990;259:216.
38. Mendenhall Associates I. 2010 Spinal Implant Price Comparisons 2010. Available from: http://spine.orthopedicnetworknews.com/archives/onn214s5.pdf.
39. Mooney V. A randomized double-blind prospective study of the efficacy of pulsed electromagnetic fields for interbody lumbar fusions. Spine. 1990;15(7):708-12.
40. Tichy J EJ, Kittinger E, Privratska J. Fundamentals of Piezoelectric Sensorics: Mechanical, Dielectric, and Thermodynamical Properties of Piezoelectric Materials: Springer; 2010.
41. Bassett CAL. Biologic significance of piezoelectricity. Calcified Tissue International. 1967;1(1):252-72.

42. Morone MA, Feuer H. The use of electrical stimulation to enhance spinal fusion. Neurosurgical Focus. 2002;13(6):1-7.
43. Platt SR, Farritor S, Haider H. On low-frequency electric power generation with PZT ceramics. Mechatronics, IEEE/ASME Transactions on. 2005;10(2):240-52.
44. Fukada E. History and recent progress in piezoelectric polymers. Ultrasonics, Ferroelectrics and Frequency Control, IEEE Transactions on. 2000;47(6):1277-90.
45. Jones RM. Mechanics of composite materials: Hemisphere Pub; 1999.
46. Wilson SA. Electric-field structuring of piezoelectric composite materials. 1999.
47. Van den Ende D, Bory B, Groen W, Van der Zwaag S. Improving the d33 and g33 properties of 0-3 piezoelectric composites by dielectrophoresis. Journal of Applied Physics. 2010;107(2):024107--8.
48. van den Ende D, van Kempen S, Wu X, Groen W, Randall C, van der Zwaag S. Dielectrophoretically structured piezoelectric composites with high aspect ratio piezoelectric particles inclusions. Journal of Applied Physics. 2012;111:124107.
49. McNulty TF, Janas VF, Safari A, Loh RL, Cass RB. Novel Processing of 1-3 Piezoelectric Ceramic/Polymer Composites for Transducer Applications. Journal of the American Ceramic Society. 1995;78(11):2913-6.
50. Randall C, Van Tassel J, Matsko M, Bowen C, editors. Electric field processing of ferroelectric particulate ceramics and composites. IEEE.
51. Wilson SA, Maistros GM, Whatmore RW. Structure modification of 0–3 piezoelectric ceramic/polymer composites through dielectrophoresis. Journal of Physics D: Applied Physics. 2005;38:175.
52. Bowen C, Newnham R, Randall C. Dielectric properties of dielectrophoretically assembled particulate-polymer composites. Journal of materials research. 1998;13(01):205-10.
53. Jones TB. Electromechanics of particles: Cambridge Univ Pr; 1995.
54. Platt SR, Farritor S, Garvin K, Haider H. The use of piezoelectric ceramics for electric power generation within orthopedic implants. Mechatronics, IEEE/ASME Transactions on. 2005;10(4):455-61.
55. Sodano HA, Inman DJ, Park G. Comparison of piezoelectric energy harvesting devices for recharging batteries. Journal of Intelligent Material Systems and Structures. 2005;16(10):799-807.
56. Cheng C, Chen H, Chen C, Lee S. Influences of walking speed change on the lumbosacral joint force distribution. Biomedical materials and engineering. 1998;8:155-66.
57. Cappozzo A. Compressive loads in the lumbar vertebral column during normal level walking. Journal of orthopaedic research. 1983;1(3):292-301.
58. Cromwell R, Schultz AB, Beck R, Warwick D. Loads on the lumbar trunk during level walking. Journal of orthopaedic research. 1989;7(3):371-7.
59. Khoo B, Goh J, Bose K. A biomechanical model to determine lumbosacral loads during single stance phase in normal gait. Medical engineering & physics. 1995;17(1):27-35.
60. Tsuang YH, Chiang YF, Hung CY, Wei HW, Huang CH, Cheng CK. Comparison of cage application modality in posterior lumbar interbody fusion with posterior instrumentation—A finite element study. Medical engineering & physics. 2009;31(5):565-70.
61. Biomet. MRI Safety Information - SpF(R) PLUS-Mini 2009. Available from: http://www.biomet.com/templates/BTBS/pdf/consumer_brochures/SpF_MRIinfo.pdf.
62. Brosch J, Morris GA, Wilson T, Talavage T, editors. Design and testing of an MRI compatible therapeutic transducer. 2001: IEEE.
63. Singh RS, Culjat M, Neurgaonkar R, White SN, Grundfest WS, Brown ER, editors. P2O-8 Single-Element PLZT Transducer for Wide-Bandwidth Imaging of Solid Materials. 2006: IEEE.
64. Jayasundere N, Smith B. Dielectric constant for binary piezoelectric 0-3 composites. Journal of Applied Physics. 1993;73(5):2462-6.

65. Maxwell J. A treatise on electricity and magnetism. With prefaces by WD Niven and JJ Thomson. Reprint of the third (1891) edition. Dover Publications, Inc., New York, N. Y; 1954.
66. Yamada T, Ueda T, Kitayama T. Piezoelectricity of a high-content lead zirconate titanate/polymer composite. Journal of Applied Physics. 1982;53(6):4328-32.
67. Ende DAvd, Bory BF, Groen WA, Zwaag Svd. Improving the d33 and g33 properties of 0-3 piezoelectric composites by dielectrophoresis. Journal of Applied Physics. 2010;107(024107):8.
68. Bowen CR, Gittings J, Turner IG, Baxter F, Chaudhuri JB. Dielectric and piezoelectric properties of hydroxyapatite-$BaTiO_3$ composites. Applied Physics Letters. 2008;89(132906):pp. 1-3.
69. Yao J, Xiong C, Dong L, Chen C, Lei Y, Chen L, et al. Enhancement of dielectric constant and piezoelectric coefficient of ceramic–polymer composites by interface chelation. J Mater Chem. 2009;19(18):2817-21.
70. Chen L, Hong Y, Chen X, Wu Q, Huang Q, Luo X. Preparation and properties of polymer matrix piezoelectric composites containing aligned BaTiO 3 whiskers. Journal of materials science. 2004;39(9):2997-3001.
71. Wang M, Pan N. Predictions of effective physical properties of complex multiphase materials. Materials Science and Engineering: R: Reports. 2008;63(1):1-30.
72. Lei A, Xu R, Thyssen A, Stoot A, Christiansen T, Hansen K, et al., editors. MEMS-based thick film PZT vibrational energy harvester. 2011: IEEE.